2014

Advancements in the Design, Synthesis, and Application of Polybenzimidazoles

Alexander Lanier Gulledge
University of South Carolina - Columbia

ADVANCEMENTS IN THE DESIGN, SYNTHESIS AND APPLICATIONS OF POLYBENZIMIDAZOLES

by

Alexander L. Gulledge

Bachelor of Science
University of South Carolina, 2010

Submitted in Partial Fulfillment of the Requirements

For the Degree of Doctor of Philosophy in

Chemistry

College of Arts and Sciences

University of South Carolina

2014

Accepted by:

Brian Benicewicz, Major Professor

Chuanbing Tang, Committee Member

Donna Chen, Committee Member

John Weidner, Committee Member

Lacy Ford, Vice Provost and Dean of Graduate Studies

DEDICATION

This dissertation is dedicated to the people that gave me the inspiration to pursue my goals, to all the teachers, friends, and family that pushed me to go further, and to my lovely wife whom helped me along the way.

ACKNOWLEDGEMENTS

I would like to thank everyone involved in helping me complete my Ph.D. Most importantly, I would like to sincerely thank Dr. Brian Benicewicz for his guidance, expertise and support throughout my graduate studies. I would also like to thank my doctoral committee members, Dr. Donna Chen, Dr. John Weidner, and Dr. Chungbing Tang for their advice and encouragement during my Ph.D. work.

I would like to express my thanks to past and present colleagues of the Benicewicz research group for their effort, support and friendship throughout my time with them. I would especially like to thank Darren Seel, Jordan Mader, Atri Rungta, Max Molleo, Xin Li, Kayley Fishel, Jason Hoffman, Ananand Viswanath, Tony Neely, Mike Bell, Lei Wang, and Junting Li for all their help, support, and advice that helped me further my own knowledge and accomplishments.

Several people outside of my research group were also extremely helpful and great friends. I would like to acknowledge Sandi and Kinkini Roy, Scott Hoy, Michael Geer, Chris Hardy, Perry Wilbon, Matt DiCarmine, Kejian Yo, Jeff Hyatt, Jim Mazzuca and Onn Wong for all of their help. I would also like to acknowledge my wife, Shadow Gulledge. Without her encouragement, love and patience, I would not have been able to achieve as much as I have.

I would also like to acknowledge my family members that have provided me with lifelong support and love, including my dad, William R. Gulledge, my brother, William

R. Gulledge Jr., my sister, Donielle Lanier, my mom, Madison Bowen, my uncle, Raymond Lanier, and my grandmother, Othella Biner. Also, I would like to thank my lifelong friends outside of graduate school, including, but not limited to, Miguel Hernandez, Daniel Manor, Alex Goff, and Eric James. They have given me support and motivation throughout my college years.

There are so many people that helped me achieve this goal, far more than just the ones listed here. I want to thank everyone who helped me in both big and small ways. I could not have done this without the help, support, and friendship everyone has offered. To everyone who has helped me, motivated me, and been a friend, I say thank you. You have all helped more than you know.

ABSTRACT

The overall goal of the work presented within this thesis is to investigate, understand, and develop structure-property relationships in regards to polymer structure, membrane stability, and device performance. Previous work has shown that material properties such as acid loading, proton conductivity, mechanical integrity, and device performance can be attributed to polymer structure, chemical functionality, and polymer architecture (homo, random, co-polymer etc.). Developing and understanding these relationships is critical to the advancement of fuel cell technology. Within this thesis, several of these relationships are investigated and reported.

Novel polymers and copolymer systems have been developed in this research and have significantly progressed the understanding of polybenzimidazole chemistries. The research reported herein contributes to the ever-developing pool of knowledge regarding polybenzimidazole chemistry and material applications.

Extensive work has been done concerning polymer structural design and investigation with regards to sequence isomerism through the design, synthesis, and utilization of novel monomer compounds. A novel diacid monomer, 2,2'-bisbenzimidazole-5,5'-dicarboxylic acid (BBDCA), was synthesized and polymerized with 3,3',4,4'-tetraaminobiphenyl (TAB) to prepare a polymer, termed i-AB-PBI, that was composed of repeating 2,5-benzimidazole units. The i-AB-PBI incorporates head-to-head, tail-to-tail, and head-to-tail benzimidazole orientations. This is in contrast to the

previously known AB-PBI which incorporates only head-to-tail benzimidazole sequences. Until this work, no other AB-type polybenzimidazole existed. AB-type polybenzimidazoles are fundamental in the family of polybenzimidazoles because they only incorporate the benzimidazole motif, i.e. no other spacer or functionality is incorporated in the polymer structure. These polymers were synthesized and characterized by molecular weight, membrane composition, ionic conductivity, thermal, mechanical, and fuel cell performance properties. A detailed report of this study is presented in Chapter 3.

This work was further progressed by the study of the AB-PBI and i-AB-PBI random copolymer system. The random copolymer system of these polymers, termed r-AB-PBI, is unique in that the chemical structure and functionality does not change across the copolymer compositional spectrum. The r-AB-PBI copolymer system introduces a sequence distribution effect with regards to benzimidazole orientation, as well as randomization of benzimidazole sequence between two well defined sequenced AB-type polymers. These polymers were synthesized and characterized by molecular weight, membrane composition, ionic conductivity, thermal, mechanical, and fuel cell performance properties. A detailed report of the unique r-AB-PBI system is described in Chapter 4.

Another set of random copolymers was developed that incorporates the AB-type polybenzimidazoles and a para-phenyl-polybenzimidazole (p-PBI). AB-PBI and p-PBI random copolymers were developed and compared to random copolymers of i-AB-PBI and p-PBI. The unique combination and contrast of properties in the AB/p-PBI and i-AB/p-PBI systems provided insight into effects resulting from structural modification,

sequence orientation, stability, and randomization. The p-PBI and AB-PBI copolymers address aspects of acid loading, stability, and structural modification, whereas the p-PBI and i-AB-PBI copolymers address comparisons of sequence isomerism and randomization between two high performance PEM materials. All copolymer materials were characterized by molecular weight, membrane composition, mechanical properties, ionic conductivities, and fuel cell performances. A detailed report of these copolymer systems and insights gained thereof are described in Chapter 5.

A sulfonated polybenzimidazole membrane (s-PBI) doped with sulfuric acid was utilized for the first time in an all-Vanadium redox flow battery (VFRB). This is the first reported utilization of polybenzimidazole in an energy storage device. Performance investigations of s-PBI in a VRFB were conducted and compared to Nafion 117, and Nafion 212. The s-PBI membranes developed were characterized in terms of molecular weight, ionic conductivity, mechanical properties, membrane composition, and overall VFRB performances under a variety of conditions. A detailed report of this work is provided in Chapter 6.

A sulfonated polybenzimidazole (s-PBI) membrane doped with sulfuric acid was utilized in the Hybrid Sulfur Electrolyzer. This work is the first report of a polybenzimidazole material being utilized in a Hybrid Sulfur Electrolyzer. Extensive research was conducted regarding device performance under a variety of conditions. All s-PBI membranes were conditioned through an acid exchange process, verified by titration, and characterized in terms of molecular weight, membrane composition, mechanical properties, ionic conductivity, and overall device performance. The s-PBI utilized in the Hybrid Sulfur Electrolyzer was compared to Nafion 117 and Nafion 112.

Prior to this work, high-temperature device operation of a Hybrid Sulfur Electrolyzer had not been evaluated. A detailed overview of this work is reported in Chapter 7.

In addition to developments of novel PBI chemistries and device applications, extensive work was conducted in regards to the development of a new solution polymerization method for PBI materials. Prior to this work, polymerization of high-molecular weight polybenzimidazole in an organic solvent had not been reported. The work conducted resulted in a viable solution polymerization method of PBI in dimethylacetamide (DMAc). Through investigation of a series of monomer functionalities, a bisulfite adduct derivative of isophthalaldehyde was developed which allowed for the synthesis of high-molecular weight PBI in DMAc at high concentrations. This work has been patented, and provides a practical synthetic avenue for the synthesis of a multitude of polybenzimidazole derivatives. PBI developed from this process was characterized in terms of NMR, IR, DSC, TGA, and molecular weight and compared to commercially produced PBI. A detailed overview of this work is reported in Chapter 8.

TABLE OF CONTENTS

LIST OF TABLES

LIST OF FIGURES

LIST OF SCHEMES

Chapter 1: Introduction

1.1 Energy Demand

Our species, as a whole, has continued to grow, develop, and consume natural resources. With the rise of global human population and technology, our consumption and demand for energy continues to increase. **Figure 1.1** illustrates the global primary energy consumption over the last twenty three years and provides a projected growth over the next two years.[1] Fossil fuel consumption contributes to more than 85% of the total world energy supply and is projected to still account for up to 80% of the global energy supply by 2040.[2] Global fossil fuel consumption has also continued to grow, and will continue to do so until alternative energy sources are developed and employed on a large scale. **Figure 1.2** illustrates the growth of global fossil fuel consumption over the past twenty six years.[3] Moreover, conventional technology utilizes heat and combustion engines to convert fossil fuels into usable energy. The efficiency of these systems, even at maximum power output, is limited as is realized by the understanding of the Carnot Cycle.[4] The combustion of fossil fuels such as oil, natural gas, and coal results in pollutant emissions of SO_X, NO_X, and CO. These pollutants contribute to the continually rising levels of carbon dioxide in our atmosphere and in turn contribute to global warming and more rapid climate change. In addition to the harmful and threatening effects of fossil fuel consumption, these resources are not renewable. The need for sustainable clean energy is evident. With the growing concerns of environmental safety to our planet, as well as the limitation and negative effects of our current energy consumption, the motivation for development of alternative clean energy technology has never been more prominent. Alternative energy refers to energy sources that have no undesired consequences such as carbon dioxide emissions.[5] Currently several types of

alternative energy sources are being utilized, including solar, wind, hydro, and geothermal. Although these sources provide clean energy, they make up for less than 20% of the world's energy sources.[6] The lack of energy provided by currently employed clean energy approaches highlights the need for additional clean energy technologies.

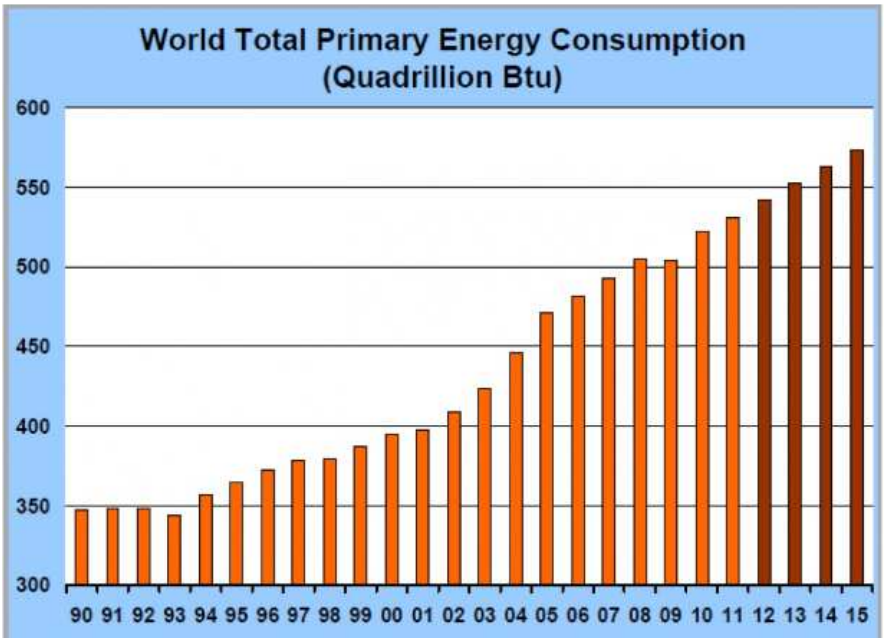

Figure 1.1: World total primary energy consumption.[1]

1.2 Introduction of Fuel Cell Technology

1.2.1 History of Fuel Cells

The development of fuel cell technology as we know it today can be traced back over 160 years to Sir William Grove's invention of the gaseous voltaic cell in 1839.[7] He defined a fuel cell as "an electrochemical device that continuously converts chemical energy into electrical energy (and some heat) as long as fuel and oxidant are supplied".[8] The history and development of fuel cells has been extensively described.[9-11] Initially,

fuel cell technology was very attractive because the energy efficiencies of other technologies were very poor. Fuel cells are not governed by Carnot-efficiency[4] unlike combustion engines or batteries, and can theoretically achieve much higher efficiencies. Moreover, the efficiency of a fuel cell is not limited by thermal losses as the electrochemical cell is driven by the Gibb's-free-energy[12] released during the chemical reaction between a fuel and oxidant. Fuel cells have been referred to as a "zero emission engine" because, when hydrogen is used as a fuel, only water and heat are produced as byproducts. As the efficiency of other technologies improved, the interest in fuel cells diminished. The intensive research and development of fuel cell technology was then reignited when Francis Thomas Bacon produced the first practical fuel cell for Britain's National Research Development Corporation in 1958. This inspired companies and government agencies such as NASA to adopt fuel cell technology and begin developmental projects. Unfortunately, nearly all of the initial development projects failed to meet performance targets, and nearly all research regarding this technology was halted by the end of the 1960s. The interest in fuel cells was not again renewed until the 1990s when concerns for energy security, economic growth and environmental sustainability began to increase.

1.2.2 Types of Fuel Cells and the Application Thereof

Since the development of fundamental fuel cell technology, many variations and applications have been investigated. Fuel cells are classified according to various parameters such as types of fuel used, fuel processing, operational device temperature, and several others. The most commonly used and widely accepted method of fuel cell classification is based upon the type of electrolyte used. Classification by the electrolyte

utilized for fuel cell operation leads to the following major types of fuel cells.[13] An overview of primary fuel cell types is given in **Table 1.1**.

1. Alkaline Fuel Cell (AFC)
2. Proton Exchange Membrane Fuel Cell (PEMFC)
3. Phosphoric Acid Fuel Cell (PAFC)
4. Molten Carbonate Fuel Cell (MCFC)
5. Solid Oxide Fuel Cell (SOFC)

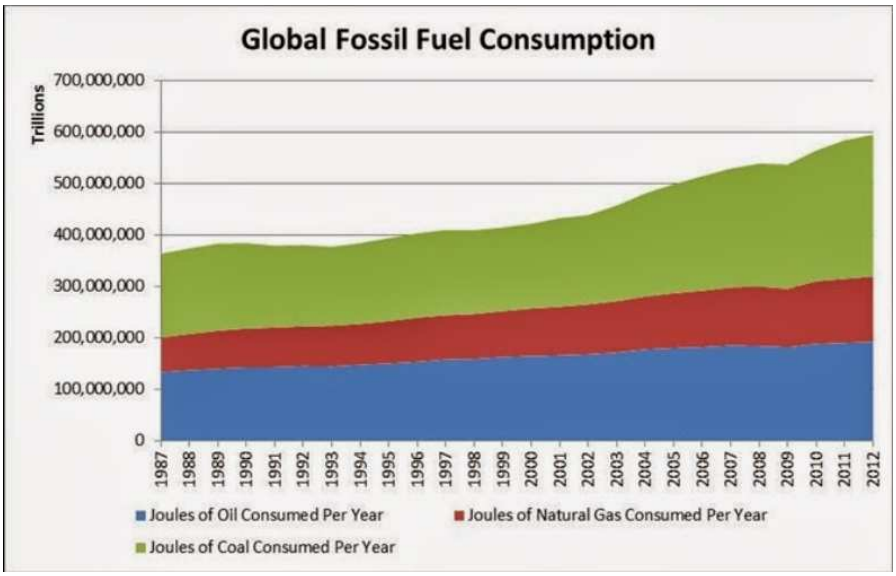

Figure 1.2: Global Fossil Fuel Consumption.[3]

Table 1.1: Fuel Cell Types and Characteristics

Fuel Cell Type		**AFC**	**PEMFC**	**PAFC**	**MCFC**	**SOFC**
Electrolyte		KOH	Polymer	Phosphoric Acid	Molten Carbonate	Solid Oxide
Charge Carrier		OH^-	H^+	H^+	CO_3^{2-}	O^{2-}
Electro-chemical Reaction	**Anode**	$H_2 + 2OH^- \rightarrow 2H_20 + 2e^-$	$H_2 \rightarrow 2H^+ + 2e^-$	$H_2 + 2OH^- \rightarrow 2H_20 + 2e^-$	$H_2 + CO_3^{2-} \rightarrow H_2O + CO_2 + 2e^-$	$H_2 + O^{2-} \rightarrow H_2O + 2e^-$

	Cathode	$\frac{1}{2}O_2 + H_2O + 2e^- \rightarrow 2OH^-$	$\frac{1}{2}O_2 + 2e^- + 2H^+ \rightarrow H_2O$	$\frac{1}{2}O_2 + H_2O + 2e^- \rightarrow 2OH^-$	$\frac{1}{2}O_2 + CO_2 + 2e^- \rightarrow CO_3^{2-}$	$\frac{1}{2}O_2 + 2e^- \rightarrow O^{2-}$
	Net	$H_2 + \frac{1}{2}O_2 \rightarrow H_2O$	$H_2 + \frac{1}{2}O_2 \rightarrow H_2O$	$H_2 + \frac{1}{2}O_2 \rightarrow H_2O$	$H2 + \frac{1}{2}O_2 + CO_2 \rightarrow H_2O + CO_2$	$H2 + \frac{1}{2}O_2 \rightarrow H_2O$
Operational Temperature*		90-100˚C	60-120˚C	150-240˚C	600-700˚C	700-1000˚C
Typical Stack Size*		10-100 kW	1-100kW	400kW	300kW-3MW	1kW-2MW
Efficiency*		60%	60%	40%	45-50%	60%
Advantages*		• Low Cost Components • Cathode Reaction Faster in alkaline electrolyte	• Solid electrolyte reduces corrosion and electrolyte management problems • Low temperature • Quick start up	• Higher temperature provides faster electrode kinetics • Increased tolerance to fuel cell impurities	• Fuel Flexibility • Variety of Catalysts	• Fuel Flexibility • Solid electrolyte
Disadvantages*		• Sensitive to CO2 in fuel and air • Electrolyte management	• Expensive Catalysts • Sensitive to fuel impurities • Humidification requirements	• Pt catalyst • Long start up time • Low current and power	• High temperature corrosion and breakdown of cell components • Long start up time • Low power density	• High temperature operation requires long start up time
Application*		• Military • Space	• Electrical utility • Portable power • Transportation	• Electrical utility • Transportation • Portable power	• Electrical utility	• Electrical utility

*: Information obtained from U.S. Department of Energy[14]

Fuel cell devices operate over a range of temperatures based on the configuration, fuel used, and electrolyte incorporated as illustrated in Table 1-1. Fuel cell device variation has developed in parallel with the discoveries of additional utilizable fuels and operational configurations. This development is key to the evolution of the technology as one device cannot be considered sufficient for all power applications. Fuel cell technology has developed in such a way that the applications have become diverse. Fuel cells can be used for stationary and portable applications, and among these can serve several practical functions. Stationary applications were the first developed with this

technology, to simply provide power. In general, fuel cell systems achieve approximately 40% fuel-to-electricity efficiency.[15] With further development, it was realized that these devices could be utilized for combined power and heat applications, as heat is a byproduct of the electrochemical reaction which will be discussed in further detail later in this thesis. With the utilization of the produced heat captured for cogeneration, the efficiency of the device can be increased up to 85%, while also reducing energy costs related to operation.[15] To date, stationary fuel cells for combined heat and power applications are utilized across the US and other countries around the world in buildings such as hospitals, schools, and utility power plants.[16] Used as either grid-independent power generators, or directly connected to grid power for supplementation, these systems provide clean, environmentally friendly, power alternatives when compared to conventional power obtained from the burning of coal and fossil fuels.

In contrast to stationary applications previously described, fuel cell device technology has also evolved to encompass portable applications. Portable fuel cell applications primarily serve to provide power in place of batteries. Considering the substantial $11.7 billion a year global battery industry[17], the development of portable applications has been a significant milestone for the continued development and utilization of this technology. Portable fuel cells are much lighter than batteries, have been shown to last longer, and generally incorporate methanol as a fuel source.[18] Moreover, these devices have been demonstrated to be applicable to small electronics such as laptop computers and cell phones.[19], while providing a significant advantage of higher energy density. Fuel cells have the potential to achieve energy densities up to sixteen time higher than that of conventional lithium ion batteries.[20] One of the primary

implementations of portable fuel cell devices is found in the automotive industry. Companies such as Nissan, Honda, Fiat, and numerous others have been researching and developing these applications over the past two decades.[21] Hybrid vehicles which incorporate alternative fuels such as hydrogen and methanol are considered to be the next generation of development in the automotive industry. This development is further driven by the limitations and cost of conventional non-renewable hydrocarbon fuels. The rise in concern for environmental standards, the limited supply and increased costs of conventional hydrocarbon fuels, and the increase in fuel cell device applications, substantially contribute to the growth and development of this innovative technology.

1.2.3 Mechanism of Fuel Cell Operation

Knowing the implications and applications of fuel cells is an important aspect for those who work in the field, however, a detailed understanding of how a fuel cell operates is still required. Understanding the operation of a fuel cell begins with the construction. A fuel cell does not incorporate any mechanically moving parts which results in low mechanical maintenance and cost.[22] For illustrative purposes within this thesis the electrochemical mechanism and construction of a polymer electrolyte membrane (PEM) fuel cell will be described. In general, a fuel cell is composed of a membrane electrode assembly (MEA) sandwiched between gas diffusion layers which are encompassed by graphite plates with gas flow channels. The flow plates are then in direct contact with current collectors, which are insulated and encased by anode and cathode endplates. The entire device is then bolted together with a set degree of compression. The construction of a PEM fuel cell is illustrated in **Figure 1.3**.

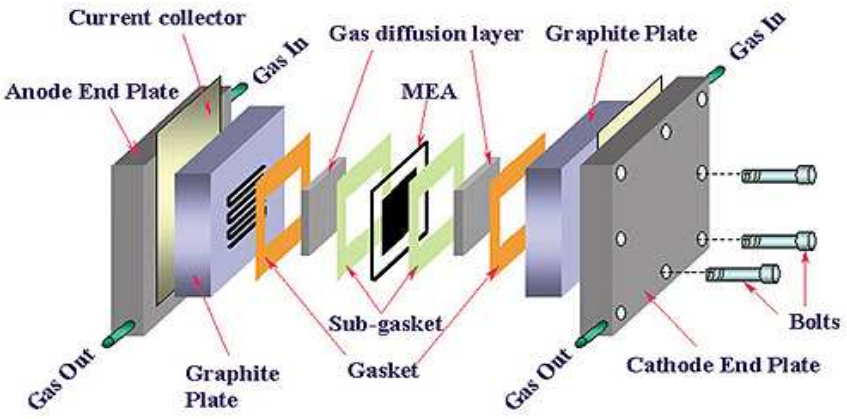

Figure 1.3: Illustration of a polymer electrolyte membrane fuel cell construction.[23]

The core component of a fuel cell is the membrane electrode assembly (MEA). In a PEM fuel cell, the MEA consists of a polymer membrane, two porous electrochemically conductive electrodes, and outer sub-gaskets. The polymer membrane used in PEM fuel cells consists of polymer matrix doped with an electrolyte that facilitates proton conduction. The porous electrochemically conductive electrodes, typically platinum or platinum alloy supported on carbon, is in contact with the polymer electrolyte membrane on both the anode and cathode side of the MEA, and comprises the catalyst layer and gas diffusion layer respectively. Finally, the MEA is completed by the addition of sub-gaskets which encompass the outer rim of the assembly to allow for safe handling. The components of the MEA are then typically hot pressed to a given degree of compression to fuse these components into a single unit. Once assembled, the MEA is sandwiched between to graphite plates with gas flow channels. This allows the gaseous fuel of the cell to pass over the surface of the MEA, penetrate the gas diffusion electrodes and electrochemically react. As previously mentioned, current collectors and insulators are placed outside of the graphite flow plates to allow for the application of an external voltage without electrifying the outer endplates (typically steel). The device assembly is

completed when the outer endplates are bolted together with a given degree of compression.

Understanding the construction of a fuel cell is only part of understanding the technology of the device. To gain a complete understanding, one must also understand the electrochemical processes that occur within the cell. All the electrochemical processes of a fuel cell occur at and within the MEA. An overview of the electrochemical processes of a PEM fuel cell are depicted in **Figure 1.4**. A gaseous fuel such as hydrogen is supplied at the anode side of the fuel cell where it penetrates the gas diffusion layer and reaches the electrode catalyst layer. When an external voltage is applied to the cell, a catalytic electrochemical reduction of the hydrogen will occur when the molecules of the gas are in contact with platinum. This results in the separation of hydrogen gas into protons and electrons. The electrons are instantaneously shuttled through the external circuit of the cell, while the protons diffuse through the polymer electrolyte membrane. The polymer electrolyte membrane must be able to facilitate proton diffusion while simultaneously inhibiting electron diffusion or conduction in order for the device to operate. This process will be discussed in further detail later in this thesis. Once the protons diffuse through the polymer electrolyte membrane, they are then catalytically oxidized on the cathode side of the cell when the oxidant gas, platinum, and protons meet. As previously defined, a fuel cell is an electrochemical device that will continuously provide heat and power as long as fuel and oxidant are supplied.[8] Typically air is used as an oxidant gas which contains a mixture of gaseous species, of which, oxygen participates in the electrochemical oxidation. Since air is comprised of approximately 23% oxygen[25], it can be used as an oxidant gas. The electrochemical half

reactions and overall net reaction which occur during the device operation are listed below.

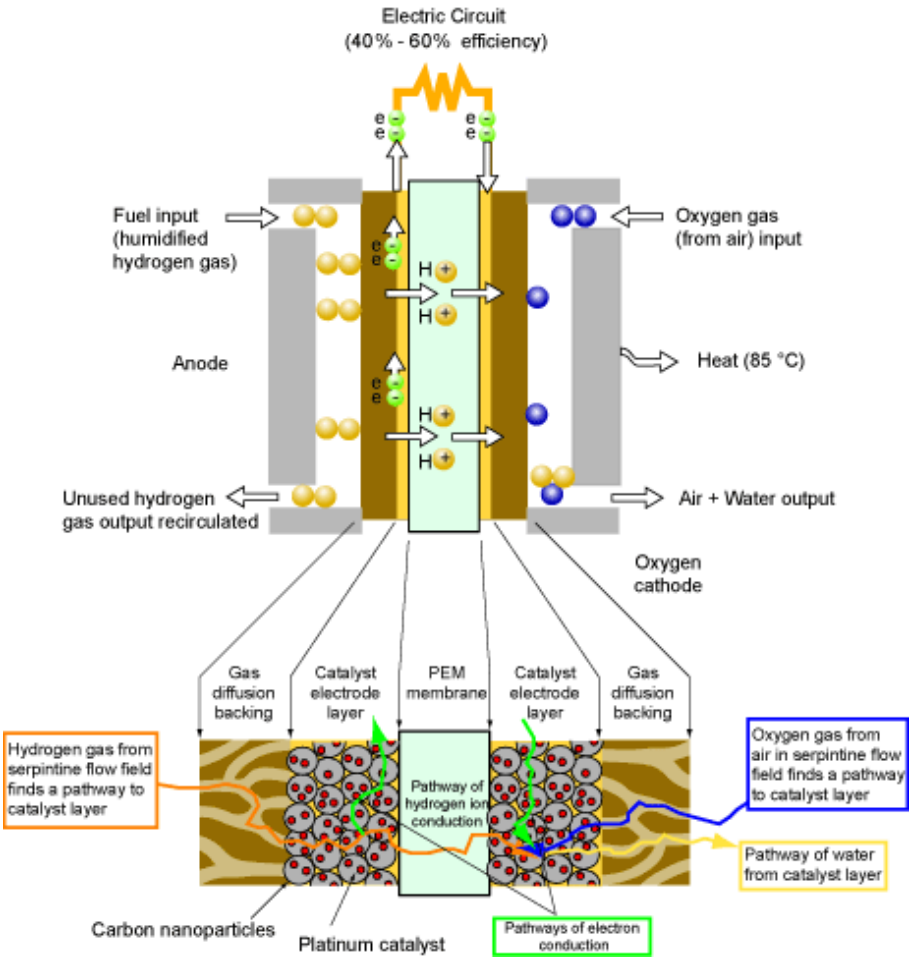

Figure 1.4: Overview of electrochemical processes within an operating PEM fuel cell.[24]

Anode: $H_2 \rightarrow 2H^+ + 2e^-$ **Equation 1-1**

Cathode: $\frac{1}{2}O_2 + 2e^- + 2H^+ \rightarrow H_2O$ **Equation 1-2**

Net: $H2 + \frac{1}{2}O_2 \rightarrow H_2O$ **Equation 1-3**

1.3 Introduction of Polymer Electrolyte Membrane Materials, Polybenzimidazole (PBI), and PBI Applications in Fuel Cells

1.3.1 Introduction to Polymer Electrolyte Membrane Materials

Perhaps the most essential component to the development and operation of PEM fuel cells is the polymer electrolyte membrane. In order for the device to function, the polymer electrolyte membrane must meet several criteria. The required properties of a material candidate for PEM fuel cell operation are as follows:

a. The ability to facilitate proton conduction in an efficient manner
b. Inhibition of electrical conduction
c. Low gas permeability to segregate the fuel and oxidant gases supplied
d. Mechanical robustness sufficient to withstand gas pressure and cell compression
e. Chemical and thermal stability in the environment of device operation

There are many other desired chemical and material properties of polymer electrolyte membranes such as low cost and ease of fabrication when considering candidates for fuel cell operation. With these requirements and desirable attributes, there is a relatively limited pool of candidates from which to select such a material. Early developments of polymer electrolyte membranes (also referred to as proton exchange membranes) resulted in proton-conducting polymers with poor tensile strengths and little resistance to cracking.[26] In 1996, Dupont developed what is currently the most widely used class of polymer electrolyte membranes in commercial production. This class of materials is known as perfluorosulfonic acid (PFSA) membranes. One subclass of these membranes, trademarked Nafion®, was developed by Dupont and met the previously

stated requirements for a desirable polymer electrolyte membrane.[27] The development of Nafion® was a derivation of a previously published perfluoro sulfonic acid material developed by DOW chemical in 1988.[28] The chemical structures of Nafion® and Dow Chemical's PFSA materials are shown in **Figure 1.5**.

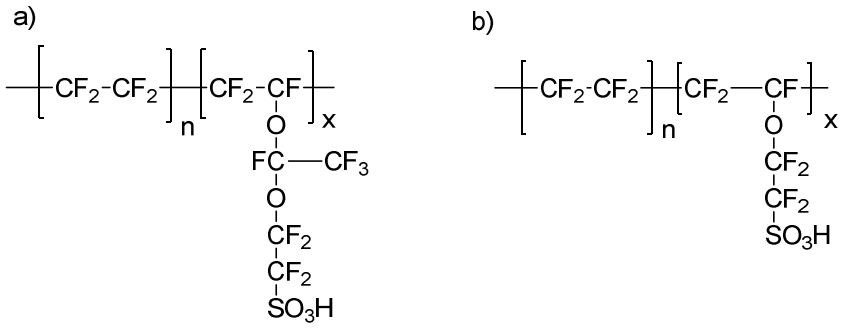

Figure 1.5: Structure of perfluorinated polymers from **a)**Dupont and **b)** Dow Chemical

The chemical structures used in PFSA membranes are comprised of a polytetrafluoroethylene (PTFE, Dupont trade name Teflon®) backbone. The Teflon® backbone of the two PFSA membranes illustrated in Figure 1-5 provide a substantial hydrophobic character to the materials. Due to the immiscibility between the backbone and side chains of PFSA membranes, an ion-clustered morphology results where the Teflon-like backbones of the polymer form semicrystalline hydrophobic regions and the pendant sulfonic acid groups form micelle-like ion clusters in a hydrophilic region of the polymer membrane's morphology.[29] The semicrystalline and micelle-like ion cluster morphology is depicted in **Figure 1.6**. The resulting structural properties exhibited by these materials exhibit a proton transport mechanism that is highly dependent upon the presence of water as an electrolyte. The proton transport mechanism of water was first described by Theodor Grotthuss in 1806[30] and later termed the Grotthuss mechanism for

proton transport.[31] As a result of the mechanism utilized, the proton conductivity and subsequent fuel cell performance are largely dependent upon the amount of water content in the membrane. Thus, water management in PFSA based fuel cell systems is a critical issue to address. Typically, water management is controlled by monitoring and adjusting humidification of the reactant gasses in the cell, and removing excess water produced during the reaction at the cathode of the cell. The above mentioned water management requirements for the operation of PFSA membrane based fuel cell imposes a significant limitation to the operational temperature of the device. Fuel cells based on PFSA membranes which use water as an electrolyte cannot operate reliably at temperatures above 100˚C.[32] This limitation has led to the pursuit of PEM materials that can operate at higher temperatures (>100˚C).

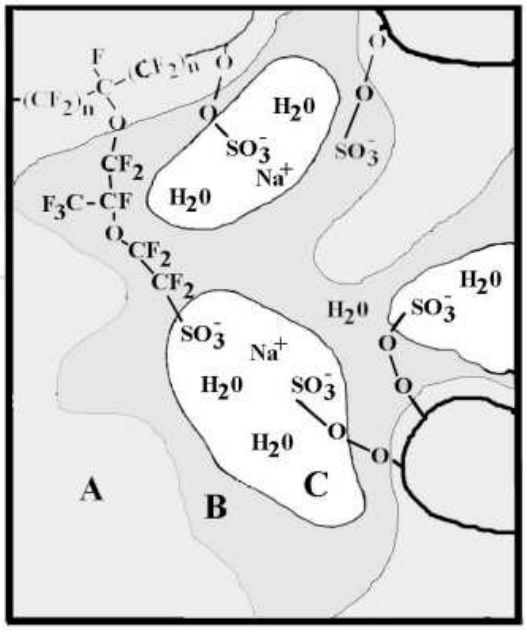

Figure 1.6: Phenomenological based Yeager Three Phase Model of Nafion® morphology.[33]

1.3.2 Approaches to High Temperature (>100˚C) Polymer Electrolyte Membranes

Fuel cell efficiency can be increased significantly by operating at elevated temperatures (>100 ˚C).[34] Higher operational temperatures have been shown to provide advantages such as faster electrode kinetics, increased resistance to fuel impurities[35] and simplified water and thermal management.[36] The pursuit of PEM materials that can operate at temperatures at or greater than the boiling point of water has followed two primary approaches. The first approach would be to develop a proton conductive material that can retain water above the normal boiling point (100˚C). This approach is seen as the first logical step when considering how to overcome the issues associated with water loss at higher temperature, and has been approached from many angles. The most extensive research using this approach is focused on inorganic/organic composite membranes. Composite membranes consist of a polymer matrix in which inorganic or inorganic-organic solid particles are dispersed. Both proton conductive polymer matrixes such as Nafion® [37,38], sulfonated polyetheretherketones (sPEEK)[40,41], and non proton conductive matrixes such as Teflon[42,43] have been developed for this approach. Moreover, the inorganic fillers can also be highly proton conductive such as heteropolyacids[39,40] and phosphonates[39] or low to non-conductive such as silica[37,38], and zirconia[44]. Over the past several decades researches have been developing new inexpensive polymer materials with good thermal stability, mechanical stability, and reasonable proton conductivity at higher temperatures. Typically these polymers consist of sulfonic or phosphonic acids attached to the polymer main chain which facilitate proton conduction when in contact with water. However, PEM membranes developed from this approach rely on water for

proton conduction, and cannot achieve operational temperatures greater that 160˚C due to insufficient water retention at those temperatures. Fuel cells operating with these materials also require high operating pressure to maintain suitable water content at elevated temperatures (>100˚C).

The second approach to the development of high temperature PEM fuel cell materials utilizes alternative electrolytes for proton conduction other than water. These alternatives include high boiling point molecules and are generally amphoteric in nature. Theoretically, any amphoteric molecules can be used as proton conductors. However, not every amphoteric molecule exhibits high proton conductivity, especially in the pure state. To date, the most common proton conductors are phosphoric acid or nitrogen-containing aromatic heterocyclic molecules.

Much research has gone into the development of alternative dopants for high-temperature PEM fuel cells, such as phosphoric acid (PA), and has been recently reviewed.[45] Phosphoric acid, which can form hydrogen bonding networks due to its unique structure, is a very good proton conductor. As opposed to water, phosphoric acid is an intrinsic proton conductor as a consequence of its high degree of self-dissociation and a very high mobility of protonic charge carriers.[46,47] Eighty five percent phosphoric acid has a conductivity of 0.053 S/cm at 30˚C which results from its extensive self-dissociation.[48-50] In addition to the self-dissociation process, phosphoric acid undergoes auto-dehydration at high temperatures.[49] This has led to extensive work on phosphoric acid doped polymer electrolyte membranes for fuel cell applications.

The majority of phosphoric acid doped polymers, such as PEI-xH_3PO_4[51,52], PEO-xH_3PO_4[53], PVDF- xH_3PO_4[54], and PMMA- xH_3PO_4[55], can only be used for low

temperature applications due to their poor mechanical or chemical stability at high temperatures. Other phosphoric acid doped polymers show good properties at high temperatures and low relative humidity such as poly-2-vinylpyridinium and derivatives thereof.[56] The most extensively studied material among all the phosphoric acid doped polymers investigated to date, showing high proton conductivity[57], low reactant permeability[58], good thermal and chemical stability[59], high fuel impurity tolerance[60], and good fuel cell performance at temperatures up to 200˚C under low relative humidity conditions[61], is polybenzimidazole.[62-82]

1.3.3 Introduction to Polybenzimidazole

A polybenzimidazole (PBI) can be formed through a polycondensation of a diacid and tetra amine, as shown in **Scheme 1.1**. As with any polycondensation polymerization and, as defined by the Carother's equation[83], an exact stoichiometric ratio is needed for the synthesis of high molecular weight polymer. Typical syntheses of bisbenzimidazoles involves a reaction between bis-ortho-phenylenediamines with a diacid or diamide in HCl or polyphosphoric acid (PPA).[84] Synthesis of 2-substituted benzimidazoles from the reaction of *o*-phenylendiamine with an imidate are also well known.[85] Synthetic knowledge of these procedures can easily be applied to polymeric systems when di-functional monomers are incorporated. Di-functional monomers with various R groups and can be used to produce a variety of polybenzimidazole derivatives (**Scheme 1.1)**.

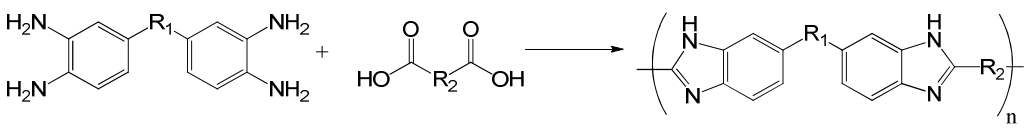

Scheme 1.1: Reaction of a tetra amine and a diacid to form a polybenzimidazole.

In 1959, the first aliphatic PBI was developed by Brinker and Robinson.[86] Shortly afterwards came the first development of an aromatic PBI by Marvel and Vogel in 1961.[87] In 1983, Celanese commercialized one type of polybenzimidazole (meta-PBI, poly(2,2'-m-phenylene-5,5'-bibenzimidazole), as shown in **Figure 1.7**. This commercialized polybenzimidazole was developed for use as fibers and textiles for thermal protective clothing and fire blocking applications.[88-91]

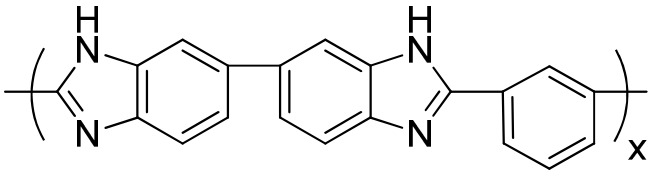

Figure 1.7: Poly(2,2'-m-phenylene-5,5'-bibenzimidazole)

Of all the derivations of polybenzimidazoles, the aromatic PBIs have received the most attention due to their excellent thermal and chemical resistance properties. Aromatic PBIs do not have a melting point due to their lack of crystallinity and exhibit very high decomposition temperatures. In addition to their high temperatures of decomposition (>500˚C), they are practically insoluble in most organic solvents.[92] Moreover, PBIs have shown outstanding stability when exposed to inorganic acids and bases when compared to other high performance fibers such as Nomex or Kevlar. [90,93]

Industrially, polybenzimidazole is polymerized by a two-stage melt-solid polymerization process. Diphenyl isophthalate (DPIP) and tetraaminobiphenyl (TAB) are reacted in bulk to produce the meta-PBI product.[94] The condensate of this reaction is a gas, and subsequent crushing of the resulting foam developed in the first stage is

required. The second stage then involves reheating the low molecular weight polymer in the solid state to synthesize high molecular weight polymer at temperatures as high as of 400˚C. The phenol gas by product of this reaction is hazardous and must be carefully collected and treated. The final product is a non-homogenous product that is separated based on particle size and molecular weight. Resulting powders from the bulk polymerization are then dissolved at high temperature and pressure in N,N-dimethylacetamide (DMAc), often with added LiCl as an aid to the dissolution process. The polymer dope solution is then filtered and spun into fibers for commercial application. These resulting fibers are then used as a raw material for thermally resistant fabrics and fire blocking applications.

In contrast to melt or bulk phase polymerization methods, solution polymerization for the synthesis of high molecular weight polybenzimidazole can be conducted with high boiling point solvents such as N,N-dimethylacetamide (DMAc) dimethylsulfoxide (DMSO) and N-methyl-2-pyrrolidinone (NMP).[95-98] Polyphosphoric acid is also a powerful solvent for the synthesis of polybenzimidazole polymers.[99] Polyphosphoric acid is composed of various condensed phosphoric acid oligomers. When polybenzimidazole is polymerized in polyphosphoric acid solution, the solvent serves multiple purposes, acting as an acid catalyst and a dehydrating agent.[99] Polymerization of polybenzimidazole in polyphosphoric acid solution has several advantages over current commercial bulk polymerization methods including:

1. Polyphosphoric acid can activate monomers by forming various phosphoric anhydrides.
2. Polyphosphoric acid solution polymerizations are homogenous

3. Cost effective monomers can be used in place of more expensive ester derivatives
4. Polyphosphoric acid is a non oxidative medium

On the contrary, there are several disadvantages of using polyphosphoric acid as a condensation solvent commercially. These include:

1. Corrosive characteristics of polyphosphoric acid
2. Limited solid content of polymer in solution
3. Multiple step isolation required for obtaining polybenzimidazole
4. High yields of phosphate waste

Considering the advantages and disadvantages for using polyphosphoric acid as a solvent for the commercial polymerization and production of polybenzimidazole, the above mentioned melt-solid state method is still utilized today. Although synthesis of polybenzimidazole in polyphosphoric acid has not proved to be the most optimal route for commercial fiber production, it is a well suited method for the development of phosphoric acid doped polybenzimidazole membranes.

1.3.4 Phosphoric Acid Doped Polybenzimidazole and The Preparation Thereof

First proposed by Litt and investigated by Savinell, Litt, and Wainright et al. at Case Western University, phosphoric acid doped polybenzimidazole emerged as a promising candidate for a low-cost and high performance membrane material applicable to high temperature polymer electrolyte membrane fuel cells.[58,62,65,68,69,73,77,100-105] Polymer electrolyte membranes of polybenzimidazole doped with phosphoric acid combine the chemical and thermal advantages of polybenzimidazole with the low volatility and high proton conductivity of phosphoric acid, leading to a promising

material candidate for high temperature PEM fuel cell applications. These membranes have significant advantages in PEM fuel cell applications over PSFA membranes including:

1. High temperature operational capabilities
2. High proton conductivity at elevated temperatures
3. Low reactant permeability

From an engineering perspective, it is understood that the material processing can greatly affect the final membrane properties. Currently, there are two methods for the synthetic preparation and processing of phosphoric acid doped polybenzimidazoles; conventional synthesis in the melt-solid polymerization process, followed by dissolution in DMAc, phosphoric acid imbibing of the film, and synthesis in polyphosphoric acid followed by an induced solution-to-gel transition.

Conventionally, preparation of phosphoric acid doped polybenzimidazole membranes for fuel cell applications starts with synthesis by the melt-solid polymerization process, and dissolution of the polymer in a high boiling point solvent, such as N,N-dimethylacetamide (DMAc). In some reports, the polymer was fractionated to isolate higher molecular weight portions. High molecular weight polymer is necessary to meet the mechanical requirements of such membranes. Once isolated, the high molecular weight polymer was then re-dissolved and subsequently cast into a thin film. These films were then thoroughly dried and washed with water to remove any trace of solvent. Once the solvent was sufficiently removed, the films were then soaked in a phosphoric acid bath at a known concentration to produce an imbibed phosphoric acid doped polybenzimidazole membrane. These membranes could be utilized for MEA

fabrication and subsequent fuel cell performance evaluations and device operations. The process of conventional imbibing is depicted in **Figure 1.8**. This process results in phosphoric acid doped polybenzimidazole films with approximately 6 moles of phosphoric acid per mole of polymer repeat unit (PA/RU). Moreover, this multi-step process is time consuming, costly, and requires the use and waste management of large amounts of organic solvents with respect to the amount of material produced.

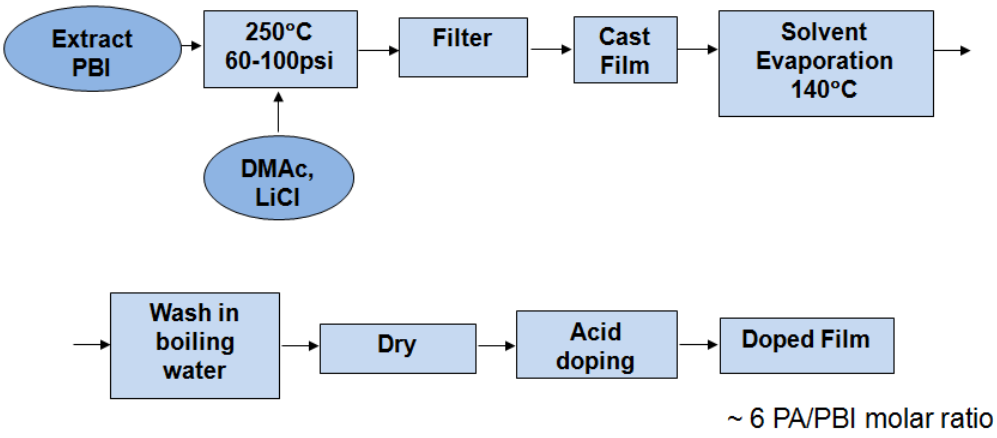

Figure 1.8: Multi-step conventional process for producing phosphoric acid doped polybenzimidazole membranes for high-temperature fuel cell applications

An alternative more direct method of developing phosphoric acid doped polybenzimidazole membranes was later developed by our research group (Benicewicz et al.). This process was termed the PPA process[106] and successfully produces phosphoric acid doped polybenzimidazole membranes with much higher acid loadings that the previously described conventional imbibing method. In addition to higher acid loadings, the membranes developed by the PPA process exhibit improved mechanical properties and fuel cell performances when compared to conventionally imbibed membranes.[106]

In the PPA process, polyphosphoric acid is utilized as a polymerization solvent and condensation agent for the reaction of tetraamines and diacids. As these functionalities react to form oligomer and subsequent polymer units, water is produced as the condensation product. Polyphosphoric acid absorbs the water, helping to shift the reaction equilibrium to the formation of product. As previously mentioned, polyphosphoric acid is an excellent solvent for the polymerization of high molecular weight polybenzimidazole. Once polymerized, the polymer solution is directly cast onto glass plates at temperatures upward of 220˚C. Since polyphosphoric acid and polybenzimidazole are both hygroscopic, water is absorbed from the atmosphere or surrounding environment. This results in hydrolysis of polyphosphoric acid into phosphoric acid. In contrast to polyphosphoric acid being a good solvent for polybenzimidazole, phosphoric acid is not. The hydrolysis of the solvent results in an arrested precipitation of polybenzimidazole, and has been described as a solution-to-gel or sol-to-gel state transition. Our observations of the PPA process are summarized in **Figure 1.9**.

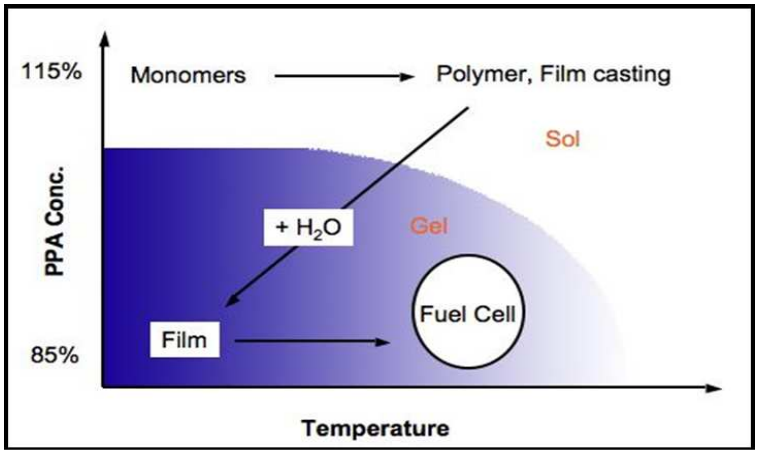

Figure 1.9: State diagram of the PPA process[106]

Experimental evaluation of the PPA process has revealed a window of gel stability of these films. This is depicted in **Figure 1.9** as the shaded region. If the temperature of the material is raised high enough, the gel membrane will revert back to a solution state. This is due to the solubility of PBI in phosphoric acid increasing with increased temperature. It should be noted that this gel-to-sol transition generally occurs at temperatures greater than 200˚C and is not problematic when considering these materials for high temperature PEM fuel cell operations which typically employ operational temperatures between 120˚C and 180˚C. It should also be noted that the above mentioned window of gel stability changes with variation of chemical structure and functionality of polybenzimidazoles.

1.4 Scope of Research

The overall goal of the work presented within this thesis is to investigate, understand, and develop structure-property relationships in regards to polymer structure, membrane stability, and device performance. Previous work has shown that material properties such as acid loading, proton conductivity, mechanical integrity, and device performance can be attributed to polymer structure, chemical functionality, and polymer architecture (homo, random, co-polymer etc.). Developing and understanding these relationships is critical to the advancement of fuel cell technology. Within this thesis, several of these relationships are investigated and reported.

With the abundance of synthetic knowledge available today, the possibilities of monomer combinations and compositional ratios of new PBIs are theoretically endless. Novel polymers and copolymer systems have been developed in this research and have significantly progressed the understanding of polybenzimidazole chemistries. The

research reported herein contributes to the ever-developing pool of knowledge regarding polybenzimidazole chemistry and material applications.

Extensive work has been done concerning polymer structural design and investigation with regards to sequence isomerism through the design, synthesis, and utilization of novel monomer compounds. A novel diacid monomer, 2,2'-bisbenzimidazole-5,5'-dicarboxylic acid (BBDCA), was synthesized and polymerized with 3,3',4,4'-tetraaminobiphenyl (TAB) to prepare a polymer, termed i-AB-PBI, that was composed of repeating 2,5-benzimidazole units. The i-AB-PBI incorporates head-to-head, tail-to-tail, and head-to-tail benzimidazole orientations. This is in contrast to the previously known AB-PBI which incorporates only head-to-tail benzimidazole sequences. AB-PBI was first developed in the early 1950s and has been extensively studied by numerous research groups.[107-111] Until this work, no other AB-type polybenzimidazole existed. AB-type polybenzimidazoles are fundamental in the family of polybenzimidazoles because they only incorporate the benzimidazole motif, i.e. no other spacer or functionality is incorporated in the polymer structure. Development of this innovate sequence isomer, i-AB-PBI, provided an opportunity to study the effects of sequence isomerism in a fundamental polybenzimidazole for the first time. These polymers were synthesized and characterized in terms of molecular weight, membrane composition, ionic conductivity, thermal, mechanical, and fuel cell performance properties. Thorough investigations of the new sequence isomer revealed significant changes and improvements in the material's properties when compared to that of the known AB-PBI. A detailed report of this study is presented in Chapter 3 of this thesis, as reported in the Journal of Polymer Science.[112]

This work was further advanced by the study of the AB-PBI and i-AB-PBI random copolymer system. The random copolymer system of these polymers, termed r-AB-PBI, is unique in that the chemical structure and functionality does not change across the copolymer compositional spectrum. The r-AB-PBI copolymer system introduces a sequence distribution effect with regards to benzimidazole orientation, as well as randomization of benzimidazole sequence between two well-defined sequenced AB-type polymers. This unique copolymer system provided insights into how properties of fundamental polybenzimidazole polymers are affected with regards to sequence distribution and orientation. Moreover, non-intuitive results were obtained in regards to solubility effects, glass transition (Tg) effects, and thermal stabilities of these polymers. These polymers were synthesized and characterized in terms of molecular weight, membrane composition, ionic conductivity, thermal, mechanical, and fuel cell performance properties. Detailed investigations in this work led to the understanding of how ordered polybenzimidazole structure properties are affected through benzimidazole sequence distribution and randomization. A detailed report of the unique r-AB-PBI system is described in Chapter 4 of this thesis, as reported in the Journal of Polymer Science.[113]

Another set of random copolymers was developed that incorporates the AB-type polybenzimidazoles and a para-phenyl-polybenzimidazole (p-PBI). p-PBI is a high performance, commercially produced polybenzimidazole that has been thoroughly studied due to its significantly desired properties in terms of fuel cell applications. AB-PBI and p-PBI random copolymers were developed and compared to random copolymers of i-AB-PBI and p-PBI. The unique combination and contrast of properties in the phenyl-

AB and phenyl-iAB systems provided insight into effects resulting from structural modification, sequence orientation, stability diversity, and randomization. The p-PBI and AB-PBI copolymer system addresses aspects of acid loading, stability, and structural modification, whereas the p-PBI and i-AB-PBI system addresses comparisons of sequence isomerism and randomization between two high performance PEM materials. The comparative evaluation of both copolymer systems provided greater insight and applicability to PEM material design than analysis of either system alone. All copolymer materials were characterized in terms of molecular weight, membrane composition, mechanical properties, ionic conductivities, and fuel cell performances. A detailed report of these copolymer systems and insights gained thereof are described in Chapter 5 of this thesis, as reported in the Journal of Polymer Science.[114]

Work in regards to expanding the electrochemical device applications of PBI materials was conducted. A sulfonated polybenzimidazole membrane (s-PBI) doped with sulfuric acid was utilized for the first time in an all-Vanadium redox flow battery (VRFB). In contrast to fuel cells, which are energy conversion devices, VRFB systems are energy storage devices. Energy storage is key to the utilization of large-scale renewable energy from solar, wind, and thermal resources. This is the first reported utilization of polybenzimidazole in an energy storage device. Performance investigations of s-PBI in a VRFB were conducted and compared to Nafion 117, and Nafion 212. Nafion materials are currently the industrial standards for VRFB applications. The PBI membranes were found to have comparable and improved performance properties when compared to the Nafion materials. The s-PBI membranes were characterized in terms of molecular weight, ionic conductivity, mechanical properties, membrane composition, and

overall VRFB performances under a variety of conditions. A detailed report of this work is provided in Chapter 6 of this thesis, as reported in the Journal of Power Sources.[115]

Other work regarding the expansion of electrochemical device applications for polybenzimidazoles was conducted. A sulfonated polybenzimidazole (s-PBI) membrane doped with sulfuric acid was utilized in the Hybrid Sulfur Electrolyzer. The Hybrid Sulfur Electrolyzer is an electrochemical energy conversion device that produces pure hydrogen and has significant large scale applications in nuclear power plants by utilizing the thermal output of the reactors that is currently discarded in cooling towers. This work is the first report of a polybenzimidazole material being utilized in a Hybrid Sulfur Electrolyzer. Extensive research was conducted regarding device performance under a variety of conditions. All s-PBI membranes were conditioned through an acid exchange process, verified by titration, and characterized in terms of molecular weight, membrane composition, mechanical properties, ionic conductivity, and overall device performance. The s-PBI utilized in the Hybrid Sulfur Electrolyzer was compared to Nafion 117 and Nafion 112. Nafion derivatives were the only materials utilized for this electrochemical device prior to this work. s-PBI was found to have comparable properties to the Nafion materials studied. Moreover, utilizing s-PBI allowed for high-temperature device operations that cannot be achieved using Nafion materials. Prior to this work, high-temperature device operation of a Hybrid Sulfur Electrolyzer had not been reported. A detailed overview of this work is reported in Chapter 7 of this thesis, as reported in ECS Electrochemistry Letters[116] and the Journal of Power Sources.[117]

In addition to developments of novel PBI chemistries and device applications, extensive work was conducted towards the development of a new solution

polymerization method for PBI materials. Prior to this work, polymerization of high-molecular weight polybenzimidazole in an organic solvent had not been reported. PBI is produced commercially through two processes, the PPA process[106] which utilizes polyphosphoric acid to produce gel membranes doped with phosphoric acid, and one involving a combination melt-solid-phase polymerization which is non-homogenous. The limited methods of development available are a direct result of the poor solubility of polybenzimidazoles. The work conducted in this thesis resulted in a viable solution polymerization method of PBI in dimethylacetamide (DMAc). Through investigation of a series of monomer functionalities, a bisulfite adduct derivative of isophthalaldehyde was developed which allowed for the synthesis of high-molecular weight PBI in DMAc at high concentrations. This work was an extension of previous attempts made in the early 1970s by Marvel and Higgins.[118] Their work utilized this monomer functionality, however failed to produce high-molecular weight PBI. The key to success with this solution process was discovered through polymerization concentration studies. High-molecular weight PBI was produced only at very high reaction concentration conditions, not previously explored. This work has been patented, and provides a practical synthetic avenue for the synthesis of a multitude of polybenzimidazole derivatives. PBI developed from this process was characterized in terms of NMR, IR, DSC, TGA, and molecular weight. A detailed overview of this work is reported in Chapter 8 of this thesis, as reported in the Journal of Polymer Science.[119]

1.5 References

1. Energy Statistics: http://visual.ly/world-total-primary-energy-consumption-quadrillion-btu (accessed Nov. **2013**).

2. Energy Statistics: http://business.financialpost.com/2013/07/25/fossil-fuels-to-remain-dominant-as-global-energy-use-set-to-rise-56-eia/?__lsa=2816-3b9a (accessed Nov. **2013**).
3. Energy Statistics: http://www.peakoilproof.com/2013_10_01_archive.html (accessed Nov. **2013**).
4. Curzon, F. L.; Ahlborn, B. *American Journal of Physics* **1975**, *43*,(1), 22-24.
5. Alternative Energy: *Alternative Energry Solutions for the 21st Century*. **2011**. http://www.altenergy.org.
6. World Primary Energy Production by Source. *Annual Energy Review*, U.S. Energy Information Administration, **2008**. http://www.eia.doe.gov/emeu/aer/pdf/pages/sec11_2.pdf.
7. Grove, W. R. *Philos. Mag.* **1839**, *14*, 127-130.
8. Fuel Cell Technology Handbook. Ed.; Hoogers, G. CRC Press LLC, **2003**.
9. Appleby, A. J. *Journal of Power Sources* **1990**, *29*, 3-11.
10. Bacon, F. T. *Electrochimica Acta* **1969**, *14* (7), 569-585.
11. Perry, M. L.; Fuller, T. F., *Journal of the Electrochemical Society* **2002**, *149* (7), S59-S67.
12. Gibbs, W. J. *Transactions of the Connecticut Academy of Arts and Sciences* **1873**, *2* (14), 382-404.
13. Hamnett, A. *Handbook of Fuel Cells*, **2003**, *Vol. 1*, 37-43.
14. Energy Efficiency and Renewable Energy. www.doe.gov. (accessed Nov. 2013).
15. Larminie, J.; Dicks, A. *Fuel Cell Systems Explained*, 2nd ed. Wiley, **2003**, *Vol. 1*, 25-43.
16. Carter, D.; Wing, J. *The Fuel Cell Industry Review 2013*, Fuel Cell Today, **2013**, 1-45.
17. Battery Manufacturing Market Research Report, NAICS 33591, Nov. **2013**. (no author listed)
18. First Element Energy: *Fuel Cell Basics*. First Element Energy LLC. **2010**.
19. Voss, D. *A Fuel Cell in Your Phone*, MIT Technology Review. **2001**, 1-4.
20. Kamitani, A.; Morishita, S.; Kotaki, H.; Arscott, S. *Journal of Micromechanics and Microengineering* **2008**, *18*, 125019-125028.
21. Fuel Cell Today: History. www.fuelcelltoday.com/about-fuel-cells/history **2014**.
22. National Renewable Energy Laboratory, US Department of Energy: *Hydrogen and Fuel Cell Research*. www.NREL.gov/hydrogen/proj_fc_market_demo.html **2013**. (accessed Dec. 2013)
23. Scientific computing world: Fuel for thought on cars of the future. www.scientific-computing.com/features/feature.php?feature_id=126 (accessed Jan. 2014)
24. National Institute of Standards and Technology (NIST): PEM Fuel Cells. www.physics.nist.gov/MajResFac/NIF/pemFuelCells.html (accessed Jan. 2014)
25. Wolfgang E. M.; Weston, C. K. *Composition and thermodynamic properties of air in chemical equilibrium*. Washington National Advisory Committee for Aeronautics **1958**, *No. NACA-TN-4265*, 1-39.
26. Steck, A. E. *Membrane Materials in Fuel Cells*. New materials for fuel systems I: proceedings of the First International Symposium on New Materials for Fuel Cell Systems, Montreal, Quebec, Canada. **1995**. p.74.

27. Heitner-Wirguin, C. *Journal of Membrane Science* **1996**, *120*, 1-33.
28. Eisman, G. A. *Journal of Power Sources* **1990**, *29*, 389-398.
29. Gierke, T. D.; Munn, G. E.; Wilson, F. C. J. *Polym. Sci. Part B: Polym. Phys.* **1981**, *19*, 1687-1704.
30. Grotthuss, C. J. T. *Ann. Chim.* **1806**, *58*, 54-73.
31. Agmon, N. *Chem. Phys. Lett.* **1995**, *244*, 456-452.
32. Nguyen, V. T.; White, R. E. *Journal of The Electrochemical Society* **1993**, *140*, 2178-2186.
33. Yeager, H. J.; Eisenberg, A. *ACS Symp. Ser., American Chemical Society: Washington DC* **1982**, *No. 180*, 41-63.
34. Ekstrom, H.; Lafitte, B.; Ihonen, J.; Markusson, H.; Jacobsson, P.; Lundblad, A.; Jannasch, P.; Lindbergh, G. *Solid State Ionics* **2007**, *178*, 959-966.
35. Qian, G.; Benicewicz, B. C. *ECS Transactions* **2011**, *41*, 1441-1448.
36. Jannasch, P. *Curr Opin Colloid Interface Sci.* **2003**, *8*, 96-102.
37. Mauritz, K. A.; Storey, R. F.; Jones, C. K. *ACS Symp. Ser.* **1989**, *395*, (multiphase Polym.: Blends Ionomers), 401-417.
38. Miyake, N.; Wainright, J. S.; Savinell, R. F., *J. Electrochem. Soc.* **2001**, *148*, A898-A904.
39. Aparicio, M.; Damay, F.; Klein, L. C., *J. Sol-Gel Sci. Technol.* **2003**, *26*, 1055-1059.
40. Mikhailenko, S. D.; Zaidi, S. M. J. *Journal of Polymer Science, Part B: Polymer Physics* **2000**, *38*, 1386-1395.
41. Bonnet, B.; Jones, D. J.; Roziere, J.; Tehicaya, L.; Alberti, G.; Casciola, M.; Massinelli, L.; Bauer, B.; Peraio, A.; Ramunni, E. *J. New Mater. Electrochem. Syst.* **2000**, *3*, 87-92.
42. Alberti, G.; Casciola, M. *Annual Review of Materials Research* **2003**, *33*, 129-154.
43. Yamaguchi, t.; Miyata, F.; Nakao, S., I. *Journal of Membrane Science* **2003**, *214*, 283-292.
44. Arico, A. S.; Baglio, V.; Di Blasi, A.; Creti, P.; Antonucci, P. L.; Antonucci, V. *Solid State Ionics* **2003**, *161*, 251-265.
45. Mader, J.; Xiao, L.; Schmidt, T. J.; Benicewicz, B. C. *Adv Polymer Sci*. **2008**, *216*, 63-124.
46. Munson, R. A. *J. Phys. Chem.* **1964**, *68*, 3374-3377.
47. Dippel, T.; kreuer, K. D.; Lassègues, J. C.; Rodriguez, D. *Solid State Ionics* **1993**, *61*, 41-46.
48. Greenwood, N. N.; Thompson, A. *J. Chem. Soc.* **1959**, 3485-3492.
49. Munson, R. A. *J. Phys. Chem.* **1964**, *68*, 3374-3377.
50. Chin, D. T.; Chang, H. *J. Appl. Electrochem.* **1989**, *19*, 95-99.
51. Tanaka, R.; Yamamoto, H.; Kawamura, S.; Iwase, T. *Electrochim. Acta* **1995**, *40*, 2421-2424.
52. Tanaka, R.; Yamamoto, H.; Shono, A.; Kubo, K.; Sakuri, M. *Electrochem. Acta* **2000**, *45*, 1385-1389.
53. Przyluski, J.; Zalewska, A.; Maron, J.; Wieczorek, W. *Pol. J. Chem.* **1997**, *71*, 968-976.

54. Zukowska, G.; Rogowska, M.; Wojda, A.; Zygadlo-Monikowska, E.; Florjanczyk, Z.; Wieczorek, W. *Solid State Ionics* **2000**, *136-137*, 1205-1209.
55. Zukowska, G.; Wieczorek, W.; Kedzierski, M; Florjanczyk, Z. *Solid State Ionics* **2001**, *144*, 163-173.
56. Narayanan, S. R.; Yen, S. P.; Liu, L.; Greenbaum, S. G. *J. Phys. Chem. B* **2006**, *110*, 3942-3948.
57. Li, Q.; jensen, J. O.; Savineli, R. F.; Bjerrum, N. J. *Progress in Polymer Science* **2009**, *34*, 449-477.
58. Wainright, S. J.; Wang, J. T.; Savinell, R. F.; Litt, M. *J. Electrochem. Soc.* **1995**, *142*, L121-L123.
59. Staiti, P.; Minutoli, M.; Hocevar, S. *J. Power Sources* **2000**, *90*, 231-235.
60. Li, Q.; Hjuler, H. A.; Bjerrum N. J. *J. Appl. Electrochem.* **2001**, *31*, 773-779.
61. Jayakody, J.R.P.; Chung, S. H.; Duantino, L.; Zhang, H.; Xiao, L.; Benicewicz, B.C.; Greenbaum, S. G. *J. Electrochem. Soc.* **2007**, *154*, B242-B246.
62. Wainright, J. S.; Wang, J. T.; Savinell, R. F.; Litt, M.; Moaddel, H.; Rogers, C. *Proceedings of the Electrochemical Society* **1994**, *94*, 255-64.
63. Gilham J. K.; *Science* **1963**, *139*, 494-495
64. Strauss, E. L. *Polymer Eng. Sci.* **1966**, *6*, 24-29.
65. Weng, D.; Wainright, J. S.; Landau, U.; Savinell, R. F. *Proceedings of the Electrochemical Society* **1995**, *95-23*, 214-225.
66. Hill, J. R. *Adhesives Age* **1966**, *9*, 32-36.
67. Delman, A. D.; Kovacs, h. N.; Simms, B. B. *Journal of Polymer Science, Part A-1: Polymer Chemistry* **1968**, *6*, 2117-2126.
68. Wang, J. T.; Savinell, R. F.; Wainright, J.; Litt, M.; Yu, H. *Electrochim. Acta* **1996**, *41*, 193-197.
69. Wang, J. T.; Wainright, J. S.; Savinell, R. F.; Litt, M. *J. Appl. Electrochem.* **1996**, *26*, 751-756.
70. Szita, J.; Marvel, Carl S. *Journal of Applied Polymer Science* **1970**, *14*, 2019-2024.
71. Korshak, V. V.; Teplyakov, m. M.; Fedorova, R. D. *Journal of Polymer Science, Part A-1: Polymer Chemistry* **1971**, *9*, 1027-1043.
72. Bingham, M. A.; Hill, B. J. *Journal of Thermal Analysis* **1975**, *7*, 347-358.
73. Wang, J. T.; Wasmus, S.; Savinell, R. F. *J. Electrochem. Soc.* **1996**, *143*, 1233-1239.
74. Hilado, C. J.; LaBossiere, L. A.; Leon, H. A.; Kourtides, D. A.; Parker, j. A.; Hsu, M. S. *Journal of Combustion Toxicology* **1976**, *3*, 211-236.
75. Kovar, R. F.; Arnold, F. E. *Journal of Polymer Science, Polymer Chemistry Edition* **1976**, *14*, 2807-2817.
76. Chatfield, D. A.; Einhorn, I. N. *Journal of Polymer Science, Polymer Chemistry Edition* **1981**, *19*, 601-618.
77. Weng, D.; Wainright, J. S.; Landau, U.; Savinell, R. F. *J. Electrochem. Soc.* **1996**, *143*, 1260-1263.
78. Xing, B.; Savadogo, O. *J. New Mater. Electrochem. Syst.* **1999**, *2*, 95-101.
79. Savadogo, O.; Xing, B. *J. New Mater. Electrochem. Syst.* **2000**, *3*, 343-347.
80. Li, Q. F.; Niels, J. B. *Dianchi* **2002**, *32*, 174-177.

81. Asensio, J. A.; Borros, S.; Gomez-Romero, P. *Electrochem. Commun.* **2003**, *5*, 967-972.
82. Coffin, D. R.; Serad, G. A.; Hicks, H. L.; Montgomery, R. T. *Textile Research Journal* **1982**, *52*, 466-472.
83. Carothers, W. *Trans . Faraday Soc.* **1936**, *32*, 39-53.
84. Berrada, M.; Anbaoui, Z.; Lajrhed, N.; Berrada, M.; Knouzi, N.; Vaultier, M.; Sekiguchi, H.; Carriere, F. *Chem Mater* **1997**, *9*, 1989-1993.
85. Holan, G.; Samuel, E.L.; Ennis, B.C.; Hinde, R. W. *J. Chem Soc, C* **1967**, *1*, 20-25.
86. Brinker, K. C.; Cameron, D. D.; Robinson, I. M. *Linear Polybenzozazoles* 2904537, **1959**.
87. Vogel, H.; Marvel, C. S. *Journal of Polymer Science, Part A: Polymer Chemistry* **1961**, *34*, 511-539.
88. Powers, E. J.; Serad, G. A., *History and Development of Polybenzimidazoles*. Elsevier Applied Science, London, **1986**, 355-73.
89. Chenevey, E. C.; Conciatori, A. B. *Polybenzimidazoles*. 65-517797 3433772, 19651230., **1969**.
90. Coffin, D. R.; Serad, G. A.; Hicks, H. L.; Montgomery, R. T. *Textile Research Journal* **1982**, *52*, 466-472.
91. Buckley, A.; Stuetz, D. E.; Serad, G. A. *Polybenzimidazoles*. Encyclopedia of Polymer Science and Engineering, **1987**, *11*, 572-601.
92. Stuetz, D. E.; DiEdwardo, A. H.; Zitomer, F.; Barnes, B. P. *Journal of Polymer Science, Polymer Chemistry Edition* **1980**, *18*, 987-1009.
93. Chung, T. S. *Polybenzimidazoles*. Plastics Engineering (New York) **1997**, *41* (Handbook of Thermoplastics), 701-731.
94. Chung, T. S. *Journal of Macromolecular Science, Reviews in Macromolecular Chemistry and Physics* **1997**, *C37*, 277-301.
95. Higgins, J.; Marvel, C. S. *Journal of Polymer Science, Part A-1: Polymer Chemistry* **1970**, *8*, 171-177.
96. Hedberg, F. L.; Marvel, C. S. *Journal of Polymer Science, Polymer Chemistry Edition* **1974**, *12*, 1823-1828.
97. Hedberg, F. L.; Marvel, C. S. *Nuova Chimica* **1974**, *50*, 51-54.
98. Neuse, E. W.; Loonat, Ms. S. *Macromolecules* **1983**, *16*, 128-136.
99. Iwakura, Y.; Uno, K.; Imai, Y. *Journal of Polymer Science, Part A: Polymer Chemistry* **1964**, *2*, 2605-2615.
100. Samms, S. R.; Wasmus, S.; Savinell, R. F. *J. Electrochem. Soc.* **1996**, *143*, 1225-1232.
101. Wainright, J. S.; Wang, J. T.; Savinell, R. F. *Proceedings of the Intersociety Energy Conversion Engineering Conference* **1996**, *31st*, 1107-1111.
102. Zecevic, S. K.; Wainright, J. S.; Litt, M. H.; Gojkovic, S. L.; Savinell, R. F. *J. Electrochem Soc.* **1997**, *144*, 2973-2982.
103. Liu, Z.; Wainright, J. S.; Savinell, R. F. *Chem. Eng. Sci.* **2004**, *59*, 4833-4838.
104. Ma, Y. L.; Wainright, J. S.; Litt, M. H.; Savinell, R. F. J. *Electrochem. Soc.* **2004**, *151*, A8-A16.
105. Wainright, J. S.; Staser, J.; Savinell, R. F. *Proceedings of the Electrochimical Society* **2005**, *2002-31*, 440-449.

106. Xiao, L.; Zhang, H.; Scanlon, E.; Ramanathan, S. L.; Choe, E. W.; Rogers, D.; Apple, T.; Benicewicz, B. C. *Chem. Mater.* **2005**, *17*, 5328-5333.
107. Ong, A.; Jung, G.; Wu, C.; Yan, W. *Journal of Hydrogen Energy* **2010**, *35*, 7866-7873.
108. Wannek, C.; Lehnert, W.; Mergel, J. *Journal of Power Sources* **2009**, *192*, 258-266.
109. Hyoung-Juhn, K.; Sung, C.; Sung, J.; Yeong, C.; Ju-Yong, K.; Hae-Kwon, Y.; Ho-Jin, K.; Kyoung, H. *Macromol Rapid Commun.* **2004**, *25*, 894-897.
110. Zheng, H.; Petrik, L.; Mathe, M. *Journal of Hydrogen Energy* **2010**, *35*, 3745-3750.
111. Wippermann, K.; Wannek, C.; Oetjen, H.; Lehnert, W. *Journal of Power Sources* **2010**, *195*, 2806-2809.
112. Gulledge, A. L.; Gu, B.; Benicewicz, B. *Journal of Polymer Science, Part A: Polymer Chemistry* **2012**, *50*, 306-313.
113. Gulledge, A. L.; Chen, X.; Benicewicz, B. *Journal of Polymer Science, Part A: Polymer Chemistry* **2014**, *52*, 619-628.
114. Gulledge, A. L.; Fishel, K.; Bottorff, M.; Benicewicz, B. *Journal of Polymer Science, Part A: Polymer Chemistry* **2014**, In preparation.
115. Gulledge, A. L.; Pezeshki, A.; Sun, C.; Mench, M.; Zawodzinski, T.; Benicewicz, B. *Journal of Power Sources* **2014**, In preparation.
116. Vishnuvarman, J.; Gulledge A. L.; Staser, J.; Benicewicz, B.; Weidner, J. *ECS Electrochemistry Letters* **2012**, *1 (6)*, F44-F48.
117. Gulledge, A. L.; Garrick, T.; Weidner, J. W.; Benicewicz, B. C. *Journal of Power Sources* **2014**, In preparation.
118. Higgins, J.; Marvel, C. S. *Journal of Polymer Science, Part A: Polymer Chemistry* **1970**, *8*,171-177.
119. Gulledge, A. L.; Hoffman, J.; Steckle, W.; Benicewicz, B. *Journal of Polymer Science, Part A: Polymer Chemistry* **2014**, In preparation.

Chapter 2: Experimental

2.1 Materials

Teraphthalic acid was purchaced from Amoco Chemical. Methyl-2,2,2-trichloroacetimidate (98 %) was purchased from Acros Organics and used as-received. TAB monomer, 3,3',4,4'-tetraaminobiphenyl (polymer grade, ~97.5 %) was donated by Celanese Ventures, GmbH (now, BASF Fuel Cell) and used as-received. Polyphosphoric acid (115 % concentration) was purchased from Aldrich and used as received. Phosphoric acid (85 %) and common solvents(e.g., DMSO, MeOH, EtOH etc.) were purchased and used as-received from Fisher Scientific. Vanadium electrolyte solutions were prepared from V(IV) sulfate oxide hydrate (99.9%, metals basis) and sulfuric acid (96%) purchased from Alfa Aesar as well as de-ionized water. CP-ESA carbon paper was obtained from SGL Carbon Group and used as-received. Nafion NR-211 and Nafion 117 membranes were purchased from Ion Power and used as-received. Purification of 3,4-diaminobenzoic acid (DABA) (10 g, Acros, 97 %) was conducted via recrystallization from water/methanol (480 mL/160 mL) using activated carbon yielding pink/tan crystals after vacuum drying, 75 %, m.p. 216.8 ˚C

2.2 Instrumentation and Characterization Techniques

FT-IR spectra were recorded on a Perkin Elmer Spectrum 100 using an attenuated total reflection (ATR) diamond cell attachment. ^{1}H-NMR were recorded using a Varian Mercury 300 spectrometer. Mechanical properties were measured in tension using an Instron 5543A with an extension rate of 5.0 mm/min and were preloaded to 0.1 N @ 3 mm/min using a 250 N load cell.

Inherent viscosity (I.V.) measurements were conducted using a Cannon Ubbelohde (size 200) viscometer at a concentration of 0.2 dL/g in Sulfuric acid (H_2SO_4) at 30.0 ˚C. A small amount of polymer solution was precipitated in water and neutralized with 0.1 N ammonium hydroxide. After thoroughly washing with water, the sample was dried under vacuum overnight at 120 ˚C and then dissolved in H_2SO_4 using a mechanical shaker. Recorded I.V. values are an average of three separate measurements and were calculated as previously reported.[1]

The phosphoric acid contents in the membranes were obtained via titration using a Metrohm 716 DMS Titrino automated titrater and a standardized 0.1 M sodium hydroxide solution following procedures reported previously.[2] Phosphoric acid concentrations were expressed as moles of PA per mole of polymer repeat unit or moles PA per benzimidazole unit.

Ionic conductivities were measured using a quadra-probe alternating current impedance method which utilized a Zahner IM6e spectrometer operating in the frequency range of 1 Hz to 100 kHz. A rectangular section of the polymer membrane was cut with the dimensions of 3.5 cm x 7.0 cm and was placed into a glass cell connected to four platinum wire current collectors. Current was supplied to the cell through two outer electrodes which were set 6.0 cm apart, while the potential drop was measured by two inner electrodes which were set 2.0 cm apart. The inner and outer electrodes of the glass cell were positioned on alternating sides of the polymer membrane to obtain through-plane bulk measurements of ionic conductivity. A programmable oven was used to house the cell so that a measure of the temperature dependence of the proton conductivity for the cell could be obtained. Two series of measurements of the conductivity were

conducted subsequently. The first series of measurements were conducted from ambient temperature to 180 ˚C, at intervals of 20 ˚C, with a 15 min pause at each temperature interval for thermal equilibrium prior to measurement. The second series of measurements were subsequently conducted in the same manner to obtain the ionic conductivity of the membranes under anhydrous conditions. A Nyquist Plot was constructed to fit the experimental curve of the resistance across the frequency range. The conductivities were calculated at different temperatures from the membrane resistance obtained using **Equation 2.1**:

$$\textbf{Eq 2.1} \qquad \sigma = \frac{D}{(W*T*R)}$$

where σ is the ionic conductivity, R is the resistance measured, W and T are the width and thickness of the membrane respectively, and D is the distance between the two inner electrodes.

Membrane Electrode Assembly (MEA) Fabrication and Fuel Cell Testing

MEA's were fabricated by hot pressing a membrane (~20 % compression) sample between two platinum doped carbon electrodes, and were 50 cm^2 in area (45.15 cm^2 active area). Gas diffusion electrodes, with a platinum loading of 1.0 mg/cm^2, were obtained from BASF Fuel Cell. A Kapton framework was also incorporated to add stability to the MEA, and to allow handling without damaging the MEA. The MEA was placed into a single-cell fuel cell apparatus for testing. The gas flow plates used were graphite with duel gas channels on the anode and triple gas channels on the cathode. Steel endplates were used to clamp the gas flow plates together. Heating pads were attached to the steel plates to regulate and monitor temperature. A commercially available fuel cell testing station (Fuel Cell Technologies, Inc.) equipped with mass flow regulators was

used to conduct and record measurements. Stoichiometric gases were supplied to the anode and cathode at a stoichiometric ratio of 1.2 and 2.0 respectively, without applied backpressure. Fuel/oxidant studies were performed with hydrogen gas, oxygen gas, and reformate gas, all without humidification. The composition of reformate gas used consisted of approximately 70 % hydrogen, 28 % CO_2, and 2 % CO.

Dynamic Mechanical Analysis

Glass transition (T_g) analysis was conducted using a dynamic mechanical thermal analyzer (DMA) (TA Instruments, model ARES-RSA3). Polymer films cast from PPA solution were heated (~60˚C) and stirred in deionized water for several days to remove the internal PA of the film. The pH of the water was monitored and water exchange was conducted over the duration of preparation until a neutral pH was observed. Polymer films of 35mm X 6mm X 1.5mm (L X W X T), were cut and hot pressed at 140˚C for approximately 1.5 h. Samples were then clamped on the film tension clamp of the pre-calibrated instrument. Scans were conducted from 300˚C to 550˚C at a heating rate of 5˚C/min. The storage modulus (E'), loss modulus (E") and tan δ values were measured at a constant frequency of 1Hz, using autotension with an initial strain of 0.08% and initial static force of 20g.

2.3 Experimental Procedures Pertaining to Chapter 3

Polymerization of Poly(2,5-benzimidazole) (AB-PBI)

Poly(2,5-benzimidazole) (AB-PBI) was prepared using the following method: Purified 3,4-diamino benzoic acid (3 g) and polyphosphoric acid (97 g) were added to a 100mL reactor. The reactor was equipped with a three neck reactor head, mechanical stirrer, nitrogen inlet/outlet and placed into a silicone oil bath with a ramp/soak

temperature controller. The polymerization began with an initial temperature of 60 ˚C and was raised to 140 ˚C over a period of 1 h. The temperature remained at 140 ˚C for 2 h to ensure all monomer was dissolved. Once the monomer had dissolved, the temperature was increased step-wise until a final polymerization temperature of 220 ˚C was obtained. Typically the polymerization reaction time at 220 ˚C was between 24-36 h, depending on the viscosity of the polymer. The Weisenberg effect was observed during the later stages of the polymerization causing the solution to climb up the stirrer. When this was observed, phosphoric acid (85 %) was added to the reaction mixture to adjust the viscosity of the solution for film casting. Analysis: ^{1}H-NMR (400 MHz, DMSO-d6) δ 6.7-7.3 (broad multiplet, aromatics, 3H).

Preparation of 2,2'-bisbenzimidazole-5,5'-dicarboxylic acid (BBDCA)

To a 1000 mL round bottom flask, purified DABA (10 g, 0.066 mol), and methanol (250 mL) were added. The mixture was then placed into an explosion proof refrigerator and cooled at 10 ˚C for approximately 20-30 min. The flask was removed from the refrigerator and methyl-2,2,2-trichloroacedimidate (4.1 mL, 0.033 mol) was immediately added drop-wise (~5 min) with stirring. After the addition was completed, the reaction flask was placed into a preheated oil bath at a temperature of 50 ˚C for 24 h. A dark orange precipitate was obtained which was filtered and washed with ethanol several times, during which the product became increasingly lighter in color. The crude product was dried at 120 ˚C overnight under vacuum.

The light orange crude product described above (5.89 g) was dissolved in approximately 200 mL of heated DMSO, followed by the addition of hot water until the solution became slightly cloudy. A yellow precipitate was obtained upon cooling to r.t.

which was filtered and washed with cold ethanol. The product was dried at 220 ˚C under vacuum to obtain a yellow powder (4.112 g, 69.8 % yield). Analysis: FT-IR: 1671m, 1625m, 1595w, 1497w, 1312s, 1295s, 1206m, 942m, 769s, 746s, 674m cm^{-1}. ^{1}H-NMR (300 MHz, DMSO-d6) δ 13.98 (s, NH), 12.86 (s, COOH), 8.325 (s, 1H), 8.159 (s, 1H), 7.94-7.63 (m, 2H), 7.63-7.60 (d, 1H, J=8.1).Elemental analysis: Calcd. for $C_{16}H_{10}N_4O_4$: C, 59.63; H, 3.13; N, 17.38. Found: C, 59.42; H, 3.23; N, 17.30.

Polymerization of New Isomeric Poly(2,5-benzimidazole) (i-AB-PBI)

In a typical polymerization procedure 3,3',4,4'-tetraaminobiphenyl (1.828 g), polyphosphoric acid (70 g), and 2,2'-bisbenzimidazole-5,5'-dicarboxylic acid (2.75 g) were added to a 100 mL reactor. The reactor was then equipped with a three neck reactor head, a stir rod attached to an overhead stirrer and a nitrogen inlet/outlet. A slow nitrogen flow of approximately 1 bubble every 2 seconds was established and monitored with an oil filled bubbler. The reactor was placed into an oil bath that was regulated using a temperature controller with ramp and soak features. The polymerization utilized the ramp/soak profile as follows:

An initial temperature of 60 ˚C was used, and the temperature was raised to 140 ˚C over a period of 1 h. The temperature remained at 140 ˚C for 2 h and was then increased to 180 ˚C over a period of 30 min. The temperature remained at 180 ˚C for 10 h, and was then increased to 220 ˚C in a period of 30 min. The reaction remained at 220 ˚C for the duration of the polymerization. Twenty hours was the typical duration of polymerization for the new sequence isomer (*i*-AB-PBI). At the end of 20 h the solution was very viscous and phosphoric acid (~15 mL) was back-added to adjust the viscosity

for casting. Analysis: ^{1}H-NMR (400 MHz, DMSO-d6) δ 6.7-7.3 (broad multiplet, aromatics, 3H), 8.2 (singlet, 1H), 8.5 (multiplet, 2H).

Polymer Electrolyte Membrane Preparation

Once an appropriate polymer viscosity was obtained, the solution was directly cast at 220 ˚C onto glass plates for membrane preparation. A heated metal casting blade (120 ˚C) with a casting thickness of 20 mil (508 μm) was used. After casting, the glass plates were separated and samples were placed into a humidification chamber maintained at a relative humidity of 55 % at 25 ˚C. The polymer samples were allowed to hydrolyze overnight. Hydrolysis of the PPA to PA induced a sol-to-gel transition that resulted in a gel membrane. The samples were then sealed in 3 mil (76.2 μm) thick polyethylene bags until testing or membrane electrode assembly (MEA) fabrication.

2.4 Experimental Procedures Pertaining to Chapter 4

Polymerization of Random AB-PBI copolymers

In a typical polymerization procedure, 2,2'-bisbenzimidazole-5,5'-dicarboxylic acid, 3,3',4,4'-tetraaminobiphenyl, 3,4-diaminobenzoic acid, and PPA were reacted on a 15mM scale with various ratios dependent upon the targeted composition. Monomer concentrations in PPA were adjusted to reflect the homopolymer closest in composition to the targeted ratio. Monomers were then added to a 100 mL reactor. The reactor was then equipped with a three neck reactor head, a stir rod attached to an overhead stirrer and a nitrogen inlet/outlet. A slow nitrogen flow was established and monitored through an oil filled bubbler. The reactor was placed into an oil bath that was regulated using a temperature controller with ramp and soak features. The polymerization utilized the ramp/soak profile as follows:

An initial temperature of 60 ˚C was used, and the temperature was raised to 140 ˚C over a period of 1 h. The temperature remained at 140 ˚C for 2 h and was then increased to 180 ˚C over a period of 30 min. The temperature remained at 180 ˚C for 10 h, and was then increased to 220 ˚C in a period of 30 min. The reaction remained at 220 ˚C for the duration of the polymerization. Twenty four to thirty six hours was the typical duration of polymerization for the random copolymers. At the end of polymerization, phosphoric acid (~15 mL) was back-added to the extremely viscous solutions to adjust the viscosity for subsequent membrane casting. Analysis: ^{1}H-NMR (400 MHz, DMSO-d6) δ 7.2-8.2 (broad multiplet, aromatics, 3H), 8.4 (singlet, 1H), 8.5 (multiplet, 2H).

Polymer Electrolyte Membrane Preparation

After adjusting the viscosity with phosphoric acid, the polymer solution was directly cast at 220 ˚C onto heated (120 ˚C) glass plates for membrane preparation. A heated metal casting blade (120 ˚C) with a casting thickness of 20 mil (508 μm) was used. After casting, the glass plates were separated and samples were placed into a humidification chamber maintained at a relative humidity of 55 % at 25 ˚C. The polymer solutions were allowed to hydrolyze overnight. Hydrolysis of the PPA to PA induced a sol-to-gel transition that resulted in a Flory type 3 gel membrane.[3] The samples were then sealed in 3 mil (76.2 μm) thick polyethylene bags until testing or membrane electrode assembly (MEA) fabrication.

Membrane Electrode Assembly (MEA) Fabrication and Fuel Cell Testing

MEA's were fabricated by hot pressing a membrane (~20 % compression) sample between two platinum doped carbon electrodes, and were 50 cm^2 in area (45.15 cm^2 active area). Gas diffusion electrodes, with a platinum loading of 1.0 mg/cm^2 on each

electrode, were obtained from BASF Fuel Cell. A Kapton framework was also incorporated to add stability to the MEA, and to allow handling without damaging the MEA. The MEA was placed into a single-cell fuel cell apparatus for testing. The gas flow plates used were graphite with dual gas channels on the anode and triple gas channels on the cathode. Steel endplates were used to clamp the gas flow plates together. Heating pads were attached to the steel plates to regulate and monitor temperature. A commercially available fuel cell testing station (Fuel Cell Technologies, Inc.) equipped with mass flow regulators was used to conduct and record measurements. Stoichiometric gases were supplied to the anode and cathode at a stoichiometric ratio (hydrogen and air) of 1.2 and 2.0 respectively, without applied backpressure. Fuel/oxidant studies were performed without humidification.

2.5 Experimental Procedures Pertaining to Chapter 5

Polymerization of AB-PBI/p-PBI random copolymers

A typical polymerization procedure for AB-PBI/p-PBI copolymer synthesis is as follows: 3,4-diaminobenzoic acid (DABA), 3,3',4,4'-tetraaminobiphenyl (TAB), terephthalic acid (TA), and PPA (116%) were reacted on a 15mM scale with various molar ratios dependent upon the targeted copolymer composition. Monomer concentrations in PPA were adjusted to reflect the homopolymer closest in composition to the targeted ratio. Monomers were then added to a 100mL kettle reactor. The reactor was then equipped with a three neck reactor head, a stir rod, and a nitrogen inlet/outlet. Once assembled, the reactor was clamped together using a 3 bolt metal clap holder, and connected to an overhead mechanical stirrer. A slow nitrogen flow was established and monitored through oil filled bubblers. The reactor was then lowered into an oil bath that

was thermally regulated using a temperature controller with ramp and soak features. The polymerization utilized the ramp/soak profile as follows:

An initial heating began at room temperature and the temperature was raised to 140 ˚C over a period of 1 h. The temperature remained at 140 ˚C for 2 h and was then increased to 180 ˚C over a period of 30 min. The temperature remained at 180 ˚C for 10 h, and was then increased to 195 ˚C in a period of 30 min. The oil bath temperature remained at 195 ˚C for the duration of the polymerization. Twenty four to thirty six hours was the typical duration of polymerization for the random copolymers. At the end of polymerization, phosphoric acid (~15 mL) was back-added to the extremely viscous solutions to adjust the viscosity for subsequent membrane casting.

Polymerization of i-AB-PBI/p-PBI random copolymers

A typical polymerization procedure for the i-AB-PBI/p-PBI random copolymers is as follows: 2,2'-bisbenzimidazole-5,5'-dicarboxylic acid (BBDCA), 3,3',4,4'-tetraaminobiphenyl (TAB), terephthalic acid (TA), and PPA (116%) were reacted on a 15mM scale with various molar ratios dependent upon the targeted copolymer composition. Monomer concentrations in PPA were adjusted to reflect the homopolymer closest in composition to the targeted ratio. Monomers were then added to a 100mL kettle reactor. The reactor was then equipped with a three neck reactor head, a stir rod, and a nitrogen inlet/outlet. Once assembled, the reactor was clamped together using a 3 bolt metal clap holder, and connected to an overhead mechanical stirrer. A slow nitrogen flow was established and monitored through oil filled bubblers. The reactor was then lowered into an oil bath that was thermally regulated using a temperature controller with ramp and soak features. The ramp/soak profile utilized for i-AB-PBI/p-PBI copolymers is

the same as the procedure described for the polymerization of AB-PBI/p-PBI copolymers, however, a final polymerization temperature of 220˚C was used.

Polymer electrolyte membrane formation

Once polymerized, random copolymer solutions were heated to 220˚C to adjust solution viscosity for casting. Solutions were then directly cast onto heated (120 ˚C) glass plates for membrane preparation. A heated metal casting blade (120 ˚C) with a casting thickness of 20 mil (508 μm) was used. After casting, the glass plates were separated and samples were placed into a humidification chamber maintained at a relative humidity of 55 % at 25 ˚C. The polymer solutions were allowed to hydrolyze overnight. Hydrolysis of the PPA to PA induced a sol-to-gel transition that resulted in a Flory type 3 gel membrane.[3] The membrane samples were then sealed in 3 mil (76.2 μm) thick polyethylene bags until further testing or membrane electrode assembly (MEA) fabrication.

Membrane Electrode Assembly Fabrication

MEA's were fabricated by hot pressing a membrane (~20 % compression) sample between two platinum doped carbon electrodes, and were 50 cm^2 in area (45.15 cm^2 active area). Gas diffusion electrodes, with a platinum loading of 1.0 mg/cm^2 on each electrode, were obtained from BASF Fuel Cell. A Kapton framework was also incorporated to add stability to the MEA, and to allow handling without damaging the MEA. The MEA was placed into a single-cell fuel cell apparatus for testing. The gas flow plates used were graphite with dual gas channels on the anode and triple gas channels on the cathode. Steel endplates were used to clamp the gas flow plates together. Heating pads were attached to the steel plates to regulate temperature. A thermocouple was attached to the steel end plate of the anode to monitor temperature. A commercially

available fuel cell testing station (Fuel Cell Technologies, Inc.) equipped with mass flow regulators was used to conduct and record measurements. Stoichiometric gases were supplied to the anode and cathode at a stoichiometric ratio (hydrogen and air) of 1.2 and 2.0 respectively, without applied backpressure. Fuel/oxidant studies were performed without humidification.

2.6 Experimental Procedures Pertaining to Chapter 6

Polymerization of s-PBI

In a typical polymerization procedure, 3,3',4,4'-tetraaminobiphenyl is reacted with mono sodium 2-sulfoterephthalate in polyphosphoric acid on a 15mM scale. Monomers were added to a 100mL reactor. The reactor was then equipped with a three neck reactor head, a stir rod attached to an overhead stirrer, and a nitrogen inlet/outlet. Nitrogen flow was established and monitored through an oil filled bubbler. The reactor was then placed in a silica oil bath which was thermally regulated using a thermal controller with ramp/soak features. The reaction follows a procedure in which the solution is heated from room temperature to a final polymerization temperature of 220˚C in a stepwise manner. The ramp/soak profile is as follows:

From an initial ambient temperature, the solution was heated to 120˚C over a period of two hours. This temperature was then held for an additional two hours before it was increased to 150˚C over three hours. The solution temperature was held at 150˚C for three and a half hours and then heated to 170˚C over a period of one hour. The solution then remained at this temperature for three hours, at which point it was increased to 190˚C over a one hour period. The solution was then held at 190˚C for ten to fifteen

hours to reach desired viscosity and finally increased to 220˚C over a period of one hour. The solution was held at 220˚C for one to four hours to adjust viscosity for casting.

Polymer Electrolyte Membrane Formation

Polymer solutions were directly cast at 220˚C onto heated (120˚C) glass plates for membrane formation. A heated metal casting blade (120 ˚C) with a casting thickness of 20 mil (508 μm) was used. Once the solution was cast, the glass plates were placed in a humidification chamber at 55%RH to hydrolyze for approximately 24 hours. Hydrolysis of the polyphosphoric acid into phosphoric acid induced a sol-to-gel transition resulting in a Flory Type III gel membrane.[3] The resulting membranes were then sealed in 3mil (76. 2μm) polyethylene bags until further analysis or testing was conducted.

Imbibing procedure for H_2SO_4 doped Polymer Membranes

The hydrolyzed polymer membranes directly cast from PPA solution were soaked in a de-ionized water bath for phosphoric acid removal. The pH of the water baths were monitored and water was replaced as needed until a neutral pH was obtained over a period of 5 days. The PBI membranes were then immersed for 3 days in a 30 wt% H_2SO_4 bath for sulfuric acid imbibing. Titration analyses were conducted at each stage of the acid exchange process.

Vanadium Electrolyte Preparation

Electrolyte solutions containing 1.7 M vanadium ions and 5 M total sulfate were prepared by dissolving V(IV) sulfate oxide in de-ionized water, followed by the addition of sulfuric acid. The solution was charged at 1.8 V with an initial 2:1 catholyte to anolyte ratio, and upon reaching a current density of 10mA cm^{-2}, one half of the catholyte was removed. One set of solutions was used for the polarization curve test; a separate set of solutions was used for both the OCV decay and cycling tests. On each side of the battery

440 mL of solution was used for polarization curve testing. To obtain 50% state of charge, the fully-charged solution was discharged at 0.9 V until 36,000 coulombs of charge were removed.

Flow Battery Experimental Procedure

Flow battery testing was carried out on a single-cell 5cm^2 (Fuel Cell Technologies) no-gap architecture[4] with serpentine flow fields. CP-ESA carbon paper compressed to ~65% of original thickness was used as the electrode in both the positive and negative half-cell. All membranes were soaked in de-ionized water prior to use. Immediately before assembly, membranes were blotted dry and the thickness was measured. Membranes were inserted between the positive and negative electrodes for testing.

All testing was carried out at 30 ˚C in a temperature controlled chamber. Electrolyte flow was delivered by a dual-channel peristaltic pump to ensure equal flow rates for the positive and negative sides. An ultra-high purity nitrogen purge was used on both sides to prevent air oxidation of the V(II) and V(III) species of the anolyte. A Biologic VMP3 potentiostat coupled with a 20A booster was used to perform electrochemical measurements and control the system.

Polarization curve testing

A single-pass configuration, in which the electrolytes from the cell outlets were directed to separate reservoirs, was used for the polarization curve test to ensure a constant electrolyte composition throughout the test. The battery was initially held at open circuit, followed by potential steps in increments of 0.1 V. The cell was held at a constant potential for 10 seconds to allow the current to stabilize. Electrochemical impedance spectroscopy (EIS) was carried out at frequencies of 500 Hz to 10 kHz to

measure the high frequency resistance (HFR) of the cell. A 10 mV sinusoidal AC signal superimposed on the steady-state DC polarization was performed to obtain the impedance spectra. The HFR was determined by the high frequency intercept of the impedance spectrum with the real axis in Nyquist plot. Multiplying HFR to the geometric area ($5cm^2$) yields the area specific resistance (ASR).

OCV decay

The open-circuit voltage (OCV) decay was measured in the cell using 50mL of solution for each side, initially charged in a separate cell. The electrolyte was circulated for approximately one minute allowing a stable OCV. The pump was subsequently switched off, resulting in a static volume of electrolyte being held within the cell and the cell OCV was monitored as a function of time in the temperature chamber.

Cycling testing

Cycling tests were carried out with 50mL of solution in both the positive and negative tanks. Electrolyte was re-circulated, in contrast with the single-pass configuration used for the polarization curve. The cell was cycled at 200 mA cm^{-2} with cutoff potentials of 1.65 and 1.2 V on charge and discharge respectively.

2.7 Experimental Procedures Pertaining to Chapter 7

Polymerization of Sulfonated Polybenzimidazole membranes

In a typical polymerization procedure, 3,3',4,4'-tetraaminobiphenyl is reacted with mono sodium 2-sulfoterephthalate in polyphosphoric acid on a 15mM scale. Monomers were added to a 100mL reactor. The reactor was then equipped with a three neck reactor head, a stir rod attached to an overhead stirrer, and a nitrogen inlet/outlet. Nitrogen flow was established and monitored through an oil filled bubbler. The reactor was then placed

in a silicone oil bath which was thermally regulated using a thermal controller with ramp/soak features. The reaction follows a procedure in which the solution is heated from room temperature to a final polymerization temperature of 220˚C in a stepwise manner. The ramp/soak profile is as follows:

From an initial ambient temperature, the solution was heated to 120˚C over a period of two hours. This temperature was then held for an additional two hours before it was increased to 150˚C over three hours. The solution temperature was held at 150˚C for three and a half hours and then heated to 170˚C over a period of one hour. The solution then remained at this temperature for three hours, at which point it was increased to 190˚C over a one hour period. The solution was then held at 190˚C for ten to fifteen hours to reach desired viscosity and finally increased to 220˚C over a period of one hour. The solution was held at 220˚C for one to four hours to adjust viscosity for casting.

Polymer Electrolyte Membrane Formation

Polymer solutions were directly cast at 220˚C onto heated (120˚C) glass plates for membrane formation. A heated metal casting blade (120 ˚C) with a casting thickness of 20 mil (508 μm) was used. Once the solution was cast, the glass plates were placed in a humidification chamber at 55%RH to hydrolyze for approximately 24 hours. Hydrolysis of the polyphosphoric acid into phosphoric acid induced a sol-to-gel transition resulting in a Flory Type III gel membrane.[3] The resulting membranes were then sealed in 3mil (76. 2μm) polyethylene bags until further analysis or testing was conducted.

Imbibing procedure for H_2SO_4 doped Polymer Membranes

The hydrolyzed polymer membranes directly cast from PPA solution were soaked in a de-ionized water bath for phosphoric acid removal. The pH of the water baths were monitored and water was replaced as needed until a neutral pH was obtained over a

period of 5 days. The PBI membranes were then immersed for 3 days in a 30 wt% H_2SO_4 bath for sulfuric acid imbibing. Titration analyses were conducted at each stage of the acid exchange process.

Membrane Electrode Assembly Fabrication

Membrane electrode assemblies (MEAs) were constructed by hot-pressing gas diffusion electrodes (1.0 mg Pt/cm2) obtained from BASF to each side of the s-PBI membranes as described previously.[5] The MEAs made with Nafion 117 (175 μm thick) and 212 (50 μm thick) membranes were loaded with 1.5 mg Pt/cm2 on each side using a procedure described previously.[6,7] The MEAs were loaded into a single cell purchased from Fuel Cell Technologies, Inc. The cell was 10 cm^2, and consisted of graphite blocks with flow channels machined into them sandwiched between two aluminum endplates to provide compression. Teflon tubing was passed through the face of the aluminum endplates directly into the graphite blocks for the reactants (i.e., SO_2 and water vapor) and products (sulfuric acid and water vapor).

Experimental Setup for Device Performance Evaluations

In this experimental setup, contact between the aluminum endplates and sulfuric acid was prevented. The cell was heated by heating rods inserted into the aluminum endplates. Gaseous SO_2 was fed into the anode compartment via a mass-flow controller at a rate corresponding to 5% conversion at each current. That is, 20 times as much SO_2 was fed than the stoichiometric amount required. The conversion of SO_2 was kept low to ensure a sufficient amount of water entered the cell. The difference between the setups for evaluating the Nafion membranes centers on the humidification of the gaseous SO_2. When using Nafion-based MEAs, dry SO_2 gas was fed to the anode and liquid water to the cathode. When using an s-PBI-based MEA, liquid water in contact with this

membrane could accelerate leaching of the acid and lead to a gradual reduction in conductivity. Therefore, for these experiments the cathode was kept dry and the gaseous SO_2 was humidified prior to introduction to the anode. The humidifier temperature was controlled separately from the electrolyzer. Prior to applying the current, the water content of the SO_2 stream was measured by condensing out the water at the exit to the cell. During cell operation, the sulfuric acid was collected at the anode exhaust of the cell and titrated against 0.1 M sodium hydroxide to determine the concentration. Membrane resistance was measured during operation by a high-frequency milliohm meter in the current interrupt technique, in which the applied current was abruptly changed and the transient potential response was monitored.

2.8 Experimental Procedures Pertaining to Chapter 8

Preparation of Isophthalaldehyde Bisulfite Adduct

7.715g sodium bisulfite (.074mol) was dissolved in 75mL deionized water. 5g isophthalaldehyde (.037 mol) was dissolved in 500mL of MeOH. Once dissolved, the solutions were combined in a 1000mL round bottom flask and stirred at room temp for 24h. After several hours, a white precipitate formed. This precipitate was confirmed via ^{1}H-NMR to be the bisulfite adduct of isophthalaldehyde (yield: 11.36g, 91.5%). Analysis: FT-IR: 1410w, 1350w, 1250w,1175s, 1000s, 650s cm^{-1}. ^{1}H-NMR (300 MHz, DMSO-d6) δ 7.7 (s, 1H), 7.5 (d, 1H, J=6.1), 7.3 (d, 1H, J=6.1), 6.0 (s, 1H), 5.1 (s, 1H).

Solution Polymerization of m-PBI

In a typical polymerization, 4g of isophthalaldehyde bisulfite adduct, 2.504g of tetraaminobiphenyl and 17.5mL of DMAc were added to a 3-neck 100mL round bottom flask under nitrogen. The flask was then equipped with a stir-rod and paddle and stir-rod

adaptor in the center flask neck. The stir-rod was then connected to an overhead mechanical stirrer. A reflux condenser with nitrogen outlet was then attached. The remaining flask neck was then fitted with a nitrogen inlet. A slow nitrogen flow rate, monitored by oil filled bubblers, was then established. The nitrogen flow rate was maintained throughout the reaction. Once assembled, the apparatus was lowered into a temperature regulated silicone oil bath. The oil bath temperature was regulated with an IR^2 thermal controller. Once the reaction was purged, the oil bath was heated to 180˚C , and maintained for the duration of the reaction. Upon refluxing of the solution, stirring was initiated at 30RPM and maintained throughout the duration of the reaction. The reaction was allowed to proceed for 24h or until the solution became too viscous to stir.

Polymer Isolation

Upon completion of the reaction, the solution was first filtered or centrifuged depending on viscosity. The polymer product was then isolated by precipitation in deionized water. The polymer product was chopped, and washed in deionized water and dried at 220˚C under vacuum for at least 12h to remove any residual DMAc solvent. Once dried, the polymer powder was used for product analysis.

2.9 References

1. Mader, J. A.; Benicewicz, B. C. *Macromolecules* **2010**, *43*, 6706–6715.
2. Mader, J. A.; Benicewicz, B. C. *Fuel Cells* **2011**, *2*, 212–221.
3. Flory, P. Principles of Polymer Chemistry; Cornell University Press: Ithaca, 1953, 321-322.
4. Aaron, D. S.; Liu, Q.; Tang, Z.; Grim, G. M.; Papandrew, A. B.; Turhan, A.; Zawodzinski, T. A.; Mench, M. M *Journal of Power Sources* **2012**, *206*, 450-453.
5. Gulledge, A. L.; Gu, B.; Benicewicz, B. C. *J. Polym. Sci. Part A: Polym. Chem.* **2012**, *50*, 306-313.
6. Staser, J.; Ramasamy, P. R.; Sivasubramanian, P.; Weidner, J. W. Electrochemcal and Solid-State Letters 2007, 10, E17-E19.
7. Staser, J.; Weidner, J. W. J. Electrochem. Soc. 2009, 156, B16-B21.

Chapter 3:
A New Sequence Isomer of AB-PBI (AB-Polybenzimidazole) For High-Temperature PEM Fuel Cells[1]

[1] Gulledge, A. L.; Gu, B.; Benicewicz, B. C.; Journal of Polymer Science, Part A: Polymer Chemistry **2012**, *50*, 306-313.

3.1 Introduction of Poly(2,5-benzimidazole) (AB-PBI)

Poly(2,5-benzimidazole) (AB-PBI) is an aromatic heterocyclic polymer and is the simplest known polybenzimidazole as shown in **Figure 3.1**. The synthesis of AB-PBI was first published by Vogel and Marvel in 1961.[1-3] Shortly after, a Japanese group of scientists also reported the synthesis of AB-PBI.[4-8] In the 1980's and 1990's, significant work went into the investigation of the physical properties of AB-PBI blended with other performance polymers such as, polybenzoxazole (PBO), and polybenzothiazole (PBT).[9,10] These polymer blends were studied as material candidates for fiber applications.[11,12] In addition, AB-PBI has been extensively studied by several research groups.[13-17] AB-PBI was not the first polybenzimidazole to be developed, but was very attractive as it offered the desirable properties of polybenzimidazole and was synthetically produced from a commercially available inexpensive monomer.[18,19] AB-PBI can be polymerized by the self condensation of 3,4-diaminobenzoic acid, and like most polybenzimidazoles, has excellent thermal and mechanical properties. AB-PBI synthesis has been reported in various solvent media including, DMAc, Eaton's reagent, and polyphosphoric acid.[20-22]

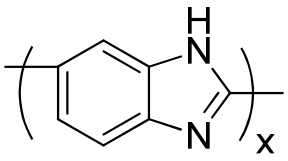

Figure 3.1: Chemical structure of Poly(2,5-benzimidazole)(AB-PBI)

Due to the small molecular size of the repeat unit, AB-PBI has a high concentration of basic sites along the polymer backbone. These basic sites along the polymer chain serve as both proton donor and acceptor sites, and as a result of their high concentration, AB-PBI has a high affinity to acids. Because of this high acid affinity, AB-PBI can be easily

doped with phosphoric acid (PA) and also sulfonated with sulfuric acid. Sulfonation of AB-PBI results in a derivative material termed sAB-PBI and can readily be achieved by heating AB-PBI is a solution of sulfuric acid.[23] In addition to derivatives of AB-PBI through post polymerization modification, substituted[24], crosslinked[25], and copolymers containing AB-PBI have also been investigated.[26] Because of the high solubility of AB-PBI in acids, membrane formation from the PPA process is challenging. The challenge of mechanically stable membrane formation with AB-PBI was overcome in the research presented by tailoring the polymer concentration, and is described herein.

3.2 Introduction of Isomeric AB-PBI (i-AB-PBI)

Many limitations of AB-PBI have arisen because of the polymer's high solubility in phosphoric acid, especially when considering the material as a candidate for high-temperature polymer electrolyte membrane fuel cell applications. These limitations led to research of similar chemically structured alternatives. A new synthetic strategy and development went into the synthesis of a novel bisbenzimidazole monomer, 2,2'-bisbenzimidazole-5,5'-dicarboxylic acid (BBDCA), which could then be polymerized with tetraaminobiphenyl (TAB) to produce a new polymer which constitutionally represents a sequence isomer of AB-PBI termed i-AB-PBI. AB-PBI is a polymer with a head-tail repeating benzimidazole sequence. The change in orientation of the benzimidazole groups incorporated into the new sequence isomer introduces two additional types of chemical bonds. In the known AB-PBI, benzimidazole groups of the polymer backbone are linked through benzimidazole-phenyl (2,5) linkages, whereas the new sequence isomer introduces two new linkages, phenyl-phenyl (5,5 linkages), and benzimidazole-benzimidazole (2,2 linkages) in addition to the benzimidazole-phenyl

linkages. The chemical structures of an expanded AB-PBI polymer sequence and the new i-AB-PBI are shown in **Scheme 3.1**.

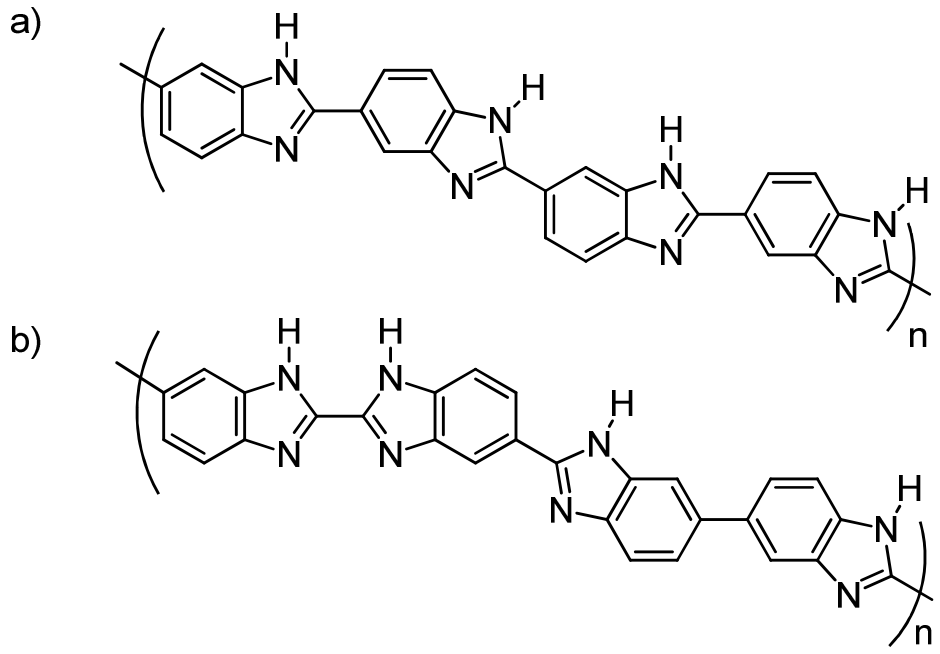

Scheme 3.1: Chemical structures of (a), poly(2,5-benzimidazole)(AB-PBI) and (b) new isomeric i-AB-PBI.

In this chapter, the investigation and evaluation of membranes prepared from the new polymer using the PPA process with respect to composition, mechanical strength, conductivity and fuel cell performance are described. The properties of the new membranes are compared to both the in-house synthesized AB-PBI prepared by the PPA process and literature data on conventionally imbibed AB-PBI membranes.

3.3 Synthesis and Purification of 2,2'-Bisbenzimidazole-5,5'-dicarboxylic Acid (BBDCA)

The key to synthesizing the new i-AB-PBI polymer was the development of a novel diacid monomer which structurally incorporated the desired benzimidazole sequence orientation. Originally, a two-step synthetic strategy was employed to obtain BBDCA, however, this synthetic procedure was inefficient and produced the product in

low yields. Further exploration of the synthesis resulted in a more efficient, higher yielding one-step process. These synthetic procedures are compared in **Scheme 3.2**.

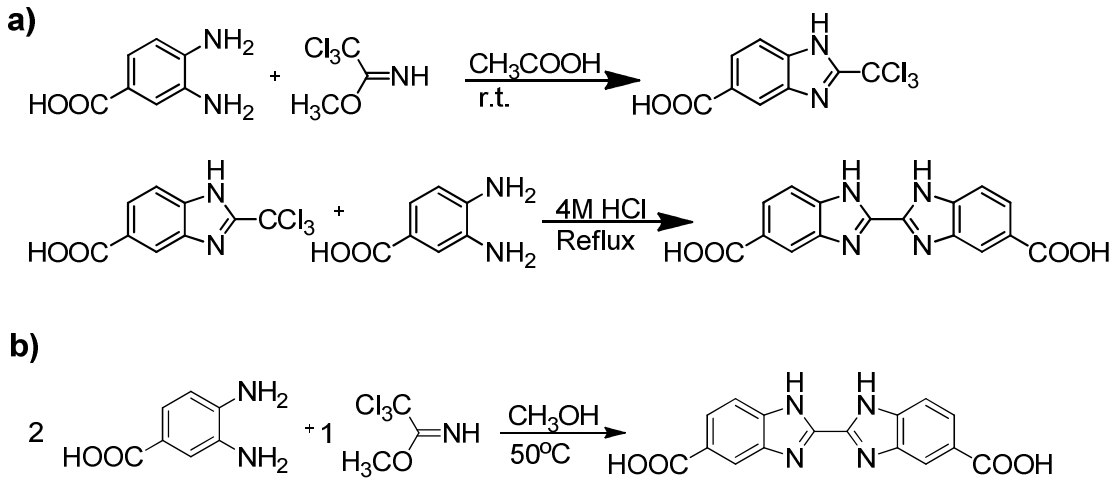

Scheme 3.2: Synthetic procedures for the (a) two-step pathway and (b) one-step pathway synthesis of 2,2'-bisbenzimidazole-5,5'-dicarboxylic acid (BBDCA).

Typical synthesis of bisbenzimidazoles involves a reaction between *o*-phenylenediamines with a diacid or diamide in HCl or polyphosphoric acid (PPA).[27] The synthesis of 2,2'-bisbenzimidazole-5,5'-dicarboxylic acid had not been previously reported in literature, however, synthesis of 2-substituted benzimidazoles from the reaction of *o*-phenylendiamine with an imidate is well known.[28] Synthesis of BBDCA was achieved by reacting purified 3,4-diaminobenzoic acid and methyl 2,2,2-trichloroacetimidate in a 2:1 stoichiometric ratio, respectively. Synthetic procedures involving 2-trichlorobenzimidazoles are often conducted at room temperature after the exothermic reaction has subsided to avoid unwanted side reactions.[29] Although these types of reactions are typically done at room temperature, an increase in reaction yield of ~10-15 % was observed in this work when the reaction was performed at 50 ˚C. It is surmised that the exothermic reaction coupled with the increased reaction temperature

provided the system with enough energy to induce reaction and ring closure of the intermediate 2-trichloro-5-carboxyl benzimidazole with a second equivalent of 3,4-diaminobenzoic acid. The crude product of this monomer was obtained in yields of 50-60 % after 24 h reaction time. The diacid monomer was found to be insoluble in most common organic solvents, but soluble in DMSO and DMAc. Purification of the diacid monomer was achieved using a mixed solvent recrystallization from DMSO and distilled water. The purified diacid monomer was a yellow colored powder after drying and was typically obtained in yields of ~60-70 %. The compound was also determined to be slightly hygroscopic, and therefore thorough drying was required prior to polymerization to achieve high molecular weight polymer. FTIR analysis was used to confirm the complete removal of the intermediate after purification by the absence of a peak at ~829cm^{-1}, which correlates to the C-Cl stretch of the intermediate. H^{1}-NMR and elemental analysis was used to verify monomer purity. The FTIR and H^{1}-NMR analysis of the BBDCA monomer are shown in **Figure 3.2** and **Figure 3.3** respectively.

3.4 Polymer Synthesis

3.4.1 Polymerization of poly(2,5-benzimidazole) (AB-PBI)

Poly(2,5-benzimidazole) (AB-PBI) was prepared by polymerizing purified 3,4-diaminobenzoic acid in PPA. Polymerization conditions for AB-PBI prepared in PPA were experimentally determined through evaluations of polymerization temperature, reaction concentration and duration. After many reaction trials, initial monomer concentrations in PPA were observed to have a direct effect on the molecular weight of the resulting polymer. A study to examine the effect of monomer concentration on polymer inherent viscosity was conducted through a series of polymerizations to determine the optimal concentration for the formation of high molecular weight polymer

and is shown in **Figure 3.4**. The optimal monomer concentration was found to be approximately 3 wt% yielding polymer samples with inherent viscosities up to 4.63 dL/g. Polymerization attempts below 2 wt% monomer concentration under the same conditions yielded lower molecular weight polymers and unstable films when the PPA solutions were cast and hydrolyzed. Polymerizations conducted above 3.5 wt% monomer concentration resulted in films with higher rigidity and less favorable mechanical properties. AB-PBI membranes prepared using the PPA process were found to have much higher acid doping levels (22-35 mol PA/mol polymer repeat unit) when compared to conventional imbibing methods (2-10 mol PA/mol polymer repeat unit).[30] However, AB-PBI membranes prepared with elevated PA doping levels (>14 molPA/mol polymer repeat unit) were found to be unstable at elevated temperatures (>130 ˚C). This is due to the elevated solubility of AB-PBI in phosphoric acid at higher temperatures as described previously. The PA level in the membranes was adjusted by soaking the membranes in PA baths with lower PA concentrations than that of the original film in an attempt to produce stable PA doped AB-PBI membranes. Membrane samples with doping levels of 29.1, 22.7 and 14.5mol PA/mol polymer repeat unit were prepared. However, the films with lower PA content still did not maintain a gel state at higher temperatures, and therefore high-temperature anhydrous conductivity and fuel cell performance analysis could not be obtained for AB-PBI membranes with these moderate levels of PA prepared using the PPA process.

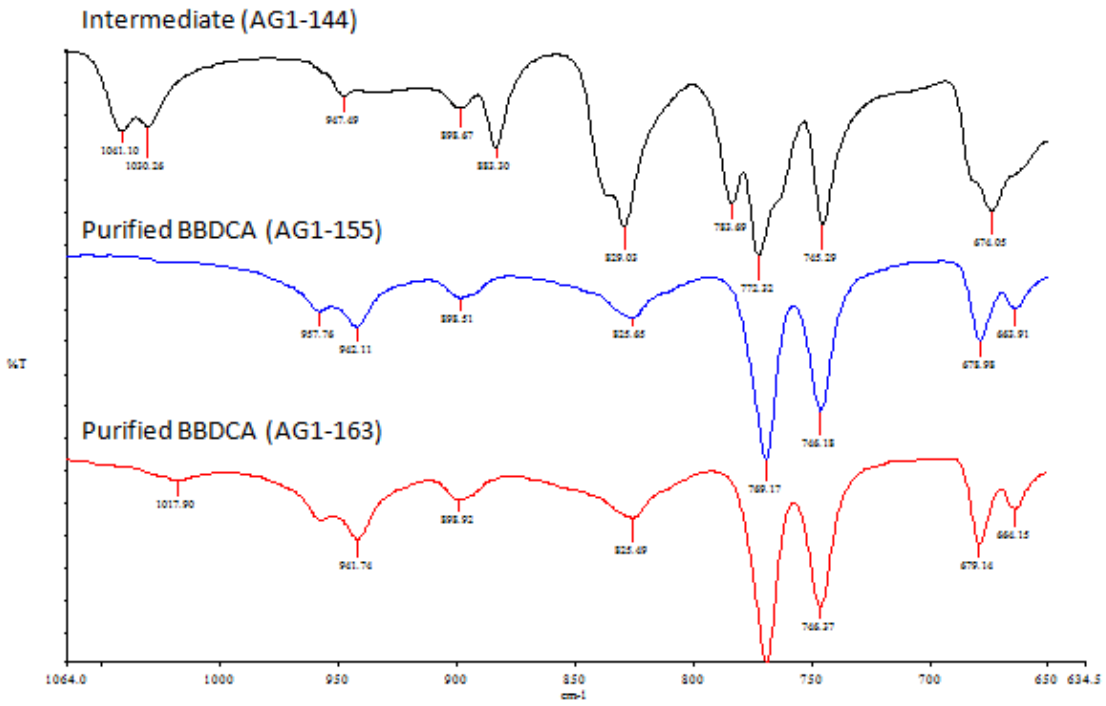

Figure 3.2: FTIR spectra of 2,2'-bibenzimidazole-5,5'-dicarboxylic acid (BBDCA)

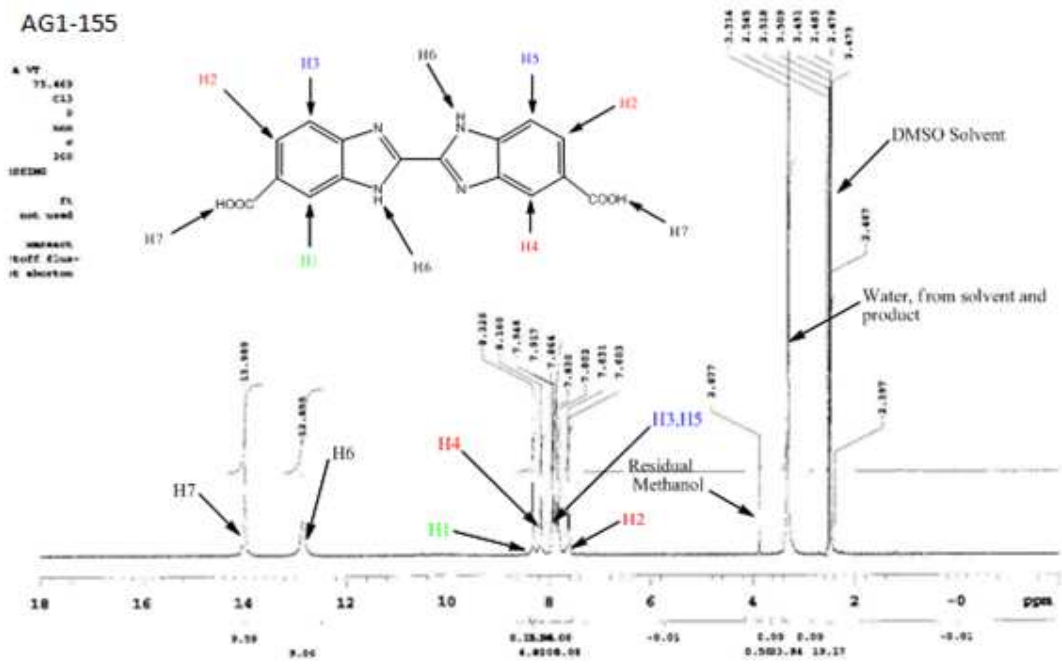

Figure 3.3: H^1-NMR spectra of purified 2,2'-bibenzimidazole-5,5'-dicarboxylic acid (BBDCA)

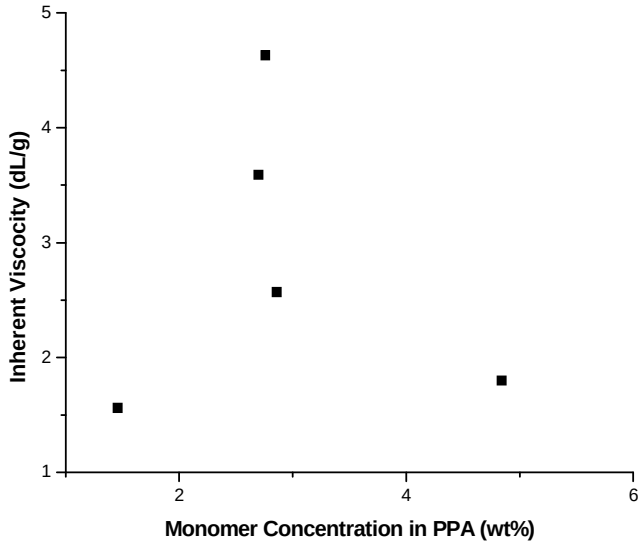

Figure 3.4: Effect of monomer concentration on inherent viscosity (I.V.) for the polymerization of 3,4-diaminobenzoic acid in PPA at 220˚C.

3.4.2 Polymerization of i-AB-PBI

The new sequence isomer of AB-PBI, i-AB-PBI, was synthesized using the synthetic scheme displayed in **Scheme 3.3**. The synthesis of i-AB-PBI is an AA-BB step polymerization and, as defined by the Carother's equation[31], an exact stoichiometric ratio of 2,2'-bisbenzimidazole-5,5'-dicarboxylic acid with 3,3',4,4'-tetraaminobiphenyl was required to achieve high molecular weight i-AB-PBI. Polymerization conditions for the new sequence isomer were experimentally determined and were conducted over a range of monomer concentrations as shown in **Figure 3.5**. A dramatic increase in polymer I.V. occurred when monomer concentration was increased from 5 to 6 wt%. The reason for this abrupt change in I.V. is not completely understood and this type of behavior has not been observed in our previous and extensive investigations of PBI polymers. Although such abrupt changes in I.V. could be indicative of a transition to an ordered or liquid

crystalline phase, all other observations were not supportive of a liquid crystalline phase morphology. Further increases in monomer concentration led to polymers with slightly lower inherent viscosities which we attributed to increased solution viscosity and difficulties in stirring during the later stages of the polymerization. Subsequent polymerizations were conducted at 6 wt% monomer concentration, which was determined to be the optimal reaction concentration to obtain high molecular weight polymer.

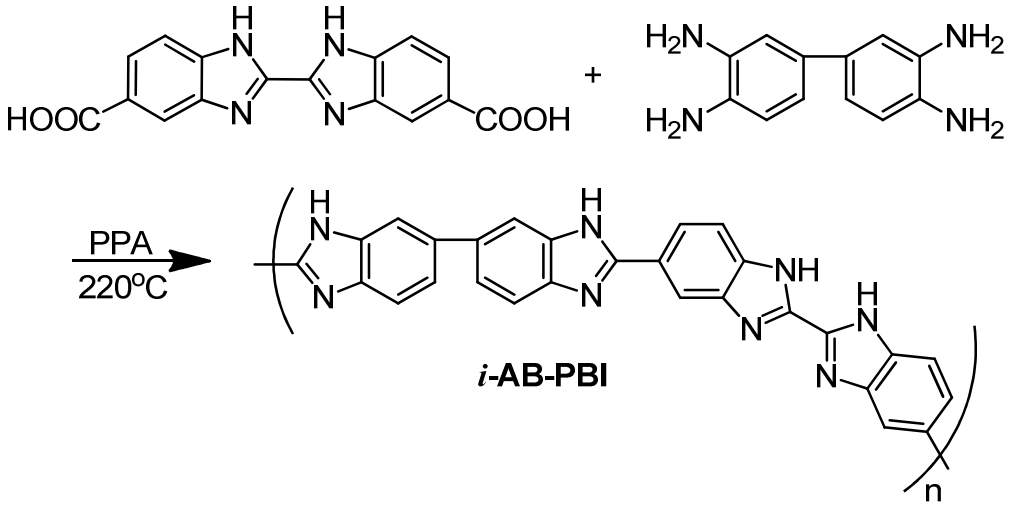

Scheme 3.3: Polymerization of i-AB-PBI.

3.5 AB-PBI and i-AB-PBI Polymer Electrolyte Membrane Formation and Properties

Polymer solutions were directly cast at 220 ˚C onto heated glass plates (120 ˚C oven temperature) using a 20 mil (508 μm) casting blade. The solutions then underwent a sol-to-gel transition as the PPA of the membrane hydrolyzed into PA and the system temperature decreased to room temperature. The membrane composition data show that the typical compositions of i-AB-PBI membranes prepared using the PPA process are

greater than 50 % phosphoric acid and have a polymer content between 7-10.5 wt%. Mechanical property evaluations of the i-AB-PBI doped membranes typically yielded Young's moduli ranging from 0.9-1.6 MPa and tensile strengths between 0.43-1.11 MPa. Membrane composition data along with other significant properties for i-AB-PBI and the in-house AB-PBI prepared using the sol-gel method are shown in **Tables 3.1** and **Table 3.2** respectively.

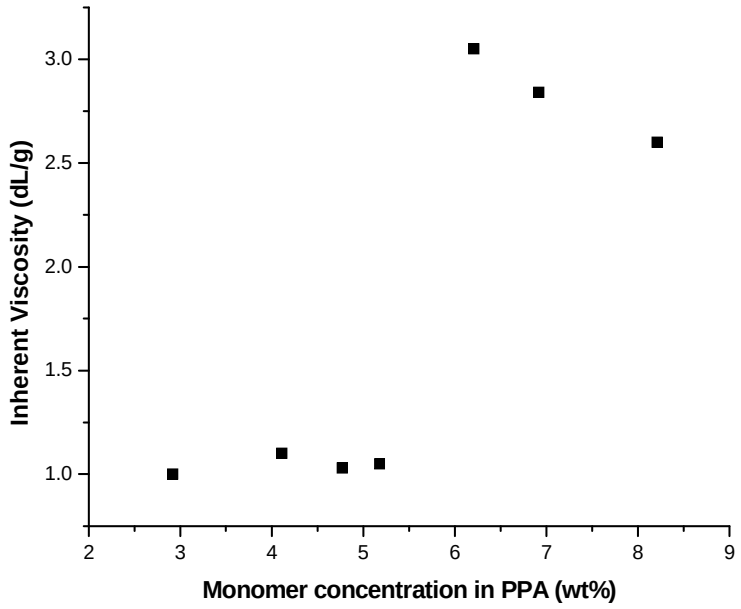

Figure 3.5: Effect of monomer concentration on inherent viscosity (I.V.) for the new isomeric AB-PBI (i-AB-PBI) at a polymerization temperature of 220˚C

Table 3.1: Characterization Results for i-AB-PBI Polymers and Membranes

Sample #	Monomer wt%	I.V. (dL/g)	Mol PA/Mol Polymer Repeat Unit	Anhydrous Conductivity at 180˚C (S/cm)	Membrane Composition(as cast) (wt%) PA	H_20	Polymer
1*	2.92	1.0	N/A	N/A	N/A	N/A	N/A
2*	4.11	1.1	N/A	N/A	N/A	N/A	N/A
3*	4.77	1.03	N/A	N/A	N/A	N/A	N/A
4	5.18	1.05	34.76	N/A	55.96	36.37	7.67
5	6.21	3.05	36.52	.202	54.98	37.76	7.26
6	6.92	2.84	24.5	.216	53.92	35.59	10.49
7	8.21	2.60	32.12	.195	54.08	37.90	8.02

* Low molecular weight samples were obtained and resulting films were unstable for testing.

Table 3.2: Characterization Results for AB-PBI Polymers and Membranes

Sample #	Monomer wt%	I.V. (dL/g)	Mol PA/Mol Polymer Repeat Unit	Membrane Composition (as cast) (wt%) PA	H_2O	Polymer
8	1.46	1.56	35.28	60.22	37.67	2.11
9	2.76	4.63	24.71	62.17	34.36	3.47
10	2.7	3.59	29.07	62.59	34.83	2.58
11	2.86	2.57	31.82	57.27	40.49	2.24
12	4.84	1.8	22.56	73.82	22.25	3.93

As previously mentioned, the new i-AB-PBI contains two additional types of chemical bonds when compared to AB-PBI, benzimidazole-benzimidazole and phenyl-phenyl linkages. ^{1}H-NMR analysis was conducted for both AB-PBI and the new i-AB-PBI. Based on the chemical structures presented, the i-AB-PBI spectrum would contain additional peaks which arise from the C-H bonds in the bi-phenyl moiety of the polymer. Spectral analysis did in fact show additional peaks at 8.2 and 8.5 ppm, which are consistent with the assignments of the bi-phenyl moiety in 2,2'-diphenyl-5,5'-bibenzimidazole, a model compound.[32] Preliminary molecular modeling using MOPAC 2009 Semi Empirical PM6 indicated slightly increased chain stiffness for i-AB-PBI as

compared to AB-PBI, and is shown in **Figure 3.6** and **Figure 3.7** respectively. Experimentally, a lower solubility for i-AB-PBI in PA at elevated temperatures (130-180 ˚C) when compared to the known AB-PBI was observed. The observed decrease in solubility is likely due to the decreased concentration of amine and imine groups along the polymer chain, as compared to that of AB-PBI. The lower solubility of the i-AB-PBI resulted in films with higher gel stability at higher temperatures, even with higher acid doping levels. Thus, films made with i-AB-PBI and doped with high levels of PA were sufficiently stable for conductivity measurements and fuel cell performance evaluations.

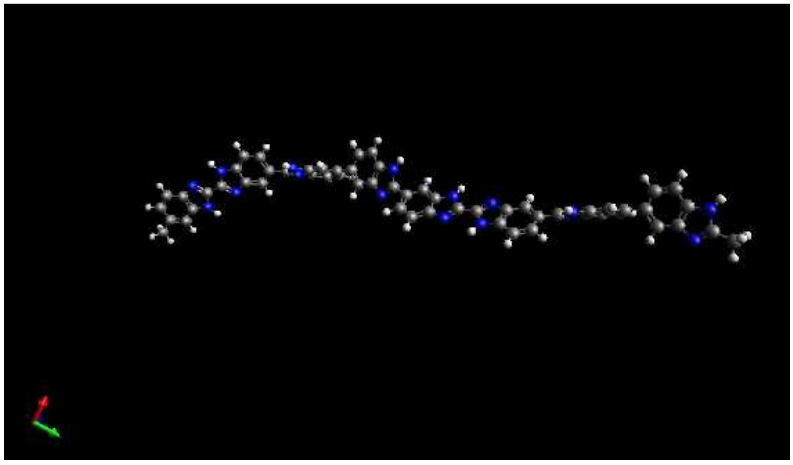

Figure 3.6: Molecular model of i-AB-PBI. Produced by Dr. Vitaly Rassolov using MOPAC 2009 Semi-Empirical PM6 molecular modeling software at the University of South Carolina.

3.6 Ionic Conductivity

The ionic conductivity data for i-AB-PBI are shown in **Figure 3.8** along with literature data for AB-PBI.[33] At 180 ˚C under anhydrous conditions, i-AB-PBI showed a nearly 10x increase in conductivity, from 0.02 to 0.2 S/cm when compared to the reported literature on the conventionally imbibed AB-PBI.[33] This is largely due to the stability of i-AB-PBI with higher acid doping levels at increased temperatures. For the

ionic conductivity comparison shown, it should be noted that the isomeric i-AB-PBI has much higher acid loadings than that of the conventionally imbibed AB-PBI reported. The i-AB-PBI membrane used for conductivity comparison had an acid loading of approximately 36 moles of phosphoric acid per mole of repeat unit, whereas, the conventionally imbibed AB-PBI membrane illustrated had 2.7 moles of phosphoric acid per mole of repeat unit. The repeat unit of the new i-AB-PBI is roughly 4 times the size of the AB-PBI repeat unit, and when corrected for these differences, the i-AB-PBI membrane has approximately 3 times the acid loading than that of the AB-PBI used for comparison. The significant differences in acid loading of the two films used to compare ionic conductivity results from the two different processes. AB-PBI membranes developed from the PPA process did in fact have much higher acid loadings than those of conventionally imbibed AB-PBI membranes and were not suitable for high temperature anhydrous conductivity analysis. Therefore, AB-PBI and i-AB-PBI membranes with similar acid loadings could not used to present a direct comparison of ionic conductivity. The high conductivity (~0.2 S/cm) for *i*-AB-PBI indicated these membranes would be an excellent candidate for high temperature PEM fuel cells and subsequent fuel cell performance analyses were conducted.

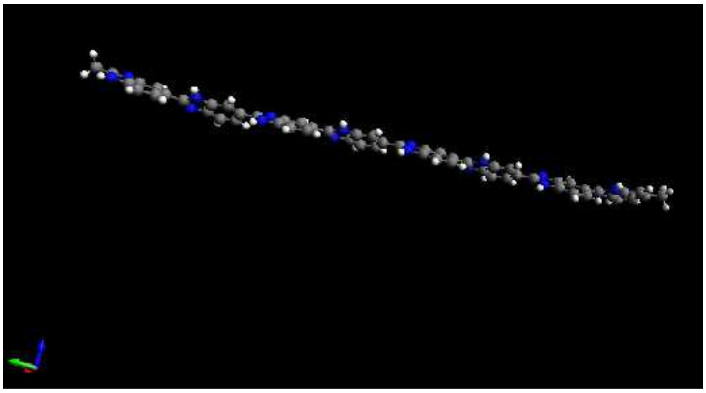

Figure 3.7: Molecular modeling of poly(2,5-benzimidazole) (AB-PBI). Produced by Dr. Vitaly Rassolov using MOPAC 2009 Semi-Empirical PM6 molecular modeling software at the University of South Carolina.

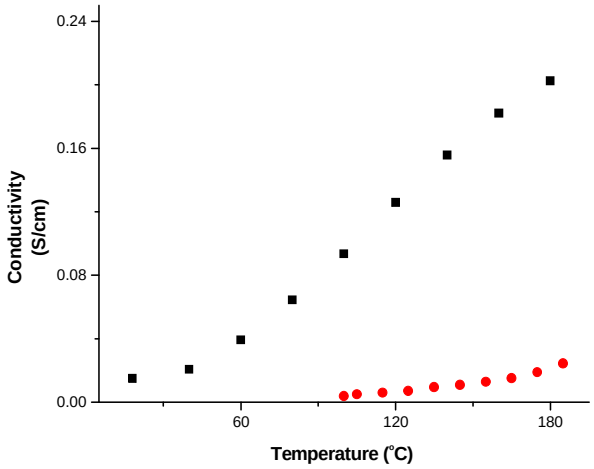

Figure 3.8: Effects of temperature on anhydrous ionic conductivity. (Squares: new isomeric i-AB-PBI (Sample 5 from Table 3-1), circles: reported literature values for poly(2,5-benzimidazole) (AB-PBI).[33]

3.7 Fuel Cell Performance

Fuel cell performance studies were conducted on i-AB-PBI membranes that included polarization curves with hydrogen/air and reformate/air fuel/oxidant combinations over a range of temperatures (120-180 ˚C). The performance of i-AB-PBI in comparison to reported literature of AB-PBI, using hydrogen/oxygen with 1.2:2.0 stoichiometric flows is shown in **Figure 3.9**. Significant increases in fuel cell performances for i-AB-PBI were observed over a range of temperatures (120-180 ˚C). At a current density of 0.2 A/cm^2, a voltage of approximately 0.65 V was observed with hydrogen and air supplied at 1.2 and 2.0 stoichiometric flows.

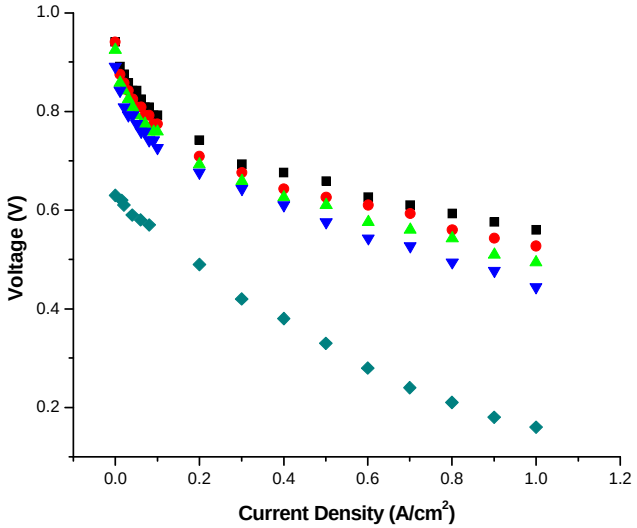

Figure 3.9: Polarization curves for i-AB-PBI membranes with hydrogen/oxygen at 1.2:2.0 stoichiometric flows respectively. [Squares: 180˚C, circles: 160˚C, triangles: 140˚C, inverted triangles: 120˚C, diamonds: reference data for poly(2,5-benzimidazole)(AB-PBI) at 130˚C.[33]]

The polarization curves for the new sequence isomer with hydrogen/air and reformate/air are shown in **Figure 3.10** and **Figure 3.11** respectively. As would be expected, a slight decrease in performance was observed when the oxidant was changed from pure oxygen to air. The reformate gas used in these polarization studies consisted of approximately 70 % hydrogen, 28 % CO_2, and 2 % CO. In the reformate/air polarization curve, it is shown that i-AB-PBI membranes maintained high performance at 180 ˚C, even in the presence of carbon monoxide, a well known fuel contaminate. At lower temperatures and in the presence of CO (2 %), a significant decrease in performance was observed, as would be expected from decreased electrode kinetics and irreversible Pt–CO binding. A lifetime performance study was conducted on *i*-AB-PBI membranes and is shown in **Figure 3.12**. An observed break-in period of around 500 h was observed before

the cell reached and maintained an average output of 0.65 V. The test was conducted over a period of 3500 h with a relatively constant output voltage of 0.65 V at 0.2 A/cm^2. Several facility events occurred during the lifetime study of i-AB-PBI which led to uncontrolled shutdowns. However, a full recovery of the cell was observed after normal re-start operations. The long (500 h) break-in period for i-AB-PBI membranes was attributed to the higher polymer content (~7-10.5%) which introduces a resistance to the transfer of internal PA of the film to the catalytic interface of the electrodes during initial fuel cell operation.

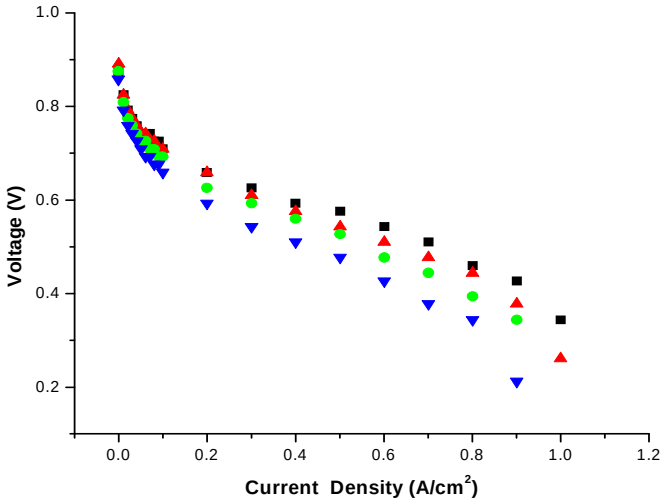

Figure 3.10: Polarization curves for i-AB-PBI membranes with hydrogen/air at 1.2:2.0 stoichiometric flows respectively. [Squares: 180˚C, triangles: 160˚C, circles: 140˚C, inverted triangles: 120˚C.]

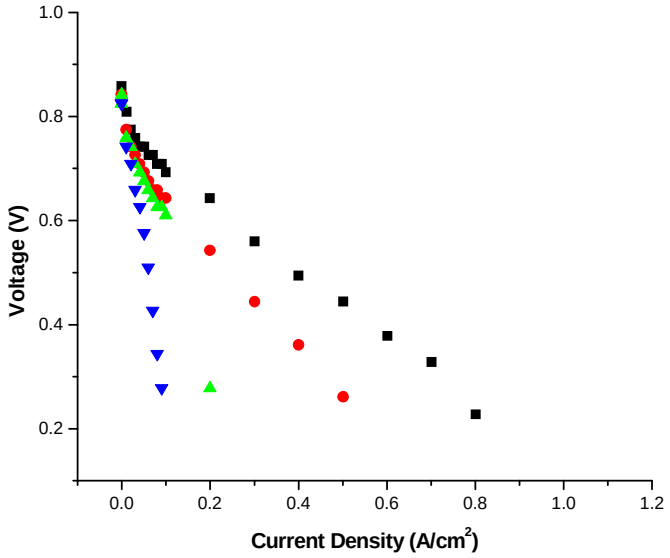

Figure 3.11: Polarization curves for i-AB-PBI membranes with reformate/air at 1.2:2.0 stoichiometric flows respectively. [Squares: 180˚C, circles: 160˚C, triangles: 140˚C, inverted triangles: 120˚C.] (Reformate composition: 70% hydrogen, 28% CO_2, and 2% CO.)

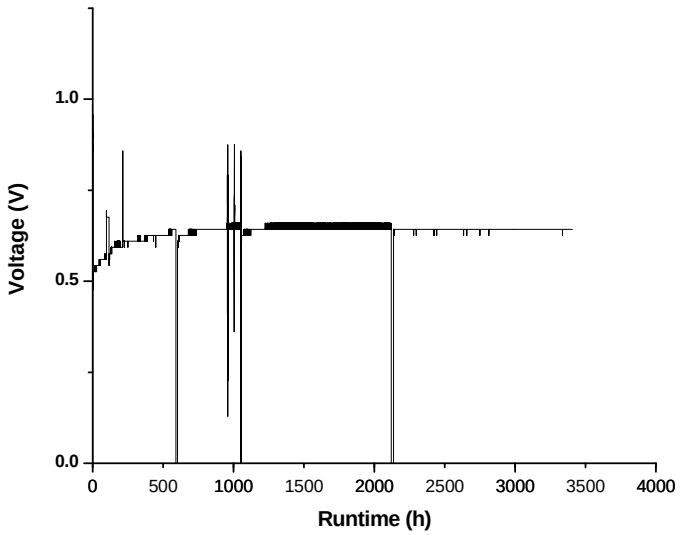

Figure 3.12: Long term performance of i-AB-PBI membrane fuel cell operated at 180˚C with hydrogen/air at 1.2:2.0 stoichiometric flows respectively. Data collected under 1atm and deviations were uncontrolled facility events.

3.8 Conclusions

AB-PBI membranes were prepared using the PPA process and compared to reported literature on the known conventionally imbibed AB-PBI membranes. A new diacid monomer was synthesized from an imidate reaction with 3,4-diaminobenzoic acid. Polymerization of this diacid monomer with 3,3'-4,4'-tetraminobiphenyl yielded a new sequence isomer of AB-PBI, termed i-AB-PBI. Polymerization studies were conducted with the new diacid which showed an unusual dependence on monomer concentration, but revealed conditions where high I.V. polymers could be prepared. Optimal conditions for the polymerization of high molecular weight i-AB-PBI membranes was determined to be 6wt% monomer charge. Membranes prepared from the PPA process exhibited higher levels of PA than typically reported for conventionally imbibed AB-PBI. The membrane mechanical property characterization and proton conductivity measurements indicated that the membranes formed from i-AB-PBI were suitable candidates for high temperature polymer membrane fuel cells.

The new sequence isomer, i-AB-PBI, was found to be less soluble in phosphoric acid and mechanically stable at elevated temperatures (120-180 ˚C) with high phosphoric acid doping levels (24-35 mol PA/mol polymer repeat unit). The changes in chain sequence incorporated into the new i-AB-PBI as compared to AB-PBI are believed to affect chain stiffness which may contribute to the observed decreased solubility and increased gel stability in phosphoric acid at high temperatures. AB-PBI membranes with higher polymer content (~7-10.5 wt%) than those prepared from the traditional AB-PBI (~3 wt%) were obtained using the PPA process. The increased solids content of the i-AB-PBI films resulted in membranes that were more mechanically robust when compared to

the in-house AB-PBI films prepared using the PPA process. Fuel cell performance evaluations were conducted using i-AB-PBI membranes and an output voltage of 0.65 V at 0.2 A/cm^2 for hydrogen/air at an operational temperature of 180 ˚C was observed. The new i-AB-PBI has been reported as a promising candidate for high temperature PEM fuel cell devices.[22] This new sequence isomer of AB-PBI represents a new type of AB polybenzimidazole and presents opportunities for the research and development of a new class of AB-type polybenzimidazoles.

3.9 References

1. Marvel, C. S.; Vogel, H. A. **1965**, *US 3174947*, 1-6.
2. Vogel, H.; Marvel, C. S. *Journal of Polymer Science: Part A* **1963**, *1*, 1531-1541.
3. Vogel, H.; Marvel, C. S. *Journal of Polymer Science: Part A* **1961**, *50*, 511-539.
4. Imai, Y.; uno, K.; Iwakura, Y. *Makromol. Chem.* **1965**, *83*, 179-187.
5. Inoue, S.; Imai, Y.; Uno, K.; Iwakura, Y. *Makromol. Chem.* **1966**, *95*, 236-247.
6. Iwakura, Y.; uno, K.; Imai, Y.; Fukui, M *Makromol. Chem.* **1964**, *77*, 41-50.
7. Iwakura, Y.; Uno, K.; Imai, Y. *Makromol. Chem.* **1964**, *77*, 33-40.
8. Iwakura, Y.; Uno, K.; Imai, Y. *Journal of Polymer Science: Part A, Polymer Chemistry* **1964**, *2*, 2605-2615.
9. Cagin, T. Materials Research *Society Symposium Proceedings*, **1993**, *291*, 321-324.
10. Hwang, W. F.; Wiff, D. R.; Verschoore, C.; Price, G. E. *Polymer Engineering and Science* **1983**, *23*, 784-788.
11. Hwang, W. F.; Wiff, D. R.; Helminiak, T. *Org. Coat. Plast. Chem.* **1981**, *44*, 32-37.
12. Krause, S. J.; Haddock, T.; Price, G. E.; Lenhert, P. G.; O'Brien, J. F.; Helminak, T. E.; Adams, W. W. *Journal of Polymer Science: Part B, Polymer Physics* **1986**, *24*, 1991-2016.
13. Ong, A.; Jung, G.; Wu, C.; Yan, W. *Journal of Hydrogen Energy* **2010**, *35*, 7866-7873.
14. Wannek, C.; Lehnert, W.; Mergel, J. *Journal of Power Sources* **2009**, *192*, 258-266.
15. Hyoung-Juhn, K.; Sung, C.; Sung, J.; Yeong, C.; Ju-Yong, K.; Hae-Kwon, Y.; Ho-Jin, K.; Kyoung, H. *Macromol Rapid Commun* **2004**, *25*, 894-897.
16. Zheng, H.; Petrik, L.; Mathe, M.; *Journal of Hydrogen Energy* **2010**, *35*, 3745-3750.
17. Wippermann, K.; Wannek, C.; Oetjen, H.; Lehnert, W. *Journal of Power Sources* **2010**, *195*, 2806-2809.
18. Gomez-Romero, P.; Chojak, M.; Cuentas-Gallegos, K.; Asensio, J. A.; Kulesza, P. J.; Casan-Pastor, N.; Lira-Cantu, M. *J Electrochem Commun* **2003**, *5*, 149-153.

19. Asensio, J. A.; Borros, S.; Gomez-Romero, P. *J Electrochem Commun* **2003**, *5*, 967-972.
20. Wainright, J. S.; Savinell, R. F.; Litt, M. H. *Handbook of Fuel Cells* **2003**, *3*, 436-446.
21. Mader, J.; Xiao, L.; Schmidt, T. J. Benicewicz, B. C. *Fuel Cells II* **2008**, Springer Berlin Heidelberg, 63-124.
22. Gulledge, A. L.; Gu, B.; Benicewicz, B. C.; Journal of Polymer Science, Part A: Polymer Chemistry **2012**, *50*, 306-313.
23. Asensio, J. A.; Borros, S.; Gomez-Romero, P. *J Electrochem Soc* **2004**, *151*, A304-A310.
24. Kumbharkar, S.; Kharul, U. *Journal of Membrane Science* **2010**, *360*, 418-425.
25. Sung-Kon, K.; Tae-Ho, k.; Taeyun, K; Jong-Chan, L. *Journal of Membrane Science* **2011**, *373*, 80-88.
26. Yang, J.; He, R.; Che, Q.; Gao, X.; Shi, L. *Polym. Int.* **2010**, *59*, 1695-1700.
27. Berrada, M.; Anbaoui, Z.; Ljrhed, N.; Knouzi, N.; Vaultier, M.; Sekiguchi, H.; Carriere, F. *Chem. Mater.* **1997**, *9*, 1989-1993.
28. Holan, G.; Samuel, E. L.; Ennis, B. C.; Hinde, R. W. *J. Chem. Soc.* **1967**, *1*, 20-25.
29. Grimmett, R.; *Imidazole and Benzimidazole Synthesis*. London; **1997** Academic Press, Inc., p 79.
30. Mader, J.; Xiao, L; Schmidt, T. J.; Benicewicz, B. C.; *Adv Polymer Sci* **2008**, *216*, 63-124.
31. Carothers, W. *Trans . Faraday Soc.* **1936**, *32*, 39-53.
32. Ryan, M. T.; Helminiak, T. E.; Polymer Preprints 1973, 14, 1317-1320.
33. Asenio, J. A.; Gomez-Romero, P. *Fuel Cells* **2005**, *No. 3*, 336-343.

Chapter 4: Investigation of Sequence Isomer Effects in AB-Polybenzimidazole (AB-PBI) Polymers[2]

[2] Gulledge, A. L.; Chen, X.; Benicewicz, B. *Journal of Polymer Science, Part A: Polymer Chemistry* **2014**, *52*, 619-628.

4.1 Introduction to Randomized AB-type Polybenzimidazole Polymers

To date, a large variety of polybenzimidazole (PBI) polymers have been synthesized and studied in the literature.[1-7] However, PBI chemistry still remains an important area of interest in the high-temperature PEM fuel cell community. Many PBI variants containing a range of structural and functional moieties have been examined to further explore the effects of polymer structure on membrane properties.[8-18] Among these, several copolymer systems have been evaluated to extensively investigate how their properties change with respect to composition.[19-22] In this work, sequence isomerism in a unique copolymer system is evaluated.

The recently reported synthesis of a novel isomeric AB-PBI, termed i-AB-PBI, was shown to have significantly improved properties resulting from a change in the benzimidazole sequence of the polymer, as compared to AB-PBI.[1] The development of this new sequence isomer with regards to AB-PBI has presented the opportunity to research and develop a new class of AB-type polybenzimidazoles. In this chapter the evaluation of random copolymers of various compositions between AB-PBI and i-AB-PBI, termed r-AB-PBI, are described. Isomerization of the benzimidazole orientation in the i-AB-PBI allowed for direct comparison with AB-PBI and provided insights into the fundamental structure property relationships of polybenzimidazoles. Variation of composition in the r-AB-PBI system allows for the direct study of how incorporation of various amounts of 2,2 and 5,5 linkages affect the properties of these materials by changing the main chain benzimidazole sequence. **Figure 4.1** shows the structural repeat units incorporated in the AB-PBI, i-AB-PBI and random AB-PBI polymers.

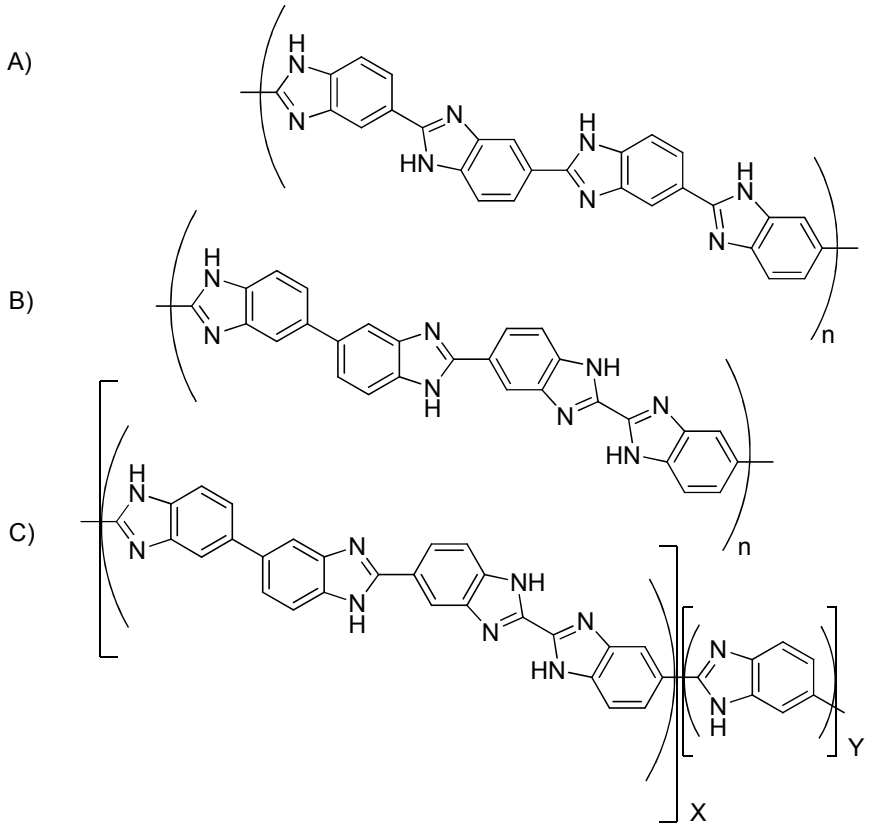

Figure 4.1: A: Poly(2,5-benzimidazole)(AB-PBI), B: Isomeric AB-PBI (i-AB-PBI), and C: Random AB-PBI (r-AB-PBI).

In this chapter, the evaluation of polymer electrolyte membranes prepared from the random copolymers of AB-PBI and i-AB-PBI are described with regards to their proton conductivity, solubility, mechanical stability, thermal properties, and high temperature fuel cell performance. Moreover, these properties are compared to both homo-polymers of AB-PBI and i-AB-PBI to gain insight on how the material properties are affected by the change and variation of main chain benzimidazole sequence.

4.2 Polymerization of Random AB-PBI copolymers (r-AB-PBI)

Using the previously reported novel bisbenzimidazole monomer[23], 2,2'-bisbenzimidazole-5,5'-dicarboxylic acid, along with recrystallized 3,4-diaminobenzoic acid and 3,3',4,4'-tetraaminobiphenyl, in PPA solution, random copolymers of AB-PBI and i-AB-PBI were prepared, as shown in **Scheme 4.1**. Assuming the Principal of Equal Reactivity[24], copolymerization of the above mentioned monomers results in a randomized benzimidazole sequence, i.e., a polymer chain composed of repeating 2,5-benzimidazole units with a random sequence of 2,5 2,2 and 5,5 linkages. Polymerization of these monomers is an AA-BB-AB type polycondensation polymerization, and as defined by the Carother's Equation[25] an exact stoichiometric ratio is needed between AA and BB monomers to achieve high molecular weight polymer. By varying the 3,4-diaminobenzoic acid molar ratio, random copolymer compositions between 0 and 100 mol % of AB-PBI and i-AB-PBI were synthesized. Polymerization conditions were adjusted from the previously reported synthetic conditions[23] of the corresponding homo-polymers as composition was varied. Random copolymers of AB-PBI and i-AB-PBI obtained had inherent viscosities ranging between 2.13 and 3.48 dL/g, indicating that high molecular weight polymers were obtained. Polymer solutions resulting from the PPA process were directly cast and hydrolyzed into polymer electrolyte membranes doped with phosphoric acid. These resulting gel films were then evaluated in terms of conductivity, mechanical stability, and high temperature fuel cell performance.

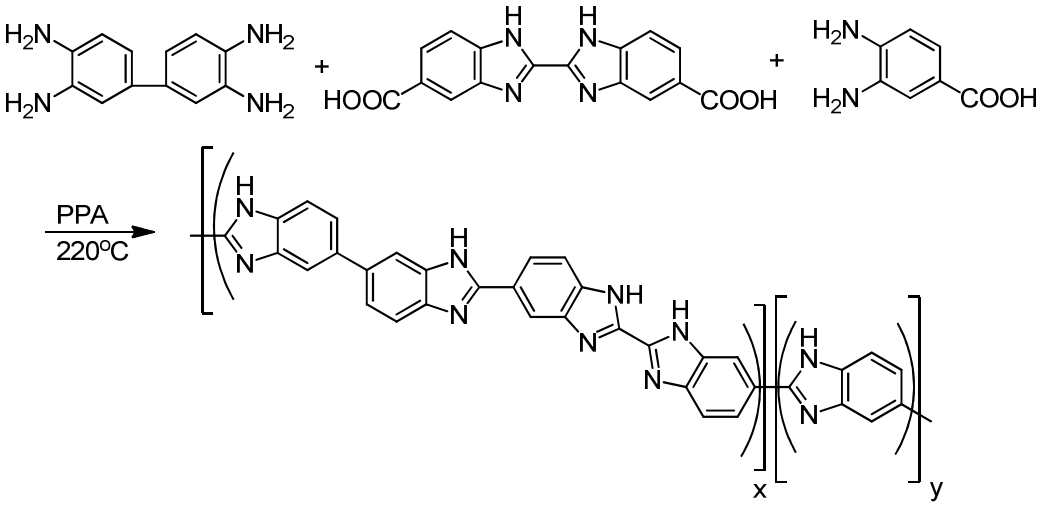

Scheme 4.1: Synthesis of Random AB-PBI Polymers.

4.3 Polymer Electrolyte Membrane Fabrication and Properties

Once polymerized, polymer solutions of r-AB-PBI were directly cast at 220˚C onto heated glass plates (120 ˚C oven temperature) using a 20 mil (508 μm) casting blade. The glass plates were then placed into a hydrolysis chamber with a controlled relative humidity of 55.5%. This induced a sol-to-gel transition as the polyphosphoric acid of the membrane hydrolyzed into phosphoric acid and the system temperature decreased to ambient conditions. Resulting membranes were then analyzed by titration to obtain compositional measurements. The membrane composition data obtained shows that the typical compositions of r-AB-PBI membranes (as cast) prepared using the PPA process are greater than 50 wt% phosphoric acid and have a polymer content ranging from 6.22-11.61 wt%. Mechanical property evaluations of the r-AB-PBI doped membranes were conducted and typically yielded Young's moduli ranging from 0.3-1.6 MPa and tensile strengths between 0.3-1.0 MPa. Membrane composition data along with other significant properties for r-AB-PBI films are shown in **Table 4.1**

Table 4.1: Characterization Results for Random AB-PBI Polymers and Membranes

	Composition i-AB:AB		Monomer Charge (wt%)	I.V.	Membrane Composition (wt%)			Mol PA/ Mol BI	Anhydrous Conductivity 180□C (S/cm)
	***i*-AB**	**AB**			**PA**	**H_2O**	**Polymer**		
1	100	0	6.21	3.05	54.98	37.76	7.26	9.09	0.202
2	90	10	5.96	2.27	52.98	38.8	8.23	7.63	0.133
3*	90	10	5.50	2.13	58.12	33.69	8.19	11.05	NA
4	80	20	6.01	2.26	58.13	35.66	6.22	9.64	0.059
5	70	30	4.50	3.38	54.81	38.03	7.16	11.09	0.2
6*	70	30	5.84	2.67	54.49	39.94	9.57	7.19	NA
7	60	40	4.97	3.48	59.17	34.48	6.35	5.11	0.18
8	50	50	5.48	2.59	64.99	24.29	10.72	7.51	0.217
9	40	60	4.96	3.11	49.38	39.01	11.61	6.5	0.112
10	30	70	5.45	3.37	55.09	36.21	8.7	7.7	0.146
11	20	80	3.61	2.30	56.17	33.58	10.25	8.65	0.0878
12	10	90	3.05	3.23	58.3	32.73	8.97	9.09	0.219
13*	0	100	2.76	4.63	62.17	34.36	3.47	7.63	NA

*Samples obtained were not suitable for high temperature proton conductivity measurements. I.V.- Inherent Viscosity, BI- Benzimidazole

4.4 Thermal Characterization and Analysis

PBI type polymers are well-known for their high thermal stabilities resulting from their fully aromatic structure and polymer chain rigidity.[13,26-28] Thermal evaluations of r-AB-PBI copolymers were conducted via TGA from ambient temperature to 750˚C with a heating rate of 5˚C/min in nitrogen. TGA curves and thermal data for several samples of the r-AB-PBI copolymers, along with AB-PBI and i-AB-PBI are shown in **Figure 4.2** and **Table 4.2** respectively. Two weight loss regions were observed in the analysis: an initial weight loss region between 100-200˚C, and a decomposition region above 600˚C. The initial weight loss region between 100-200˚C results from loss of bound water,

despite thorough drying under vacuum at 120˚C. PBI polymers are very hygroscopic and have been shown to absorb approximately 10-15% (by weight) of water, even in short sample handling times.[45] Thermal degradation of the polymer backbone is observed between 580˚C and 600˚C. Above 600˚C, rapid weight loss is observed. **Figure 4.2** and **Table 4.2** show that less than 10% weight loss is observed at 570˚C and 600˚C for AB-PBI and i-AB-PBI respectively, indicating the high thermal stabilities of ordered polybenzimidazoles. Randomized polybenzimidazoles samples showed slightly lower thermal stability and a higher degradation rate, as would be expected from disrupted chain packing. The randomized polybenzimidazoles also showed an unusual drop between 200-300˚C that was not observed in the corresponding homopolymers.

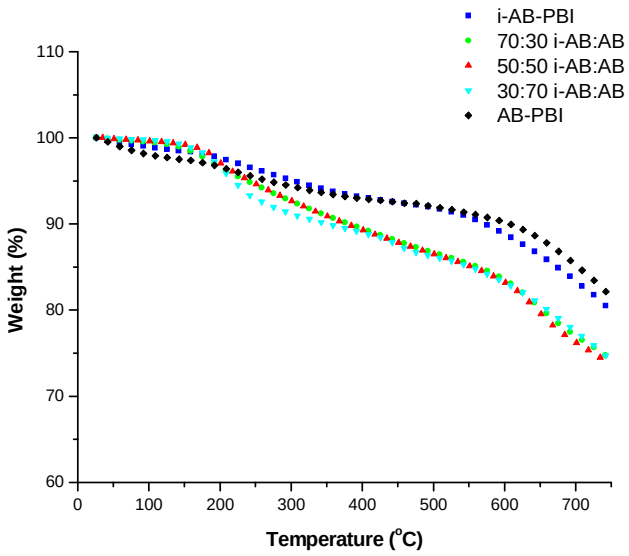

Figure 4.2: TGA curves for AB-PBI, i-AB-PBI, and r-AB-PBI in nitrogen.

Table 4.2: Thermal Properties for AB-PBI Polymers Under Nitrogen

Sample	T_g	T_{d5}	T_{d10}
i-AB-PBI	500˚C	304˚C	572˚C
70:30 r-AB	512˚C	238˚C	381˚C
50:50 r-AB	515˚C	242˚C	378˚C
30:70 r-AB	379˚C	220˚C	351˚C
AB-PBI	520˚C	268˚C	606˚C

Td5: Temperature at 5% weight loss
Td10: Temperature at 10% weight loss

All samples were then investigated using TGA-MS to analyze the off-gas in that temperature range. The TGA-MS analysis showed loss of water and trace amounts of residual DMSO solvent used in monomer purification. **Figure 4.3** shows a representative TGA-MS analysis showing trace amounts of DMSO and DMSO-H2O complexes. TGA curves of AB-PBI, i-AB-PBI and r-AB-PBI suggest that thermal stability is inversely proportional to the randomization of benzimidazole sequence.

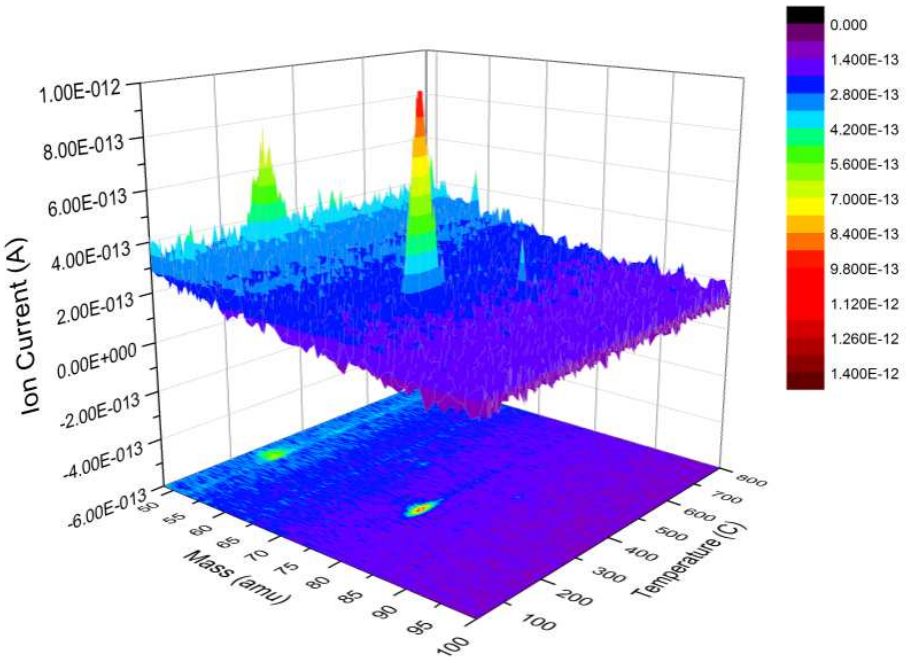

Figure 4.3: TGA-MS analysis of 30:70 r-AB-PBI copolymer.

4.5 Glass Transition Temperature (Tg) Effects

DSC measurements were conducted over the compositional range of the copolymers as an initial method of observing T_g. The DSC thermograms revealed information about the glass transitions, but were not prominent enough for accurate interpretation. Therefore DMA measurements were conducted to precisely determine the glass transition temperatures of the copolymers. Glass transition events were clearly observed as shown in **Figure 4.4** which shows a representative DMA tan δ plot of a 30:70 (i-AB:AB) r-AB-PBI. As the compositional spectrum of the copolymers was evaluated, an anomalous T_g effect was observed. The T_g values for r-AB-PBI compositions are shown in **Figure 4.5**. The theoretical T_g values for the r-AB-PBI were calculated by the Fox equation[29], **Equation 4.1**.

Equation 4.1: $$\frac{1}{T_g} = \frac{W_1}{T_{g,1}} + \frac{W_2}{T_{g,2}}$$

where W_1 and W_2 are the weight fractions and T_{g1} and T_{g2} are the glass transition temperatures of the corresponding homopolymers. The experimental values were compared to theoretical T_g values, and showed a sharp deviation from the predicted values corresponding with the region of highest randomization. The DMA results were confirmed when new polymer batches were evaluated and the measurements were reproduced. The deviation of the experimentally determined Tg values from those predicted by the Fox equation are unusual, but are not unprecedented in literature.[30-32] N.W. Johnston has reviewed sequence distribution glass transition effects in copolymer systems and gave numerous examples of copolymer systems in which deviations from predicted Tg values using the Fox equation were observed.[33] It was observed that as randomization of the benzimidazole sequence approached a maximum, the T_g of the

material was lowered. The lowest T_g value of 379 ˚C was observed in the compositional region where randomization was maximized, near 20:80 i-AB:AB due to weight contribution. This measurement was confirmed using a second sample from a subsequent polymerization. It is surmised that the disrupted regularity of the benzimidazole sequence impacts inter-chain associations and chain packing, resulting in lowered glass transition temperatures. **Figure 4.6** shows the width of the tan δ peak at half-max, which also supports our conclusion that the randomization lowers the inter-chain association. To further evaluate this effect, other fundamental properties such as solubility were evaluated.

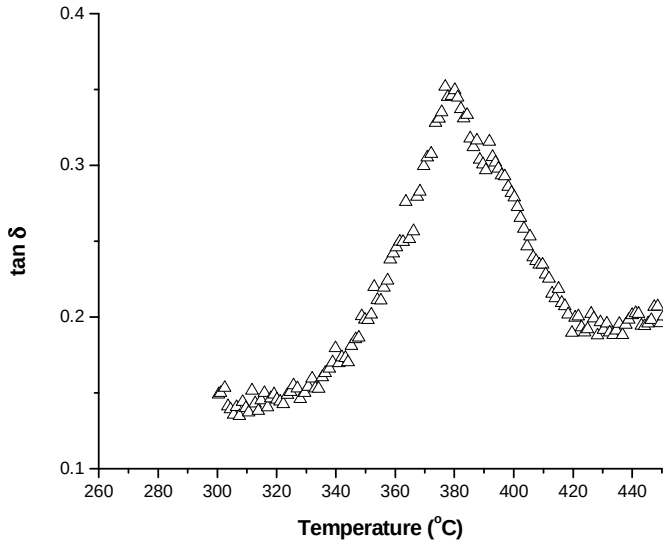

Figure 4.4: DMA tan δ plot of r-AB-PBI (30:70 i-AB:AB).

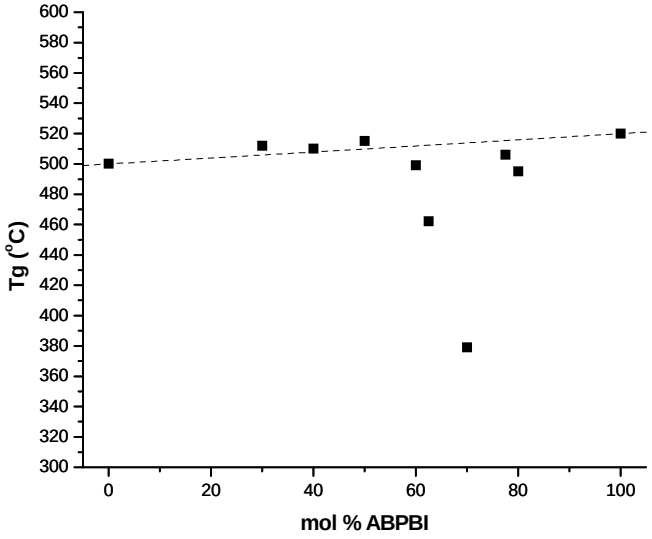

Figure 4.5: Effect of copolymer composition on glass transition temperature, T_g. Repeat measurements were conducted and error of $\pm 1^{\circ}C$ was determined. Dashed line is a calculated plot of the Fox Equation.

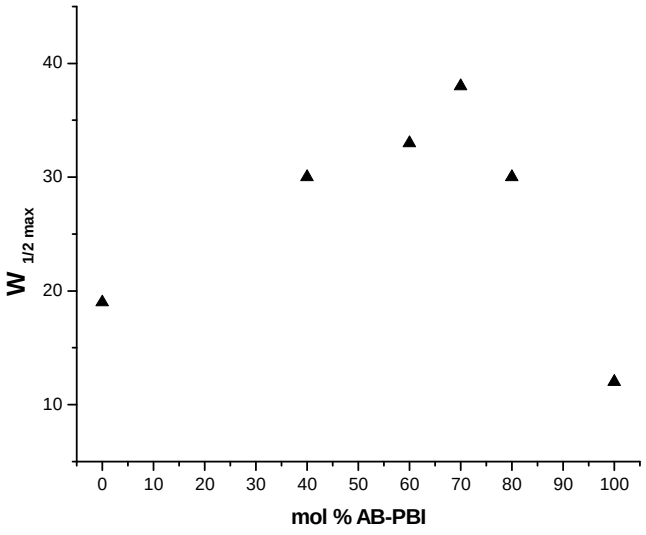

Figure 4.6: Plot of tan δ peak width at half-max with respect to copolymer composition.

4.6 Solubility Study

Polybenzimidazoles are known for their low solubility and are generally only soluble in aprotic or strong acid solvents.[34] Several attempts to increase the solubility of PBI type polymers have been made by incorporation of soluble linkages, functionalities and copolymerizations.[35-39] In this work, the effects of randomization of the benzimidazole sequence on solubility were examined.

Based upon the earlier work of Vogel and Marvel[40,41] concerning solubility of polybenzimidazoles, the solubility of AB-PBI, i-AB-PBI, and r-AB-PBI copolymers were evaluated in several common organic solvents. It was found that all of the AB type PBIs have very low solubility in the organic solvents evaluated, however, a change in solubility was observed across the compositional spectrum of r-AB-PBI samples. This change in solubility results from the randomization of benzimidazole sequence as the chemical composition and functionality are not changed in the r-AB-PBI copolymers. The results of the evaluation, illustrating the sequence dependence on solubility, are shown in **Table 4.3**. Although the change in solubility is not dramatic, it does show that the orientation of the benzimidazole nitrogen atoms in the polymer main chain effects polymer-solvent interactions. These effects were also noted in the previously reported evaluation of the isomeric AB-PBI.[23] To further evaluate these effects, studies of the proton conductivity of phosphoric acid doped membranes were conducted.

4.7 Ionic Conductivity

As previously mentioned, PBI has both proton acceptor and donor sites that contribute to polymer-solvent interactions. These interactions greatly affect the retention of phosphoric acid in PBI membranes. Since proton conduction is proposed to occur by means of the Grotthuss-type (hopping) mechanism[42], orientation of benzimidazole motifs along the polymer chain may affect the proton conduction of the material when

doped with phosphoric acid. In previous work, we have shown that changes in the benzimidazole sequence within the polymer main chain affect the acid retention in the membrane, which in turn affects proton conductivity.[23] In the present work, the proton conductivity of several samples across the compositional spectrum of r-AB-PBI were evaluated. AB-PBI homopolymer samples are not shown in the conductivity evaluations because the membranes with high acid content formed from AB-PBI using the PPA process were found to be unstable at temperatures greater than 100˚C, reverting back to the solution state. A trend was observed in the r-AB-PBI samples, indicating that as randomization of the benzimidazole sequence increased, the conductivity of the material was lowered. **Figure 4.7** shows the temperature dependence of the conductivities measured for i-AB-PBI and r-AB-PBI samples. Repeat measurements were conducted to determine the error of the measurement and to also confirm the observed trend. Moderate to high conductivities were observed for the r-AB-PBI copolymers as compared to previous literature results for AB-PBI with lower amounts of phosphoric acid dopant[43]. The conductivities of the membranes generally scaled with the PA/BI in the membrane. Several of the compositions were found to have very high proton conductivity (~0.2 S/cm) and indicated these membranes were suitable candidates for high temperature fuel cell applications.

Table 4.3: Solubility Evaluation Results for r-AB-PBI Polymers

Polymer	Polymer IV (dL/g)	Qualitative Solubility				
		DMAc (158˚C)	Formic Acid (98˚C)	NMP (195˚C)	DMAc/LiCl (158˚C)	Formic Acid/m-cresol (98˚C)
i-AB-PBI	3.05	+	++	+	+	++
70:30 r-AB-PBI	2.67	++	+	++	+	+

50:50 r-AB-PBI	2.59	+	++	+	++	+
30:70 r-AB-PBI	3.37	+	++	++	+++	+++
AB-PBI	4.63	+	+++	+	++	++

+++: Soluble, ++: Mostly Soluble, +: Very little solubility with polymer swelling, - : No solubility
Solutions were made at 1wt% and held at temperature for 6 days with constant stirring
Observations made on hot solutions.

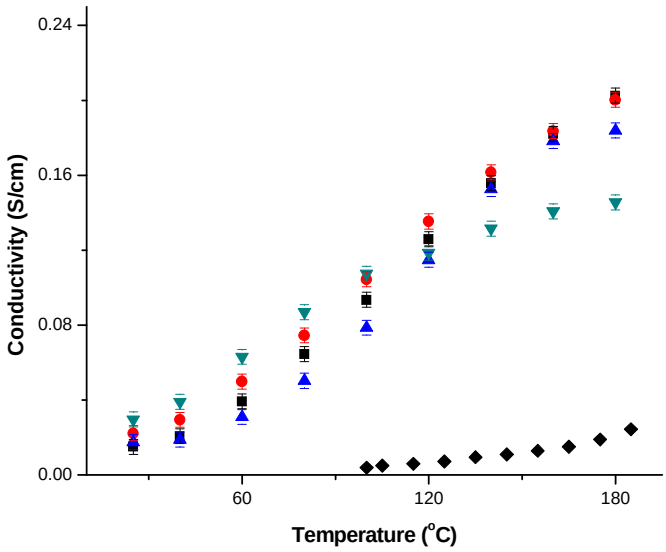

Figure 4.7: Anhydrous conductivity evaluation for r-AB-PBI at 180˚C. [Squares: *i*-AB-PBI, circles: 70:30 i-AB:AB, triangles: 50:50 *i*-AB:AB, inverted triangle: 30:70 *i*-AB:AB, diamonds: reported literature values for poly(2,5-benzimidazole)(AB-PBI).[43]]

Since conductivity is very closely associated with the electrolyte doping level in polymer electrolyte membranes, the relationship between PA retention and r-AB-PBI composition was investigated. **Figure 4.8** shows that compositions above 50 mol % i-AB-PBI in AB-PBI copolymers generally retained more PA than compositions below that percentage. Previous work showed that the i-AB-PBI membranes were more stable with respect to phosphoric acid loading than AB-PBI membranes and had a higher acid retention.[23] This correlates with the trend discussed in **Figure 4.7**. When conductivity

was examined with respect to PA retention, a very clear relationship was observed and is shown in **Figure 4.9**. A critical doping level was observed between 7 and 8 moles of PA per moles of benzimidazole. Above this critical level, conductivities of 0.2 S/cm were consistently observed, whereas below this level, the maximum conductivity achieved was 0.1 S/cm. We believe this trend in acid loading, gel stability and proton conductivity correlates with the Tg trend discussed earlier, and is indicative of the difference in chain packing associated with the sequence randomization.

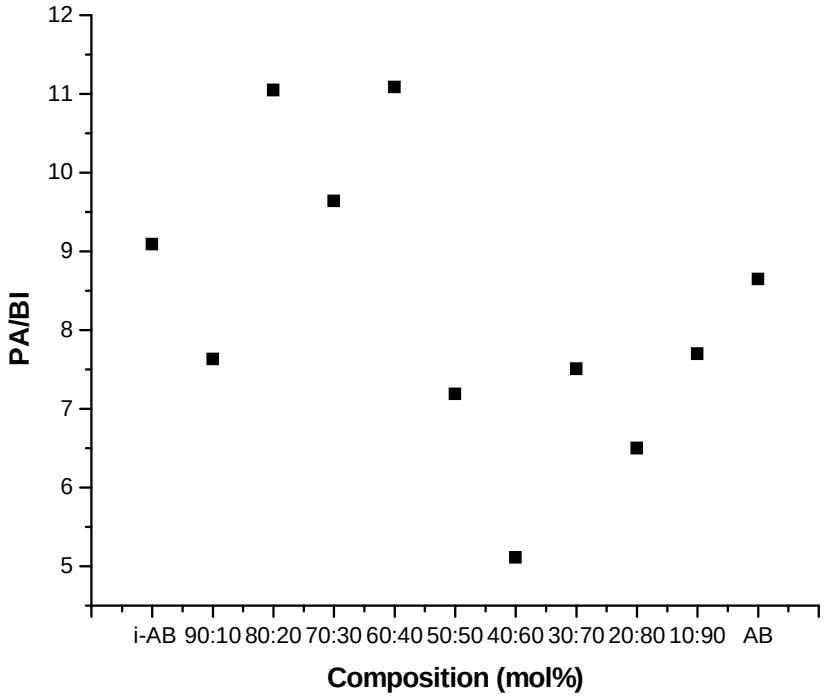

Figure 4.8: Variation of acid loading with copolymer to composition for r-AB-PBI copolymers. PA/BI: moles PA per mole of benzimidazole.

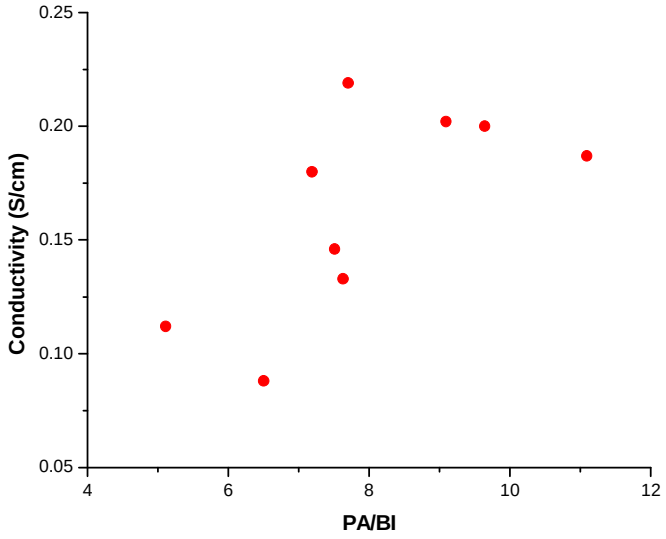

Figure 4.9:Effect of phosphoric acid loading on ionic conductivity at 180˚C for r-AB-PBI copolymers. PA/BI: moles PA per mole of benzimidazole.

4.8 Fuel Cell Performance

Fuel cell performance evaluations were conducted on the r-AB-PBI membranes which included polarization curves using a hydrogen/air fuel/oxidant combination over a range of temperatures (120-180 ˚C). Representative polarization curves are shown for the 60:40 (i-AB:AB) r-AB-PBI along with i-AB-PBI in **Figure 4.10** and **Figure 4.11** respectively. These two samples were selected since they have similar phosphoric acid loadings and similar high temperature anhydrous ionic conductivities. A decrease in performance over the range of temperatures evaluated was observed for the randomized AB-PBI when compared to i-AB-PBI and might indicate a change in polymer-phosphoric acid interactions or an effect of polymer order on the conduction pathways. Lifetime performance studies were conducted on the r-AB-PBI membranes and an average output voltage ranging from 0.5-0.6 V at a current density of 0.2 A/cm^2 was observed which

appear to be stable over several hundred hours, as shown in **Figure 4.12**. A trend in fuel cell performance was observed as the compositional spectrum was shifted towards that of AB-PBI and is shown as the inset of **Figure 4.12**. The trend observed for the fuel cell performance in r-AB-PBI compositions correlates directly with the results observed for conductivity.

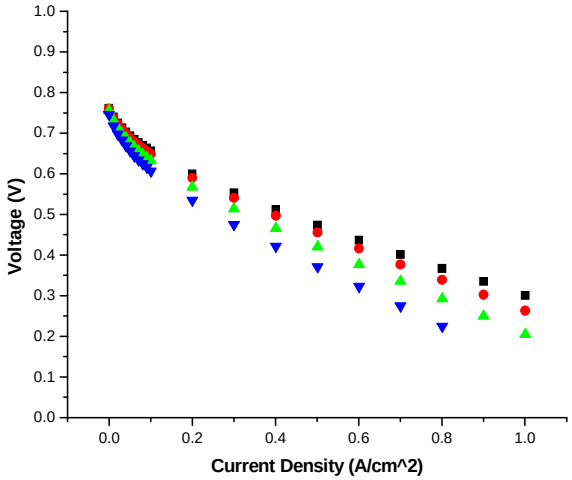

Figure 4.10: Polarization curves for 60:40 *i*-AB-PBI:AB-PBI using H2:Air 1.2:2.0 stoichiometric flows respectively. [Squares: 180˚C, circles: 160˚C, triangles: 140˚C, inverted triangles: 120˚C.]

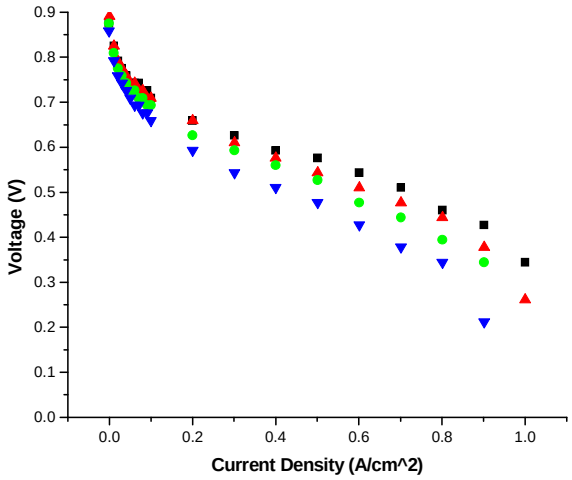

Figure 4.11: Polarization curves for *i*-AB-PBI using H2:Air 1.2:2.0 stoichiometric flows respectively. [Squares: 180˚C, circles: 160˚C, triangles: 140˚C, inverted triangles: 120˚C.]

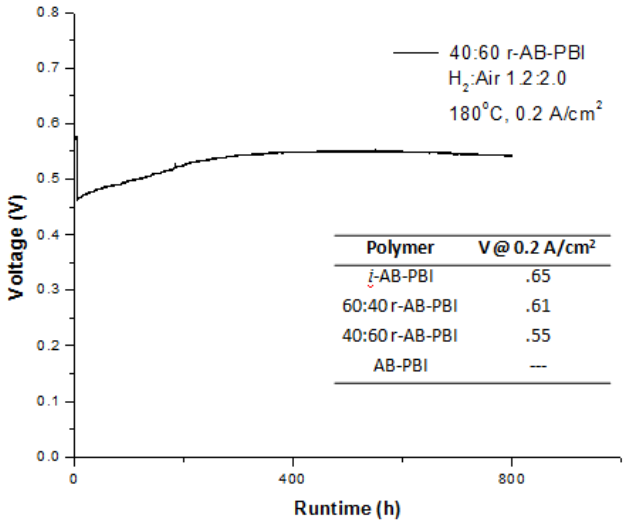

Figure 4.12: Lifetime fuel cell performance of 40:60 (*i*-AB:AB) r-AB-PBI membrane. Inset: Fuel cell performance observed over compositional range for the r-AB-PBI copolymer system. Data collected from fuel cells operated at 180˚C supplied with hydrogen/air at 1.2:2.0 stoichiometric flows respectively, under 1 atm without applied backpressure or humidification.

4.9 Conclusions

A combination of monomer design and copolymerization techniques were used to prepare high molecular weight AB type polybenzimidazoles comprised of a randomized benzimidazole sequence. Disrupted regularity of sequence in the polymer main chain was found to affect fundamental polymer properties, such as chain packing, solubility, glass transition (T_g) temperatures as well as membrane properties for high-temperature fuel cell application.

Phosphoric acid doped random co-polymer membranes of AB-PBI and *i*-AB-PBI were developed using the PPA process. The random AB-PBI polymers had inherent viscosities >2.0 dL/g, and formed mechanically robust films. Thermal evaluations of the

randomized AB-PBI copolymers showed a slight decrease in thermal stability when compared to the ordered structures of AB-PBI and i-AB-PBI. Glass transition (T_g) values measured for the r-AB-PBI showed an unexpected depression when compared to theoretical values, and a maximum T_g depression of 140˚C was observed.

Randomized AB-PBI copolymers showed several differences across the compositional spectrum when compared to the AB-PBI and i-AB-PBI homopolymers, indicating primary chemistry and sequence affect properties of both the polymer and membranes derived thereof. A sequence dependence of solubility was observed as well as trends regarding conductivity, PA retention, and fuel cell performance. Random AB-PBI copolymer membranes were evaluated for mechanical integrity, ionic conductivity and fuel cell performance. An output voltage ranging between 0.5 and 0.6 V at 0.2 A/cm^2 for hydrogen/air at an operational temperature of 180˚C was observed for several r-AB-PBI compositions, indicating these materials would be suitable candidates for high temperature fuel cell applications. When comparing films with similar PA doping and conductivity, an effect on fuel cell performance from sequence isomerism was observed. Thus it appears that both high PA loadings and a more ordered polymer structure contribute to high conductivities and membrane properties.

Overall, this unique copolymer series provided an opportunity to evaluate fundamental properties of polybenzimidazole that would not be achievable in other copolymer systems. Because the copolymers evaluated consist of only repeating 2,5 benzimidazole units, without extraneous functionality or spacers, the fundamental properties of polybenzimidazole regarding sequence, orientation, and regularity are reported.

4.10 References

1. Mader, J.; Xiao, L.; Benicewicz, B. C. *Fuel Cells* **2008**, *No. 3-4*, 165-174.
2. Li, Q.; Jensena, J. O.; Savinell, R. F.; Bjerrum, N. *J. Prog. Polym. Sci.* **2009**, *34*, 449-477.
3. Seel, D. C.; Benicewicz, B. C.; Xiao, L.; Schmidt, T. J. *Handbook of Fuel Cells* **2009**, *5*, 300-312.
4. Sannigrahi, A.; Arnbabu, D.; Sankar, R. M.; Janna, T. *J. Phys. Chem. B.* **2007**, *111*, 12124-12132.
5. Kulkarni, M. P.; Thomas, O. D.; Peckhm, T. J.; Holdcroft, S. *Macromolecules* **2007**, *40*, 983-990.
6. Maity, S.; Jana, T. *Macromolecules* **2013**, *46*, 6814-6823.
7. Xiao, L; Zhang, H.; Jana, T.; Scanlon, E.; Chen, R.; Choe, E. W.; Ramanathan, L. S.; Yu, S.; Benicewicz, B. C. *Fuel Cells* **2005**, *No. 2*, 287-295.
8. Deimede, V.; Voyiatzis, G. A.; Kallitsis, J. k.; Qingfeng, L.; Bjerrum, N. J. *Macromolecules* **2000**, *33*, 7609-7617.
9. Arunbabu, D.; Sannigrahi, A.; Jana, T. *J. Phys. Chem. B.* **2008**, *112*, 5305-5310.
10. Hazarika, M.; Jana, T. *ACS Appl. Mater. Interfaces* **2012**, *4*, 5256-5265.
11. Hazarika, M. *Eur. Polym. J.* **2013**, *49*, 1564-1576.
12. Savinell, R.; Yeager, E.; Tryk, D.; Landau, U.; Wainright, J.; Weng, D.; Lux, K.; Litt, M.; Rogers, C. *J. Electrochem. Soc.* **1994**, *141*, L46-L48.
13. Jayakody, J. R. P.; Chung, S. H.; Duantino, L; Zhang, H.; Xiao, L.; Benicewicz, B. C.; Greenbaum, S. G. *J. Electrochem. Soc.* **2007**, *154*, B242-B246.
14. Choe, E. W.; Choe, D. D. *Polymeric Materials Encyclopedia*; Salamone, J. C., Ed.: CRC Press: New York, **1996**.
15. Samms, S. R.; Wsmus, S.; Savinell, R. R. *J. Electrochem. Soc.* **1996**, *143*, 1225-1232.
16. Yu, S.; Benicewicz, B. C. *Macromolecules* **2009**, *42*, 8640-8648.
17. Kang, S.; Zhang, C.; Xiao, G.; Yan, D.; Sun, G. *Journal of Membrane Science* **2009**, *334*, 91-100.
18. Quan, G.; Benicewicz, B. C. *Journal of Polymer Science, Part A: Polymer Chemistry* **2009**, *47*, 4064-4073.
19. Arindam, S.; Sandip, G.; Sudhangshu, M.; Janna, T. *Polymer* **2010**, *51*, 5929-5941.
20. Ng, F.; Bae, B.; Miyaltake, k.; Watanabe, M. *Chemical Communications* **2011**, *47*, 8895-8897.
21. Mader, J.; Benicewicz, B. *Fuel Cells* **2011**, *No. 2*, 222-237.
22. Seel, D.; Benicewicz B C. *Journal of Membrane Science* **2012**, *405-406*, 57-67,
23. Gulledge, A.; Gu, B.; Benicewicz, B. *Journal of Polymer Science: Part A* **2012**, *50*, 306-313.
24. Flory, P. *Principles of Polymer Chemistry*. Cornell University Press. pp. 321-322.
25. Carothers, W. *J. Amer. Chem. Soc.* **1929**, *51*, 2548-2559.
26. Neuse, E. W. *Adv. Polym. Sci*. **1982**, *47*, 1-42.
27. Buckley, A.; Stuetz, D. E. Serad, G. A. *Encyclopedia of Polymer Science and Technology*, Wiley, NY **1988**, *11*, 572-601.
28. Chung, T. S. *Plastics Engineering* **1997**, *41*, 701-731.

29. Fox, T. G.; Flory, P. J. *Journal of Applied Physics* **1950**, *21*, 581-591.
30. Beevers, R. B. *Trans. Faraday Soc.* **1962**, *58*, 1465-1472.
31. Johnston, N. W. *J. Macromol. Sci. Chem.* **1973**, *A7*, 531-545.
32. Johnston, N. W. *Polym. Prep. Am. Chem. Soc. Div. Polym. Chem.* **1969**, *10*, 608-614.
33. Johnston, N. W. *J. Macromol. Sci. Rev. Macromol. Chem.* **1976**, *C14*, 215-250.
34. Ma, T.; Li, Y. F.; Zhang, S. J.; Yang, C. F.; Gong, C. L.; Zhao, J. J.; Li, Y. F. *Chin. Chem. Lett.* **2011**, *21*, 976-978.
35. Kalehn, J. R.; Orme, C. J.; Peterson, E. S.; Stewart, F. F. Urban-Klaehn, J. M. *Membr. Sci. Technol. Ser*. **2011**, *14*, 295-307.
36. Liang, Z.; Jiang, X.; Xu, H.; Chen, D.; Yin, J. *Macromol. Chem. Phys.* **2009**, *210*, 1632-1639.
37. Kumbharkar, S. C.; Islam, N.; Potrekar, R. A.; Kharul, U. K. *Polymer* **2009**, *50*, 1403-1413.
38. Korshak, V. V.; Izyneev, A. A.; Novak, I. S.; Etonova, E. M.; *Doklady Adademii Nauk SSSR* **1975**, *220*, 597-600.
39. Maity, S.; Sannigrahi, A. Ghosh, S. Jana T. *Eur. Polym. J.* **2013**, *49*, 2280-2292.
40. Vogel, H.; Marvel, C. S. *J. Polym. Sci.* **1961**, *50*, 511-539.
41. Vogel, H.; Marvel, C. S. *J. Polym. Sci. Part A* **1963**, *1*, 1531-1541.
42. Agmon, N. *Chem. Phys. Lett.* **1995**, *224*, 456-462.
43. Asensio, J. A.; Gomez-Romero, P. *Fuel Cells* **2005**, *5*, 336-343.

Chapter 5: Structure Property Relationships in Phenyl-AB Polybenzimidazole Copolymer Systems[3]

[3] Gulledge, A. L.; Fishel, K.; Bottorff, M.; Benicewicz, B. *Journal of Polymer Science, Part A: Polymer Chemistry* **2014**, In preparation.

5.1 Introduction

Polybenzimidazoles (PBIs) are a class of aromatic heterocyclic polymers that are well suited for high-temperature applications.[1] PBIs are well known for their high chemical and thermal stabilities during high temperature fuel cell operation conditions.[2] PBI possesses both proton donor and acceptor sites that allow for specific interactions with polar solvents such as PA.[3,4] PBI polymers doped with PA are readily achievable and have been noted as a promising material for use as polymer electrolyte membranes in high-temperature PEM fuel cell devices.[5] PBI polymer membranes doped with PA used in PEM fuel cells are capable of operating at temperatures up to 200˚C because they do not rely on water for proton conduction.[6] Due to the excellent thermal and chemical properties of PBI membranes doped with PA, these materials are excellent candidates for low-cost and high-performance fuel cell applications. To date, a large variety of PBI polymers have been synthesized and studied in the literature,[7-12] however, PBI chemistry still remains an important area of interest in the high-temperature PEM fuel cell community.

With the evolution of polymer science in terms of copolymer structure, chemical functionalization, and targeted applications, structure property relationships have become an increasingly important aspect of new materials development. Generally, specific structure property relationships are evaluated that apply only to the parent chemistry of the system. Herein, we have performed a side by side comparison of AB/p-PBI type polybenzimidazoles to determine structure-property relationships that can be applied broadly to polymer electrolyte membrane systems. The unique combination and contrast of properties in the AB/p-PBI and i-AB/p-PBI systems provided insight into effects

resulting from structural modification, sequence orientation, stability, and randomization. The AB-PBI and p-PBI system addresses aspects of acid loading, stability, and structural modification, whereas the i-AB-PBI and p-PBI system addresses comparisons of sequence isomerism and randomization between two high performance PEM materials. The comparative evaluation of both copolymer systems provided greater insights and applicability to PEM material design than analysis of either system alone. The structures and corresponding synthetic schemes are shown in **Scheme 5.1** and **Scheme 5.2** for the AB/p-PBI and i-AB/p-PBI systems, respectively. Polymer electrolyte membranes from these copolymer systems were prepared using the PPA process and were evaluated in terms of composition, mechanical integrity, ionic conductivity and fuel cell performance. The properties of the copolymer membranes were compared to all corresponding homopolymer structures.

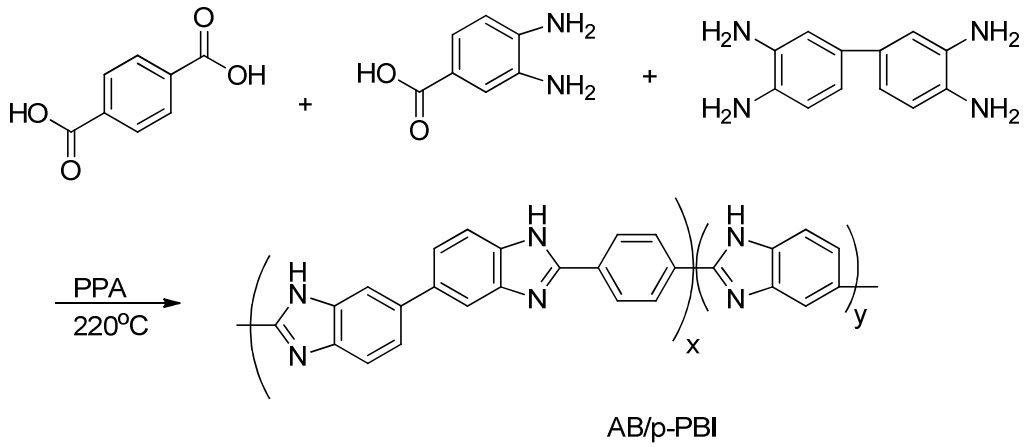

Scheme 5.1: Reaction scheme for the polymerization of AB/p-PBI copolymers.

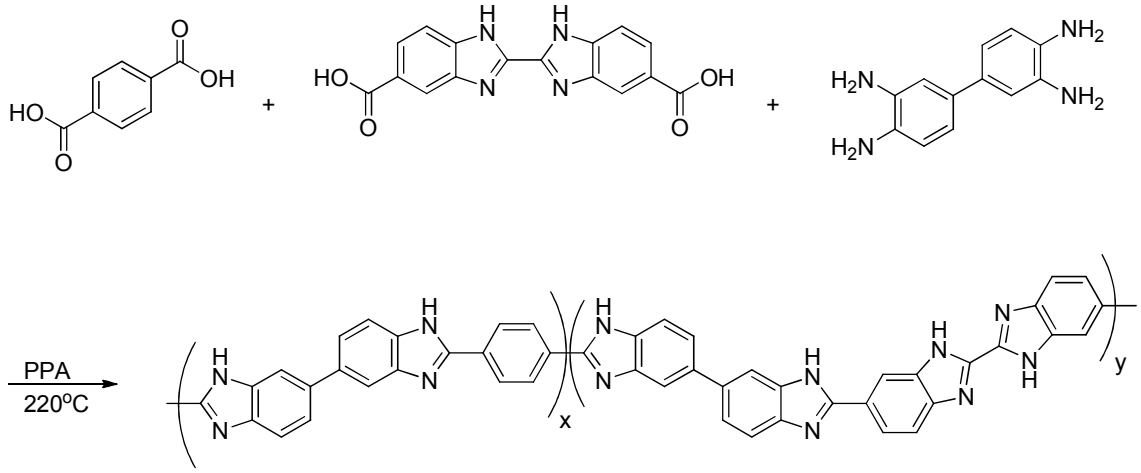

i-AB/p-PBI

Scheme 5.2: Reaction scheme for the polymerization of i-AB/p-PBI random copolymers.

5.2: Polymerization of Copolymer Systems

Random AB/p-PBI copolymers were synthesized by the PPA process[13] using 3,4-diaminobenzoic acid, 3,3',4,4'-tetraaminobiphenyl, and terephthalic acid monomers as shown in **Scheme 5.1**. Assuming the principal of equal reactivity,[14] polymerization of the above monomers results in randomized incorporation of the AB benzimidazole and *p*-phenyl PBI motif within the polymer backbone. Polymerization of the above described system is an AA-BB-AB polycondensation. Molar increments between 0 and 100% of the corresponding homopolymers were synthesized by variation of AB monomer content while maintaining an exact stoichiometric ration between the AA and BB monomers. As defined by the Carothers equation[15], an exact stoichiometric ratio is needed between AA and BB monomers to achieve high-molecular weight polymer. Polymerization conditions were modified from the previously reported synthetic conditions of AB-PBI[16] and p-PBI[17] based on copolymer composition. Polymer solutions were then directly cast and humidified to obtain corresponding gel-membranes. Mechanical properties, ionic

conductivity, and high-temperature fuel cell performance were then measured on the gel membranes.

Random i-AB/p-PBI copolymers were also synthesized by the PPA process[13] using 2,2'-bisbenzimidazole-5,5'-dicarboxylic acid, 3,3',4,4'-tetraaminobiphenyl, and terephthalic acid monomers as shown in **Scheme 5.2**. Randomized incorporation of the 2,2 and 5,5 benzimidazole linkages and p-phenyl PBI motifs is assumed considering the principal of equal reactivity[14] and is consistent with our previous studies.[18] Polymerization of the above monomers is an AA-BB-AA type polycondensation polymerization in which two different diacid monomers were used. Molar increments ranging from 0 to 100% of each corresponding homopolymer were synthesized by varying the ratio of the diacid monomers. Polymerization conditions were modified from previously reported synthetic conditions of i-AB-PBI and p-PBI based on copolymer composition. Polymer solutions were then directly cast and humidified to obtain corresponding gel-membranes. Mechanical properties, ionic conductivity, and high-temperature fuel cell performance were measured on the gel membranes.

5.3: Membrane Compositional Analysis

All polymer membranes were evaluated via titration to determine the phosphoric acid, water, and polymer content. The data provided in **Table 5.1**, showed that there was no significant change in polymer, acid or water content as the copolymer composition shifted from p-PBI to AB-PBI. The 90:10 (AB/p-PBI) copolymer showed an unusually high polymer content and lower acid loading. This is likely due to a shorter time allowed for hydrolysis. Comparison of the AB-PBI and p-PBI homopolymers indicates a higher acid retention for AB-PBI. The relatively consistent acid compositions of the AB/p-PBI

copolymers indicates that adding even a small amount of AB-PBI to the p-PBI system increases the acid retention properties of the copolymer membranes.

The data shown in **Table 5.2** for the i-AB/p-PBI copolymers indicated consistent acid and water percentages although a gradual increase in polymer content was observed. A gradual change in the polymer content was expected as the increase in final polymer content of the membranes directly correlates with an increase in monomer charge of the polymerization. The relatively consistent percentages of water and acid as the composition was changed from one homo-polymer to the other indicates the acid retention effect in this system was equally offset by the polymer content of the membranes. For membranes with higher i-AB-PBI content, a lower acid retention was observed as these membranes had higher polymer content and equal acid percentages than corresponding membranes with higher p-PBI content and lower percentage polymer content. This indicates a naturally higher acid retention of p-PBI than i-AB-PBI polymers. This is also supported by comparison of the p-PBI and i-AB-PBI homopolymers evaluated. The higher acid retention of p-PBI over i-AB-PBI had evident effects when evaluating this system's mechanical properties and ionic conductivity.

5.4: Mechanical Property Evaluations

The mechanical properties of both copolymer systems were evaluated at room temperature. The properties reported are an average result of five random area membrane samples. The mechanical properties measured in the ABp-PBI copolymer system are shown in **Table 5.3**. The AB/p-PBI copolymers showed both stress and elongation at break in the range of 1.0-3.7MPa and 130-890%, respectively. The stress-at-break remained relatively consistent across the copolymer compositional range, but was very

low for the AB-PBI homopolymer. This is likely due to the high acid retention of pure AB-PBI. The elongation-at-break approximately followed the same pattern as the stress-at-break throughout the copolymer compositional spectrum. The 60:40 (AB:para) region of the copolymers showed an increase in both stress-at-break and elongation-at-break, however, this result directly correlated with an increased inherent viscosity, and is therefore not attributed to the copolymer composition.

Table 5.1: Characterization Results for AB/p-PBI Copolymers and Membranes

Sample	Composition (mol %)		Monomer Charge (wt%)	IV† (dL/g)	Membrane Composition (wt %)			Mol PA/BI*
	AB-PBI	p-PBI			H_2O	Polymer	PA#	
1	0	100	3.25	3.05	41.20	3.50	55.30	12.51
2	10	90	4.95	2.71	22.81	4.78	72.41	23.50
3	20	80	5.15	2.38	23.75	4.62	71.63	23.70
4	30	70	4.87	3.51	25.42	4.16	70.42	25.44
5	40	60	4.94	1.98	24.43	4.84	70.73	21.55
6	50	50	5.53	4.51	26.65	4.63	68.72	21.41
7	60	40	5.32	6.41	26.24	4.23	69.53	23.11
8	70	30	5.02	4.45	27.34	4.68	67.98	19.80
9	80	20	4.10	3.23	29.67	6.68	63.65	12.52
10	90	10	4.50	1.89	30.00	8.73	61.28	8.81
11	100	0	4.84	1.8	22.25	3.93	73.82	22.56

†: IV: Inherent viscosity as measured in H_2SO_4 at 30˚C
#: PA: Phosphoric acid
*: Mol PA/BI: Mol of Phosphoric acid per mol benzimidazole

Table 5.2: Characterization Results for i-AB/p-PBI Copolymers and Membranes

Sample	Composition (mol %)		Monomer Charge (wt%)	IV† (dL/g)	Membrane Composition (wt%)			Mol PA/BI*
	i-AB-PBI	p-PBI			H_2O	Polymer	PA#	
1	0	100	3.25	3.05	41.20	3.50	55.30	12.51
12	10	90	3.05	1.46	41.72	7.20	51.08	8.40
13	20	80	4.01	2.13	43.77	6.76	49.47	8.67
14	30	70	4.09	1.96	42.26	6.67	51.07	9.07
15	40	60	3.92	1.44	40.90	6.94	52.16	8.90
16	50	50	4.49	1.27	41.27	7.31	51.42	8.33

17	60	40	4.99	0.94	42.12	7.38	50.50	9.07
18	70	30	4.95	1.60	37.84	7.35	54.81	8.84
19	80	20	5.01	1.64	40.20	8.30	51.50	7.34
20	90	10	5.98	1.52	41.30	9.00	49.70	6.53
21	100	0	6.21	3.05	37.76	7.26	54.98	9.08

†: IV: Inherent viscosity as measured in H_2SO_4 at 30˚C
#: PA: Phosphoric acid
*: Mol PA/BI: Mol phosphoric acid per mol benzimidazole

Table 5.3: Mechanical Evaluation Data for AB/p-PBI Copolymer Membranes*.

Sample	AB-PBI content (mol %)	p-PBI content (mol %)	IV (dL/g)	Stress at break (MPa)	St. dev.	Elongation at break (%)	St. dev.
1	0	100	3.05	1.93	0.11	798	10
2	10	90	2.71	2.40	0.2	453	29
3	20	80	2.38	1.80	0.2	295	56
4	30	70	3.51	1.40	0.1	230	34
5	40	60	1.98	0.95	0.1	132	9
6	50	50	4.51	1.90	0.1	258	14
7	60	40	6.41	3.70	0.3	889	11
8	70	30	4.45	1.70	0.2	575	46
9	80	20	3.23	1.30	0.2	413	47
10	90	10	1.89	1.20	0.2	382	52
11	100	0	1.80	0.30	0.02	35	4.9

*: Mechanical properties are an average of five random area samples measured at room temperature.

The mechanical evaluations for the i-AB/p-PBI copolymer system are shown in **Table 5.4**. This data indicates that the stress-at-break and elongation-at-break were affected by randomization of the homopolymers. As the composition shifted to a higher degree of randomization, these properties decreased, and as composition approached a more ordered sequence, these properties increased. This result is not completely unexpected as p-PBI and i-AB-PBI are both mechanically robust high-performance polymer electrolyte membrane materials. The stress strain curves of the i-AB/p-PBI copolymers shown in **Figure 5.1** indicates a higher Young's modulus for copolymers that are higher in i-AB-PBI content. This effect can be understood by comparing the flexibility of the para-phenyl moiety to the locked benzimidazole sequence of i-AB-PBI.

The increased Young's modulus of the higher i-AB-PBI content copolymers could indicate that the copolymers with a higher p-PBI content have a higher degree of polymer chain flexibility, however, further research would be needed to confirm this.

Table 5.4: Mechanical Evaluation Data for i-AB/p-PBI Copolymer Membranes*.

Sample	i-AB-PBI content (mol %)	p-PBI content (mol %)	IV (dL/g)	Stress at break (MPa)	St. dev.	Elongation at break (%)	St. dev.
1	0	100	3.05	1.93	0.11	798	10
12	10	90	2.71	1.51	0.19	282	47
13	20	80	2.38	1.44	0.08	210	09
14	30	70	3.51	1.22	0.05	186	07
15	40	60	1.98	0.94	0.06	107	12
16	50	50	4.51	0.64	0.11	69	16
17	60	40	6.41	0.26	0.04	14	4
18	70	30	4.45	0.39	0.02	42	4
19	80	20	3.23	0.57	0.03	64	7
20	90	10	1.89	1.99	0.16	309	42
21	100	0	1.8	1.09	0.03	186	13

*: Mechanical properties are an average of five random area samples measured at room temperature.

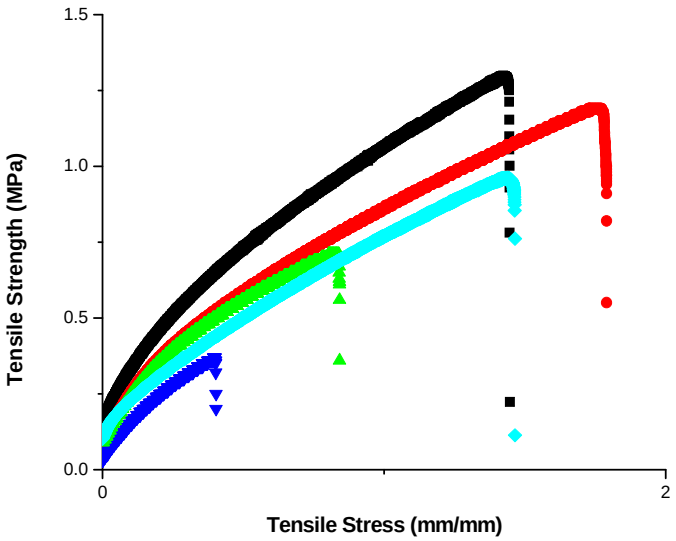

Figure 5.1: Stress strain curves for the i-AB/p-PBI random copolymers. [squares: i-AB-PBI, circles: 70:30 i-AB/p-PBI, triangles: 50:50 i-AB/p-PBI, inverted triangles: 30:70 i-AB/p-PBI, diamonds: p-PBI]

5.5: Ionic Conductivity

Ionic conductivities were evaluated for all polymer electrolyte membranes. The conductivities for AB/p-PBI random copolymers are shown in **Figure 5.2**. As AB-PBI content increased, ionic conductivity decreased. AB-PBI has been reported to be unstable at high temperatures when produced by the PPA process.[13] This is evident in the 90:10 (AB/p-PBI) copolymer, where conductivity decreased significantly as the temperature increased above 60˚C. Attempts to measure the ionic conductivity of pure AB-PBI were unsuccessful for these high phosphoric acid content membranes. Notably, all of the other compositions were stable up to 160˚C.

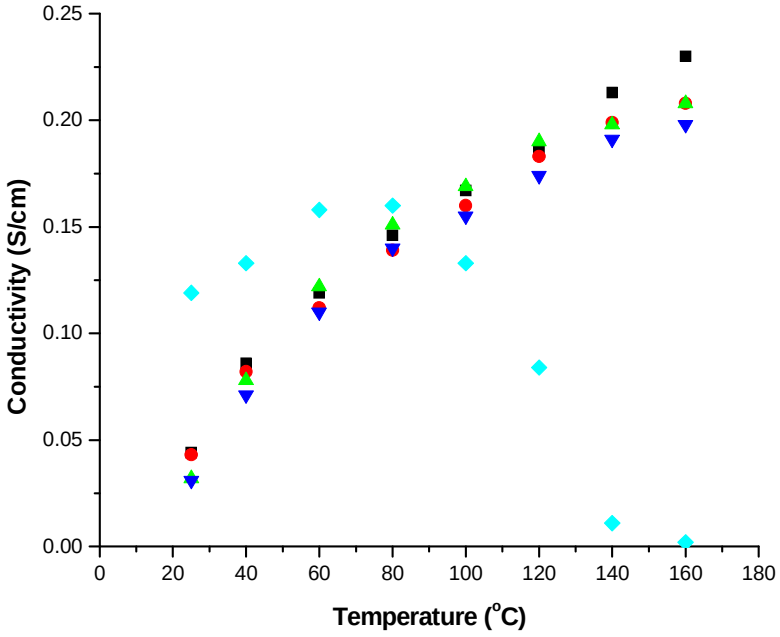

Figure 5.2: Ionic conductivities for AB/p-PBI random copolymers. [squares: 10:90 AB/p-PBI, circles: 30:70 AB/p-PBI, triangles: 50:50 AB/p-PBI, inverted triangles: 70:30 AB/p-PBI, diamonds: 90:10 AB/p-PBI]

The ionic conductivities of the i-AB/p-PBI random copolymers are shown in **Figure 5.3**. The conductivities of the i-AB/p-PBI random copolymers showed a correlation between ionic conductivity and p-PBI content. As mentioned previously, as the copolymer composition shifted from i-AB-PBI to p-PBI higher acid retention was observed for copolymers with higher p-PBI content. It has been shown that PA doping levels in these systems directly affects the proton conductivity measured.[16] All i-AB/p-PBI copolymers showed desirable proton conductivities for high-temperature fuel cell applications.

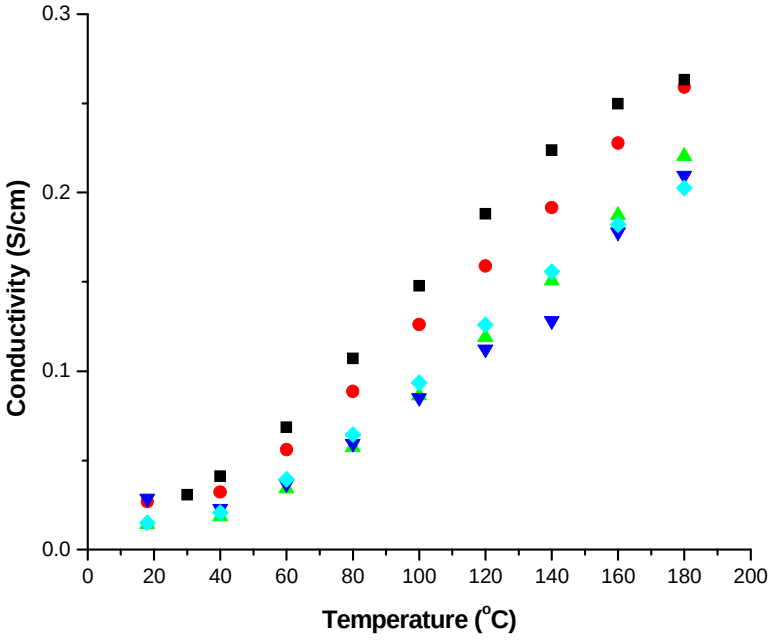

Figure 5.3: Ionic conductivities for i-AB/p-PBI random copolymers. [squares: p-PBI, circles: 30:70 i-AB/p-PBI, triangles: 50:50 i-AB/p-PBI, inverted triangles: 70:30 i-AB/p-PBI, diamonds: i-AB-PBI]

5.6: Fuel Cell Performance

Fuel cell polarization curves for the AB/p-PBI copolymers are shown in **Figure 5.4**. Among the AB/p-PBI copolymers evaluated for high-temperature fuel cell performance, similar performances were observed and directly correlated with the percentages of PA in the membranes (Table 5.1). Stable performance was not observed when AB-PBI content was higher than 70%. This is directly related to the instability of AB-PBI membranes doped with phosphoric acid at these temperatures.

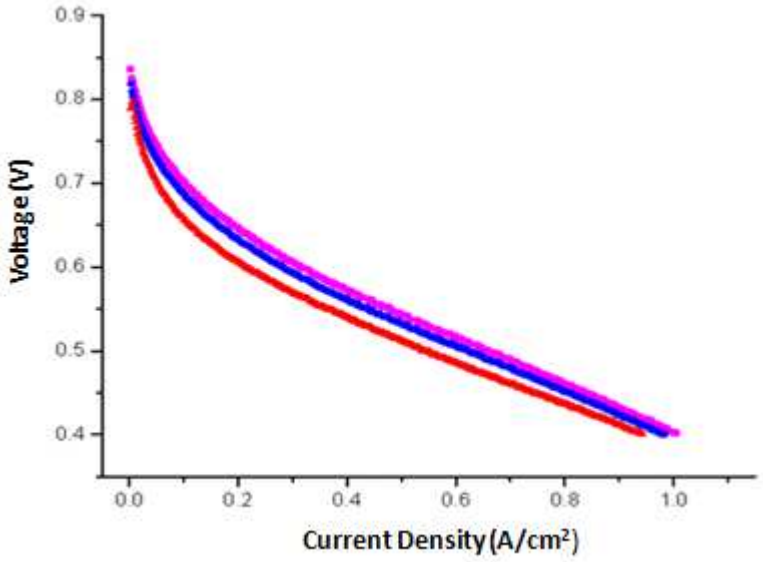

Figure 5.4: Polarization curves for AB/p-PBI copolymers at 160˚C using H_2:Air 0.6:2.0 stoichiometric flows, respectively. Performance evaluations were conducted without applied pressure or humidification. [squares: 60:40 AB/p-PBI, circles: 30:70 AB/p-PBI, triangles, 70:30 AB/p-PBI]

Fuel cell polarization curves for the i-AB/p-PBI copolymers are shown in **Figure 5.5**. The data for the i-AB/p-PBI copolymers indicates an effect of randomization on fuel cell performance. As the PBI sequence was randomized, fuel cell performances decreased, and were observed to increase as compositions moved towards a more ordered sequence. The fuel cell performance evaluations for the i-AB/p-PBI copolymers did not

correlate with the percentage of PA of the membranes. This is consistent with trends observed in the mechanical properties for this copolymer system. Several of the i-AB/p-PBI random copolymers were also evaluated in lifetime studies. All i-AB/p-PBI copolymers showed stable performances for the entire duration measured (over 1000 hours) as shown in **Figure 5.6**.

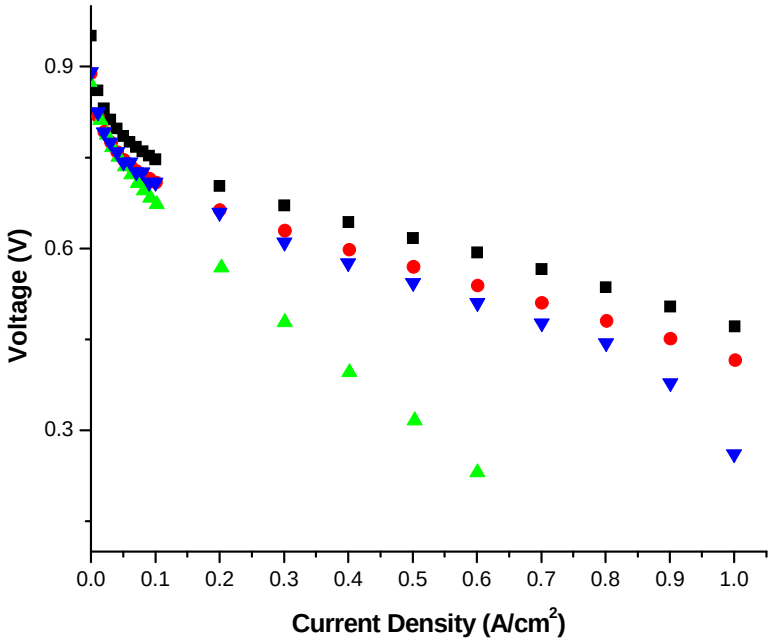

Figure 5.5: Polarization curves for i-AB/p-PBI copolymers at 180˚C using H_2:Air 1.2:2.0 stoichiometric flows respectively. Performance evaluations were conducted without applied pressure or humidification.[squares: p-PBI, circles: 30:70 i-AB/p-PBI, triangles: 50:50 i-AB/p-PBI, inverted triangles: i-AB-PBI]

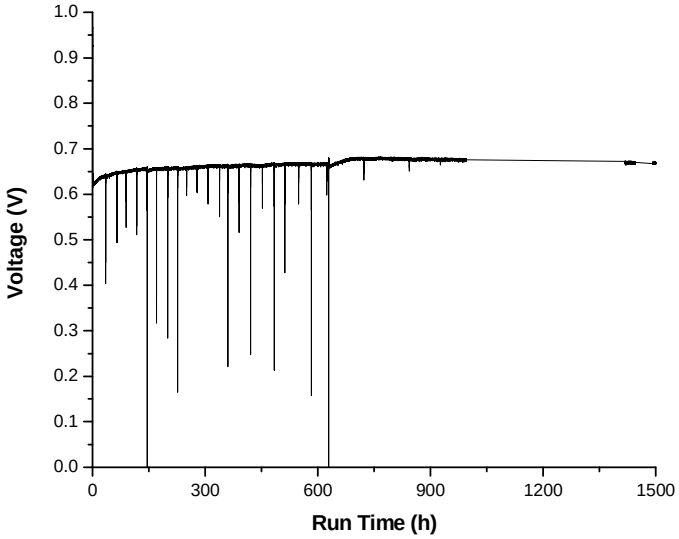

Figure 5.6: Lifetime performance for 30:70 i-AB/p-PBI copolymer at 180˚C at 0.2 A/cm^2 with H_2:Air 1.2:2.0 stoichiometric flows, respectively. Momentary drops in voltage are attributed to interruptions of measurement by the voltage detector. Data was recorded every 2 seconds for 1500 hours.

5.7: Conclusions

Random copolymers of AB-PBI and p-PBI termed AB/p-PBI and of i-AB-PBI and p-PBI termed i-AB/p-PBI were synthesized via the PPA process and evaluated for membrane composition, mechanical properties, ionic conductivities, and high-temperature fuel cell performances. Random copolymers were synthesized under conditions similar to optimized conditions for the corresponding homopolymer closest in composition.

Compositional analysis of the AB/p-PBI copolymers showed similar membrane compositions in terms of phosphoric acid, water, and polymer content. Comparison of the random AB/p-PBI copolymers and the AB-PBI and p-PBI homopolymers indicated that a small amount of AB-PBI incorporation caused an increase in the acid retention of the system which remained relatively constant throughout the copolymer compositional

series. In the i-AB/p-PBI copolymer system, acid retention was gradually increased as the composition was shifted from i-AB-PBI to p-PBI, but was offset by the increase in polymer content of the final membrane resulting in relatively consistent acid doping levels. These results were further supported when comparisons were made with the i-AB-PBI and p-PBI homopolymers.

Room-temperature mechanical evaluations were conducted for acid doped membranes for both copolymer systems. Evaluation of the AB/p-PBI copolymer system indicated that mechanical properties were relatively consistent in terms of polymer structure as the copolymer composition was varied. Changes that were observed in the mechanical properties were attributed to differences in inherent viscosity and acid loadings, and could not be attributed to polymer compositional changes. However, mechanical property evaluation of the i-AB/p-PBI copolymers indicated that the changes were attributable to the polymer composition. The stress-at-break and elongation-at-break decreased as randomization of the system increased. This is consistent with previous evaluations of randomization in ordered systems.[18] A decrease in Young's moduli of the i-AB/p-PBI copolymers was observed as the p-PBI content increased. This could be attributed to an increased flexibility of the para-phenyl moiety of p-PBI as compared to the locked benzimidazole structure of i-AB-PBI.

Ionic conductivity measurements were conducted under anhydrous conditions at temperatures up to 180˚C for both random copolymer systems. Evaluations of the AB/p-PBI random copolymers showed a decrease of ionic conductivity as AB-PBI content increased. Since the AB/p-PBI copolymers had similar acid loadings, this effect was attributed to the instability of AB-PBI membranes with high acid loadings at elevated

temperatures. This effect was also evident by the ionic conductivity behavior of the 90:10 (AB/p-PBI) copolymer, which exhibited a significant drop in ionic conductivity above 80˚C. AB-PBI homopolymer membranes were unstable at elevated temperatures and ionic conductivity measurements could not be conducted. The i-AB/p-PBI copolymer membranes showed an increase in ionic conductivity with increased p-PBI content. These effects were largely attributed to the acid-to-polymer ratio of the membranes.

Fuel cell performance evaluations were conducted on both the AB/p-PBI and i-AB/p-PBI copolymer membranes. Fuel cell performances of the AB/p-PBI copolymer membranes directly correlated with the percent acid content of the membrane. Membranes with greater than 70% AB-PBI content were found to be unstable under the fuel cell operation conditions, indicative of the instability of PA-doped AB-PBI membranes at elevated temperature. Fuel cell performances of the i-AB/p-PBI copolymer membranes decreased as randomization of the copolymers increased. Although the fuel cell performance decreased with randomization, all i-AB/p-PBI copolymer membranes were found to have suitable high-temperature fuel cell performances. Lifetime evaluations were conducted for several i-AB/p-PBI compositions and all showed stable fuel cell performances for more than 1000 hours.

These studies highlight an important design criterion for membrane gel stability. Copolymerization of PBI polymers that create highly randomized polymer sequences seem to disrupt chain packing in the highly swollen gel state. Thus, even when the phosphoric acid content in the membranes is retained, the gel thermal stability is likely to decrease, thus rendering these membranes unsuitable for long-term stability at high temperatures.

5.8 References

1. Yu, S.; Xiao, L.; Benicewicz, B. C, *Fuel Cells* **2008**, *3-4*, 165-174.
2. Shogbon, C.; Brousseau, J.; Zhang, H.; Benicewicz, B. C.; Akpalu, Y. *Macromolecules* **2006**, *39*, 9409-9418.
3. Kojima, T. *J. Polym. Sci. Polym. Phys. Ed.* **1980**, *18*, 1685-1695.
4. Sannigrahi, A.; Arunbabu, D.; Sankar, R. M.; Janna, T. *Macromolecules* **2007**, *40*, 2844-2851.
5. Savinell, R.; Yeager, E.; Tryk, D.; Landau, U.; Wainright, J. Weng, D.; Lux, K.; Litt, M.; Rogers, C. *J. Electrochem. Soc.* **1994**, *141*, L46-L48.
6. Jayakody, J. R. P.; Chung, S. H.; Durantino, L.; Zhang, H.; Xiao, L.; Benicewicz, B. C.; Greenbaum, S. G. *J. Electrochem. Soc.* **2007**, *154*, B242-246.
7. Mader, J.; Xiao, L. Benicewicz, B. C. *Adv. Polym. Sci.* **2008**, *216*, 63-124.
8. Li, Q.; Jensen, J. O.; Savinell, R. F.; Bjerrum, N. J. *Prog. Polym. Sci.* **2009**, *34*, 449-477.
9. Seel, D. C.; Benicewicz, b. C. Xiao, L. Schmidt, T. J. *Handbook of Fuel Cells* **2009**, *5*, 300-312.
10. Sannigrahi, A.; Arunbabu, D.; Sankar, R. M.; Jana, T. *J. Phys. Chem. B* **2007**, *111*, 12124-12132.
11. Kulkarni, M. P.; Thomas, O. D.; Peckhm, T. J.; Holdcroft, S. *Macromolecules* **2007**, *40*, 983-990.
12. Maity, S.; Jana, T. *Macromolecules* **2013**, *46*, 6814-6823.
13. Xiao, L.; Zhang , H.; Jana, T.; Scanlon, E.; Chen, R.; Choe, E. W.; Ramanathan, L. S.; Yu, S.; Benicewicz, B. C. *Fuel Cells* **2005**, *2*, 287-295.
14. Flory, P. *Principles of Polymer Chemistry*; Cornell University Press: Ithaca, **1953**, pp 321-322.
15. Carothers, W. J. *J. Am. Chem. Soc.* **1929**, *51*, 2548-2559.
16. Gulledge, A. L.; Gu, B.; Benicewicz, B. C. *J. Polym. Sci. A* **2012**, *50*, 306-313.
17. Yu, S.; Zhang, H.; Xiao, L.; Choe, E. W.; Benicewicz, B. C. *Fuel Cells* **2009**, *9*, 318-324.
18. Gulledge, A. L.; Chen, X.; Benicewicz, B. *Journal of Polymer Science, Part A: Polymer Chemistry* **2014**, *52*, 619-628.

Chapter 6: Sulfuric Acid-Doped Polybenzimidazole based Membrane for All-Vanadium Redox Flow Battery Application[4]

[4] Gulledge, A. L.; Pezeshki, A.; Sun, C.; Mench, M.; Zawodzinski, T.; Benicewicz, B. *Journal of Power Sources* **2014**, In preparation.

6.1 Introduction

As the global demand for energy increases, the need for and development of energy technology becomes more relevant. Effective utilization of renewable energy resources, such as wind, solar and geothermal, are required to sustain our ever-growing population while also decreasing our carbon emissions.[1,2] As a plausible solution to this challenge, large scale energy storage is envisioned to serve as an important component of energy sustainability. Technologies concerning energy storage are complementary with renewable energy technologies such as solar and wind power that cannot produce energy on a continuous basis.[3,4]

Among energy storage devices, redox flow batteries (RFB) with the capability to decouple energy and power densities are relatively easy to scale up and hence hold a great potential for large scale energy storage applications.[5] Of the variety of RFB systems known to date, one of particular interest is the all-vanadium redox flow battery (VRFB). VRFBs operate through the redox couples of vanadium ions among four oxidation states, V(II)/V(III) and V(IV)/V(V) for negative and positive respectively, mediated by concentrated acidic solutions.[6-10] By adopting the same metal for both sides of the electrochemical cell, concerns raised by the cross-contamination in multi-element systems is then eliminated. VRFBs are therefore among the more well-studied and characterized RFB system.

The typical cell is comprised of two electrodes separated by a polymer electrolyte membrane. As each electrode governs the redox reaction individually during operation, the membrane mediates ionic conduction and prevents crossover of the species between the two compartments. Nafion, is the most commonly used membrane material in VRFB

studies, and possesses a good balance between conductivity and stability. However, the high cost of the perfluorinated polymer hinders large-scale implementation and drives the demand for hydrocarbon alternatives.[11-14]

Polybenzimidazole (PBI) membranes have been shown to have exceptional performance in various electrochemical devices because of their high ionic conductivity when imbibed with various acid electrolytes.[15,16] PBI, with promising chemical and thermal stability[17,18], is a basic polymer (pka ~5.25)[19] and possesses both proton donor and acceptor sites. This property induces a specific interaction between the proton acceptor/donor sites and polar solvents, allowing direct acid incorporation into the polymer matrix. [20-22] To date, a large variety of PBI polymers have been synthesized and studied in the literature[23-45]; however, a sulfonated polybenzimidazole might be best suited for VRFB applications. Sulfonated PBI (s-PBI) has been shown to be stable in a sulfuric acid environment[46,47], which is incorporated in VRFB systems.[48] Compared to the commonly adopted ion-conducting polymers, the acid-doped PBI possesses a distinct conduction mechanism which drives interest in VRFB application.[49]

Herein, for the first time, sulfuric acid doped s-PBI was adopted as a membrane material in a VRFB system. The s-PBI polymer and membrane was characterized by molecular weight measurements, membrane composition, ionic conductivity, and mechanical properties. Polarization curves and cycling test analyses were performed to examine the membrane and overall cell performance. Furthermore, the decay of the cell open circuit voltage (OCV) was also monitored to evaluate the vanadium permeation of the membranes. Nafion films were identically tested for comparison.

6.2 Polymerization of Sulfonated Polybenzimidazole (s-PBI)

A large variety of PBI and PBI derivative membranes, including homopolymer[50-52], random copolymer[53-55], and polymer blends[56-59], have been evaluated for use as proton exchange materials in various electrochemical devices[47,60,61]. Among these, when selecting a potential candidate for VRFB systems, sulfonated PBI was selected due to its high stability in sulfuric acid.[22] As illustrated in **Scheme 6.1**, this variant of PBI is synthesized with a pre-sulfonated monomer, mono-sodium 2-sulfoterephthalate. Using a pre-sulfonated monomer allows for controlled placement of and incorporation of the sulfonate group in every repeat unit of the polymer. Alternate sulfonation techniques, such as post polymerization sulfonation[62-64], or chemical grafting of functionalized motifs[65,66], often result in random placement of the sulfonate group in addition to non-uniform or uncontrolled sulfonation. As previously mentioned, PBI has both proton acceptor and donor sites that contribute to polymer-solvent interactions. These interactions significantly contribute to the retention of sulfuric acid in PBI membranes. Since proton conduction is proposed to occur by means of the Grotthuss-type (hopping) mechanism[67], it is surmised that uniform orientation of sulfonate motifs along the polymer chain may facilitate the proton conduction of the material when doped with sulfuric acid. Ionic conductivities for s-PBI membranes imbibed in 30wt% sulfuric acid baths have been reported to be greater than 0.5S/cm at 100˚C.[22] For these reasons, s-PBI was chosen as a potential candidate to serve as the separator in the VRFB system.

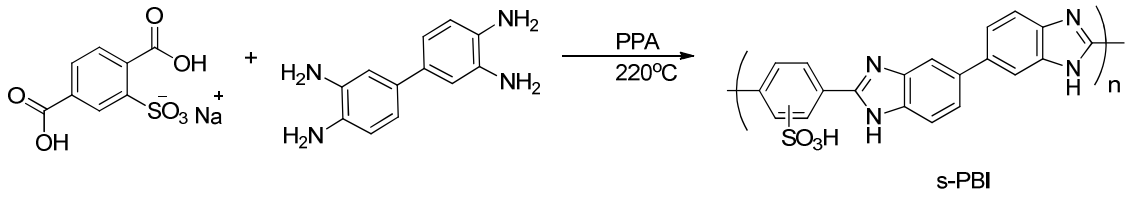

Scheme 6.1: Polymerization of s-PBI.

6.3: Material Processing

The s-PBI utilized for the reported experimental evaluations was synthesized following a previously reported procedure.[22] The resulting polymer solution was cast as previously described resulting in a phosphoric acid doped membrane. To achieve the sulfuric acid doped analogue of the membrane, an acid exchange procedure was conducted. At this phase, prior to experimental evaluations of the material, removal of the phosphoric acid and subsequent sulfuric acid imbibing required verification. Acid exchange was confirmed via titration using the difference in pKa and equivalence points between sulfuric acid (-3, 1.92) and phosphoric acid (2.15, 7.20, 12.35) respectively. Moreover, titration across the full pH spectrum post acid exchange revealed only two equivalence points, verifying that only sulfuric acid remained in the membrane. Once the acid exchange was verified, subsequent evaluation of the material was conducted.

6.4 Mechanical Analysis

Mechanical properties of the s-PBI membranes were evaluated with both phosphoric acid and sulfuric acid for determination of how the material was affected mechanically by the acid exchange process. It has been shown that the type of electrolyte dopant and doping levels can affect the mechanical properties of gel membranes.[68] **Figure 6.1** shows the stress-strain curves of five random area samples taken from the as-

cast phosphoric acid doped s-PBI membranes. The samples evaluated that were doped with phosphoric acid had Young's moduli ranging from 2.152 MPa to 2.858 MPa and an average Young's modulus of 2.48 MPa. With a relatively low measured Young's modulus, the phosphoric acid doped s-PBI would most likely require some type of structural support for device application. However, as previously mentioned, the sulfuric acid doped s-PBI is of interest. **Figure 6.2** shows the stress-strain curves of five random area samples taken from the sulfuric acid doped s-PBI membranes. The samples evaluated that were doped with sulfuric acid had Young's moduli ranging from 6.467 MPa to 8.043 MPa and an average Young's modulus of 7.32 MPa, a 295% increase. This increase is partially attributed to the lower doping level of sulfuric acid as compared to phosphoric acid, but does not completely account for the significant increase in the Young's modulus of the material. During the acid exchange process, shrinking of the membrane as a result of phosphoric acid removal was observed. Subsequent swelling of the membrane was also observed when imbibing with sulfuric acid. The thickness of the films was reduced from 0.35mm to 0.27mm as measured from the phosphoric acid doped and sulfuric acid doped films respectively. It is surmised that the reduction in acid doping level and overall decrease in film thickness attributed to the significant increase in the Young's modulus. Mechanical properties, as well as other significant material properties, are shown in **Table 6.1**.

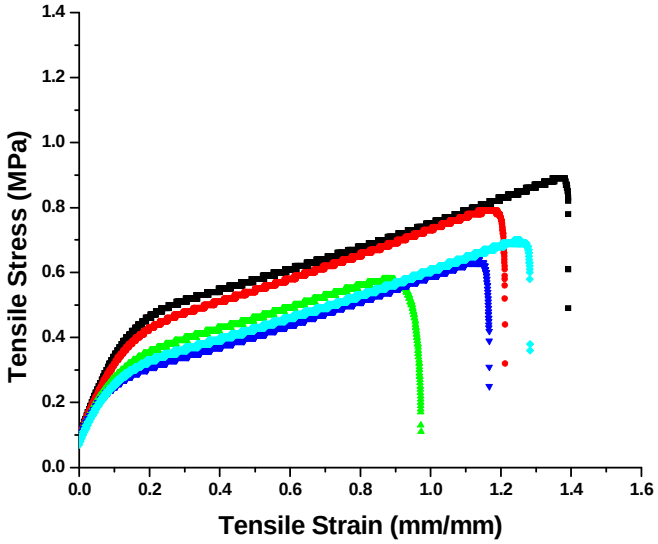

Figure 6.1: Stress-strain curves for as cast PA doped s-PBI membranes. Mechanical analyses were conducted at ambient temperature. Multiple samples from random membrane area are shown.

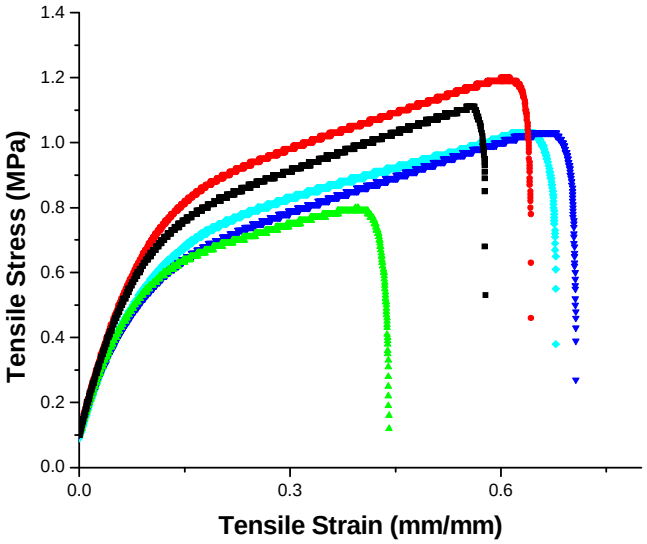

Figure 6.2: Stress-strain curves for sulfuric acid doped s-PBI membranes. Mechanical analyses were conducted at ambient temperature. Multiple samples from random membrane area shown.

Table 6.1: Characterization analysis for s-PBI membranes.

Sample	IV (dL/g)	Tensile Strength (MPa)	*Young's Moduli (MPa)	Membrane Composition (wt%)		
				H_2O	Phosphoric Acid	Polymer
s-PBI	0.96	0.76	2.42	34.61	58.26	7.13
				Membrane Composition (wt%)		
				H_2O	Sulfuric Acid	Polymer
		1.09	7.52	53.11	36.11	10.78

*: Average of five samples measured at ambient temperature.

6.5: Polarization Curve Analysis

Polarization curves for cells with s-PBI, Nafion 117 and Nafion NR-211 were obtained at 50% state of charge in single-pass mode as shown in **Figure 6.3** and the corresponding ASR is plotted as a function of current density in **Figure 6.4**.Given that the s-PBI membrane was considerably thicker (**Table 6.2**) than Nafion NR-211 with similar measured ASR, the conductivity of s-PBI in an operating VRFB was noticeably higher than NR-211. At low current densities (<500mA/cm^2), the iR-free polarization curves are similar for all three membranes. As charge transfer and ohmic over-voltages within the electrode are considered as the dominating losses in this regime, this result is expected since the voltage loss contributed by the membrane resistance has been corrected and identical electrodes were used. Nevertheless, the difference in iR-free voltage was observed for current densities at 600mA/cm^2 and above implying distinct mass transport behavior. We suspect that this is caused by the differences in the membrane swelling properties, i.e. more significant s-PBI swelling may compress the electrode more strongly, resulting in a change in porous structure and increased concentration polarization relative to a Nafion-based membrane.

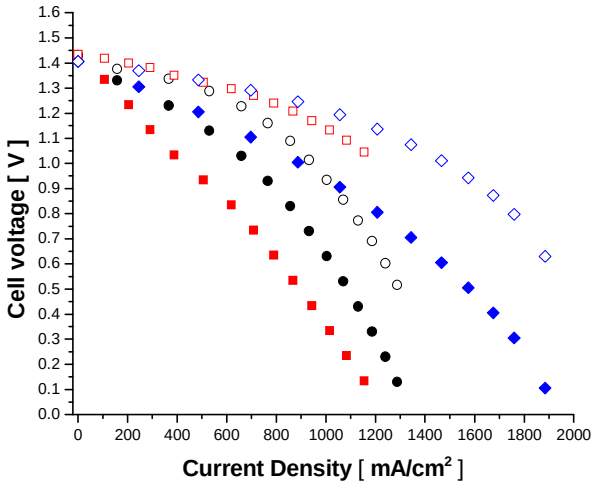

Figure 6.3: Actual and iR-free polarization curves at 50% state of charge. [Circles: s-PBI, squares: N117, diamonds: NR-211; solid: cell voltage, hollow: iR-corrected cell voltage]

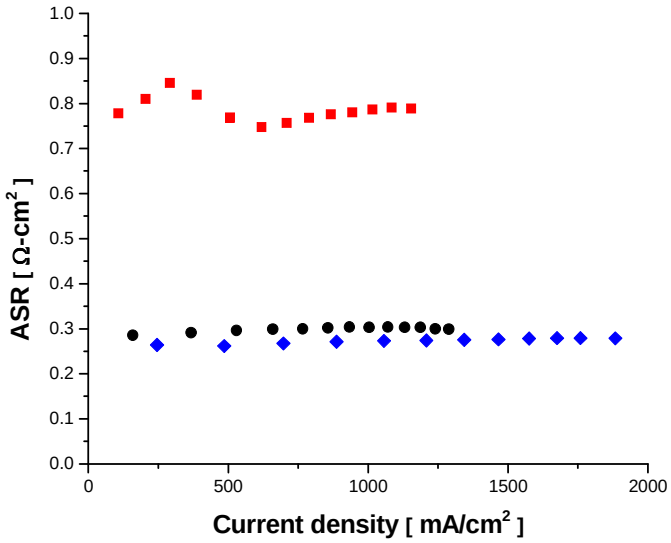

Figure 6.4: Area square resistance measured during 50% state of charge polarization curves. [Circles: s-PBI, squares: N117, diamonds: NR-211]

Table 6-2: Membrane thickness

Sample	Thickness* (μm)
s-PBI	62
NR-211	34
N117	193

*: Membranes were soaked in de-ionized water at room temperature for one hour and subsequently blot-dried prior to cell assembly.

6.6: Open Circuit Voltage (OCV) Decay

The open-circuit voltage decay, shown in **Figure 6.5** shows that Nafion NR-211 permits a high rate of vanadium diffusion, resulting in a rapid voltage loss for a cell held at open circuit. S-PBI exhibits a slower rate of voltage decline, with N117 showing the greatest suppression of vanadium ion crossover. Apparent in the s-PBI voltage decay curve is a significant drop in voltage at 0.7 hours; this large rapid drop is attributed to a complete depletion of V(II) in the negative half-cell, as probed using a reference electrode. The initial rapid drop in voltage seen in all curves is due to the sensitivity of the Nernst equation to small changes in species concentrations at high states of charge. Combining **Figure 6.4** and **Figure 6.5**, it is clearly shown that the membrane thickness dominates the trade-off between membrane resistance and vanadium crossover for Nafion materials. However, s-PBI with a distinct conduction mechanism shows a similar membrane resistance to NR-211 but with twice the thickness to exhibit moderate OCV decay caused by vanadium permeation.

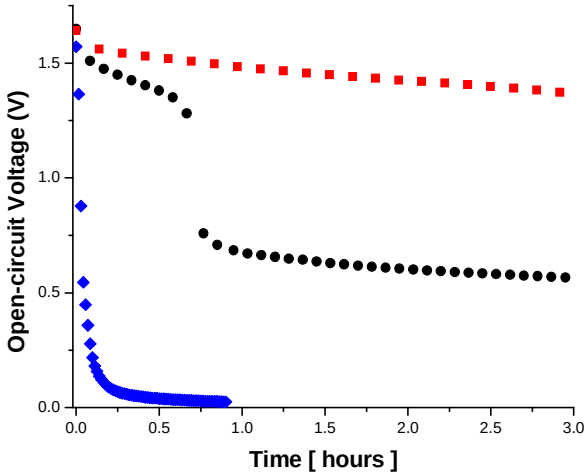

Figure 6.5: Open-circuit cell voltage decay from fully charged with static pumps. [Circles: s-PBI, squares: N117, diamonds: NR-211]

6.7: Cycling Performance

While the polarization curve analysis suggested Nafion NR-211 as the superior membrane, results of the OCV decay experiment indicate that s-PBI suppresses vanadium crossover much more effectively. Charge/discharge cycle profiles are shown in **Figure 6.6**. Indeed, as seen in **Figure 6.7**, cycling tests carried out show that Nafion NR-211 has an unacceptably low coulombic efficiency below 60% due to significant vanadium species crossover, whereas s-PBI has a coulombic efficiency near 100%, on par with the much thicker Nafion 117 membrane. Nafion NR-211 has a slightly higher voltage efficiency as a result of a slightly lower ASR. s-PBI appears to combine the superior coulombic efficiency of Nafion 117 with the high voltage efficiency of NR-211, resulting in the highest overall energy efficiency, with an average energy efficiency of 84% compared to 77% with Nafion 117 and 45% in NR-211. Capacity fade is an inevitable feature of VRFBs, as vanadium crossover results in a net depletion of vanadium species

in one half-cell. **Figure 6.8** shows the discharge capacity for each membrane tested; Nafion NR-211 and s-PBI have much higher absolute capacities as a result of lower cell resistances widening the operating window of the battery. That is, the lower ohmic losses allow the battery to reach further into the state of charge window without reaching the cutoff potential. The normalized capacity was calculated by dividing the cycle absolute discharge capacity by the absolute discharge capacity of 1st cycle for each membrane. The s-PBI membrane exhibits the least drastic normalized capacity fade. The ASR was measured at the end of each charge and discharge step, as shown in **Figure 6.9**. The results indicate a stable ASR for s-PBI, similar to the stability of the ASR seen in Nafion-based membranes, suggesting negligible membrane degradation within the given testing period.

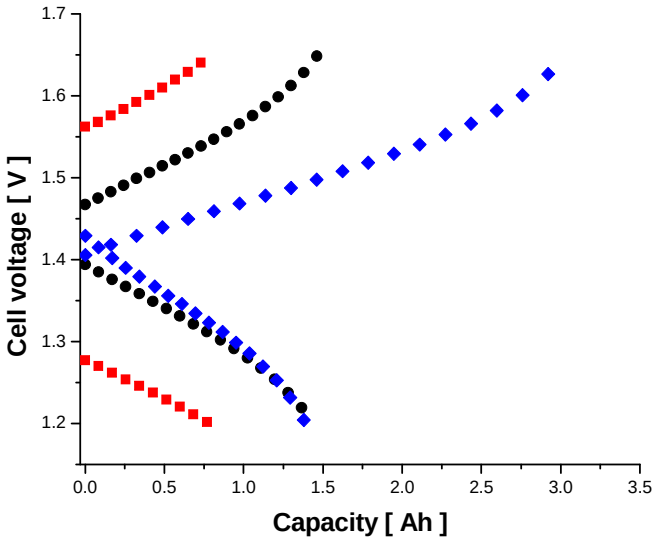

Figure 6.6: Charge and discharge profiles of first cycle during cycling performance tests. [Circles: s-PBI, squares: N117, diamonds: NR-211]

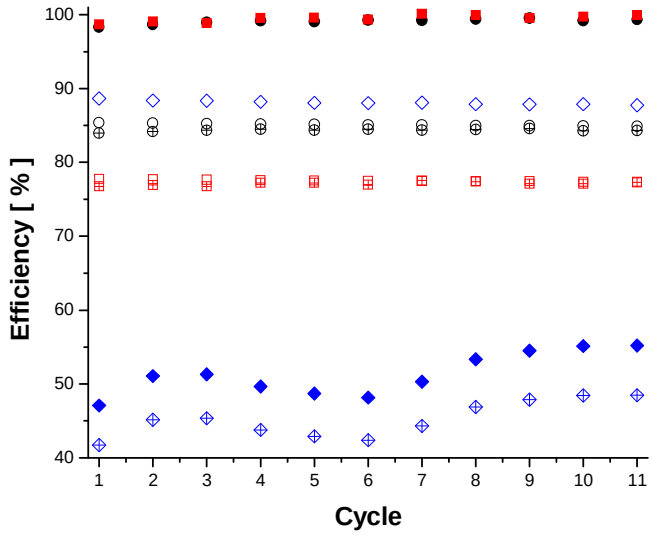

Figure 6.7: Cycle efficiencies for cycling performance tests. [Circles: s-PBI, squares: N117, diamonds: NR-211; solid: coulombic efficiency; hollow: voltage efficiency; crosses: energy efficiency]

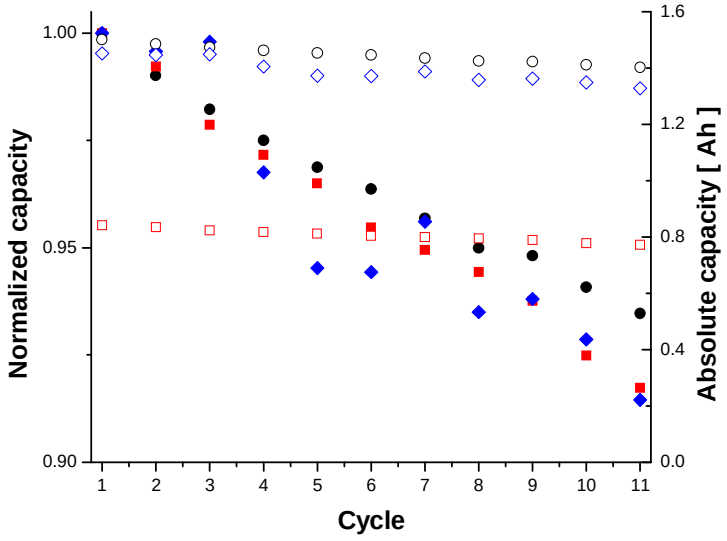

Figure 6.8: Normalized and absolute discharge capacities from cycling performance tests. [Circles: s-PBI, squares: N117, diamonds: NR-211; solid: normalized capacity, hollow: absolute capacity]

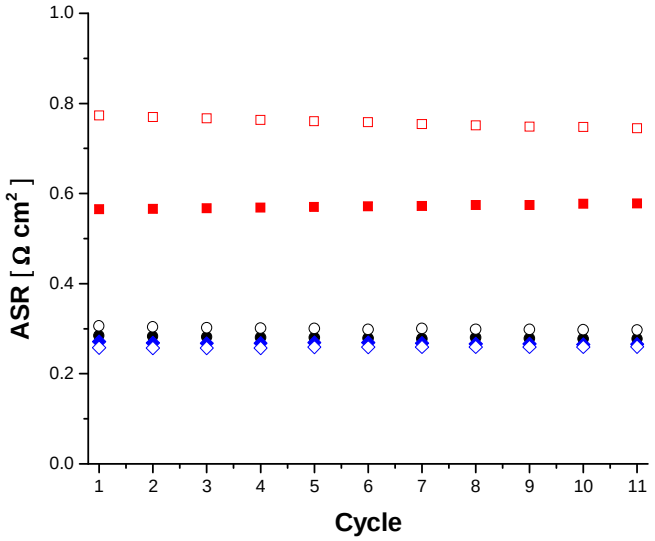

Figure 6.9: Cell ASR measured at end of charge and discharge steps from cycling performance tests. [Circles: s-PBI, squares: N117, diamonds: NR-211; solid: end of charge, hollow: end of discharge]

6.8: Conclusions

s-PBI membranes were synthesized with uniformly placed sulfonate groups along the polymer backbone utilizing a pre-sulfonated monomer. s-PBI membranes were prepared via the PPA process and subsequently imbibed with sulfuric acid. s-PBI membranes doped with sulfuric acid were selected for evaluations in a VRFB due to the exceptionally high conductivity and material stability in sulfuric acid. Mechanical analysis of the as-cast and sulfuric acid doped s-PBI membranes showed a significant increase in the Young's modulus of the material (295%). The increase in mechanical properties was attributed to membrane composition and thickness changes during the acid exchange process. Complete acid exchange was verified via titration analysis.

Performance evaluations were conducted on sulfuric acid doped s-PBI membranes in an operating single-cell VRFB. Polarization curves, OCV decay, and cycle

testing were carried out. Exact replicate evaluations were performed on Nafion 117 and Nafion NR-211 for comparison. Obtained ASR data indicates a notably higher conductivity for s-PBI than Nafion in an operating VRFB. Differences in cell voltage at higher current densities were attributed to differences in membrane swelling. Swelling of the s-PBI membrane compressed the electrode, resulting in lower porosity and increased concentration polarization relative to Nafion-based materials.

Open circuit voltage decay studies indicated that the s-PBI membranes evaluated exhibited a slower rate of voltage decline and vanadium diffusion than that of Nafion NR-211. Cycle testing evaluations also indicated that s-PBI suppresses vanadium crossover much more effectively than Nafion NR-211. Coulombic efficiency of s-PBI was measured to be nearly 100%, comparable with the much thicker Nafion 117 membrane. Discharge capacity evaluations showed excellent discharge capacities for both Nafion NR-211 and s-PBI, allowing for a greater window of operation for VRFB systems. s-PBI also showed the least drastic normalized capacity fade, indicative of the vanadium crossover resistance of the material. Stable area specific resistances were observed for s-PBI, suggesting minimal performance degradation within the testing period.

Overall, s-PBI was found to be an excellent material candidate as a high-performance membrane for VRFB systems. s-PBI appears to combine the superior coulombic efficiency of Nafion 117 with the high voltage efficiency of Nafion NR-211, resulting in the highest overall energy efficiency, with an average efficiency of 84% compared to 77% with Nafion 117 and 45% in Nafion NR-211. Future work will consist

of preparing thinner s-PBI membranes for performance evaluations in VRFB systems and evaluating reinforcement strategies to lower membrane swelling.

6.9: References

1. Hoffert, M. I.; Caldeira, K.; Jain, A. K.; Haltes, E. F.; Harvey, D. L.; Potter, S. D.; Schlesinger, M. E.; Schneider, S. H.; Watts, R. G.; Wigley, T. M. L.; Wuebbles, D. J. *Nature* **1998**, *39*, 881-884.
2. Lior, N. *Energy* **2010**, *35*, 3976-3994.
3. Dresselhaus, M. S.; Thomas, I. L. *Nature* **2001**, *414*, 332-337.
4. Hoffert, M. I.; Caldeira, K.; Benford, G.; Criswell, D. R.; Green, C.; Herzog, H.; Jain, A. K.; Kheshgi, H. S.; Lackner, K. S.; Lewis, J. S.; Lightfoot, D. H.; Manheimer, W.; Mankins, J. C.; Mauel, M. E.; Perkins, J. L.; Schlesinger, M. E.; Volk, T.; Wigley, T. M. L. *Science* **2002**, *298*, 981-987.
5. Weber, A. Z.; Mench, M. M.; Meyers, J. P.; Ross, P. N.; Gostick, J. T.; Liu, Q. *Journal of Applied Electrochemistry* **2011**, *41*, 1137-1164.
6. Kazacos, M.; Cheng, M.; Skyllas-Kazacos, M. *Journal of Applied Electrochemistry* **1990**, *20*, 463-467.
7. Rychik, M. Skyllas-Kazacos, M. *Journal of Power Sources* **1987**, *19*, 45-54.
8. Rychik, M. Skyllas-Kazacos, M. *Journal of Power Sources* **1988**, *22*, 59-67.
9. Skyllas-Kazacos, M. *Journal of the Electrochemical Society* **1986**, *133*, 1057-?.
10. Sum, E. Skyllas-Kazacos, M. *Journal of Power Sources* **1985**, *15*, 170-190.
11. Chen, D.; Hickner, M. A. *Physical Chemistry Chemical Physics: PCCP* **2013**, *15*, 11299-11305.
12. Fujimoto, C. H.; Hickner, M. A.; Cornelius, C. J.; Loy, D. A. *Macromolecules* **2005**, *38*, 5010-5016.
13. Hickner, M. A.; Ghassemi, H.; Kim, Y. S.; Einsla, B. R.; McGrath, J. E. *Chemical Reviews* **2004**, *104*, 4587-4611.
14. Kim, S.; Yan, J.; Schwenzer, B.; Zhang, J.; Li, L.; Liu, J.; Yang, Z. G.; Hickner, M. A. *Electrochemistry Communications* **2010**, *12*, 1650-1653.
15. Quan, G.; Benicewicz, B. C. *Journal of Polymer Science Part A: Polymer Chemistry* **2009**, *47*, 4064-4073.
16. Perry, K.; Eisman, G.; Benicewicz, B. Journal *of Power Sources* **2008**, *117*, 478-484.
17. Yu, S.; Xiao, L.; Benicewicz, B. C. *Fuel Cells* **2008**, *No. 3-4*, 165-174.
18. Shogbon, C.; Brousseau, J.; Zhang, H.; Benicewicz, B. C.; Akpalu, Y. *Macromolecules* **2006**, *39*, 9409-9418.
19. Sannigrahi, A.; Ghosh, S.; Maity, S.; Jana, T. *Polymer* **2010**, *51*, 5929-5941.
20. Kojima, T.; *Journal of Polymer Science: Polymer Physics Ed.* **1980**, *18*, 1685-1695.
21. Sannigrahi, A.; Arunbabu, D.; Sankar, R. M.; Jana, T. *Macromolecules* **2007**, *40*, 2844-2851.
22. Mader, J. A.; Benicewicz, B. C. *Macromolecules* **2010**, *43*, 6706-6715.
23. Mader, J.; Xiao, L.; Schmidt, T. J.; Benicewicz, B. C.; *Adv. Polym. Sci.* **2008**, *216*, 63-124.

24. Li, Q.; Jensena, J.O.; Savinell, R.F.; Bjerrum, N.J. Prog. *Polym. Sci.* **2009**, *34*, 449-477.
25. Seel, D.C.; Benicewicz, B.C.; Xiao, L.; Schmidt, T.J. *Handbook of Fuel Cells* **2009**, *5*, 300-312.
26. Wainright, J. S.; Wang, J. T.; Savinell, R. F.; Litt, M.; Moaddel, H.; Rogers, C. *Proceedings of the Electrochemical Society* **1994**, *94*, 255-64.
27. Gilham J. K.; *Science* **1963**, *139*, 494-495
28. Strauss, E. L. *Polymer Eng. Sci.* **1966**, *6*, 24-29.
29. Weng, D.; Wainright, J. S.; Landau, U.; Savinell, R. F. *Proceedings of the Electrochemical Society* **1995**, *95-23*, 214-225.
30. Hill, J. R. *Adhesives Age* **1966**, *9*, 32-36.
31. Delman, A. D.; Kovacs, h. N.; Simms, B. B. *Journal of Polymer Science, Part A-1: Polymer Chemistry* **1968**, *6*, 2117-2126.
32. Wang, J. T.; Savinell, R. F.; Wainright, J.; Litt, M.; Yu, H. *Electrochim. Acta* **1996**, *41*, 193-197.
33. Wang, J. T.; Wainright, J. S.; Savinell, R. F.; Litt, M. *J. Appl. Electrochem.* **1996**, *26*, 751-756.
34. Szita, J.; Marvel, Carl S. *Journal of Applied Polymer Science* **1970**, *14*, 2019-2024.
35. Korshak, V. V.; Teplyakov, m. M.; Fedorova, R. D. *Journal of Polymer Science, Part A-1: Polymer Chemistry* **1971**, *9*, 1027-1043.
36. Bingham, M. A.; Hill, B. J. *Journal of Thermal Analysis* **1975**, *7*, 347-358.
37. Wang, J. T.; Wasmus, S.; Savinell, R. F. *J. Electrochem. Soc.* **1996**, *143*, 1233-1239.
38. Hilado, C. J.; LaBossiere, L. A.; Leon, H. A.; Kourtides, D. A.; Parker, j. A.; Hsu, M. S. *Journal of Combustion Toxicology* **1976**, *3*, 211-236.
39. Kovar, R. F.; Arnold, F. E. *Journal of Polymer Science, Polymer Chemistry Edition* **1976**, *14*, 2807-2817.
40. Chatfield, D. A.; Einhorn, I. N. *Journal of Polymer Science, Polymer Chemistry Edition* **1981**, *19*, 601-618.
41. Weng, D.; Wainright, J. S.; Landau, U.; Savinell, R. F. *J. Electrochem. Soc.* **1996**, *143*, 1260-1263.
42. Xing, B.; Savadogo, O. *J. New Mater. Electrochem. Syst.* **1999**, *2*, 95-101.
43. Savadogo, O.; Xing, B. *J. New Mater. Electrochem. Syst.* **2000**, *3*, 343-347.
44. Li, Q. F.; Niels, j. B. *Dianchi* **2002**, *32*, 174-177.
45. Asensio, J. A.; Borros, S.; Gomez-Romero, P. *Electrochem. Commun.* **2003**, *5*, 967-972.
    Coffin, D. R.; Serad, G. A.; Hicks, H. L.; Montgomery, R. T. *Textile Research Journal* **1982**, *52*, 466-472.
46. Mader J.; Benicewicz B. *Fuel Cells No. 2* **2011**, *11*, 212-221.
47. Jayakumar, J; Gulledge, A.; Staser, J.; Kim, C.; Benicewicz, B.; Weidner, J. *ECS Electrochem. Lett.* **2012**, *1*, F44-F48.
48. Aaron, D; Tang, Z; Papandrew, B. A; Zawodzinski, T. *Journal of Applied Electrochemistry* **2011**, *41*, 1175-1182.
49. Kreuer, K. D. *Journal of Membrane Science* **2001**, *185*, 29-39.
50. Yu, S.; Benicewicz, B. C. *Macromolecules* **2009**, *42*, 8640-8648.

51. Yu, S.; Zhang, H.; Xiao, L.; Choe, E. W.; Benicewicz, B. *Fuel Cells*, **2009**, *No. 4*, 318-324.
52. Gulledge, A. L.; Chen, X.; Benicewicz, B. C. *Journal of Polymer Science, Part A: Polymer Chemistry* **2014,** *52*, 619-628.
53. Chuang, S. W.; Hsu, S. L. C.; Liu, Y. H. *Journal of Membrane Science* **2007**, *305*, 353-363.
54. Daletou, M. K.; Kallitsis, J. K. *Journal of Membrane Science* **2009**, *326*, 76-83.
55. Deimede, V.; Voyitazis, G. A.; Kallitsis, J. K.; Li, Q.; Bjerrum, N. *Macromolecules* **2000**, *33*, 7609-7617.
56. Arunbabu, D.; Sannigrahi, A.; Jana, T. *J. Phys. Chem. B* **2008**, *112*, 5305-5310.
57. Hazarika, M.; Jana, T. *ACS Appl. Mater. Interfaces* **2012**, *4*, 5256-5265.
58. Hazarika, M. *Eur. Polym. J.* **2013**, *49*, 1564-1576.
59. Perry, K. A.; Eisman, G. A.; Benicewicz, B. C. *Journal of Power Sources* **2008**, *117*, 478-484.
60. Jones, D. J.; Roziere, J. *Journal of Membrane Science* **2001**, *185*, 41-58.
61. Ariza, M. J.; Jones, D. J.; Roziere, J. *Desalination* **2002**, *147*, 183-189.
62. Staiti, P.; Lufrano, F.; Arico, A. S.; Passalacqua, E.; Antonucci, V. *Journal of Membrane Science* **2001**, *188*, 71-78.
63. Asensio, J. A.; Borros, S.; Gomez-Romero, P. *Electrochim. Acta* **2004**, *49*, 4461-4466.
64. Bai, J. M.; Honma, i.; Murata, m.; Yamamoto, T.; Rikukawa, m.; Ogata, N. *Solid State Ionics* **2002**, *147*, 189-194.
65. Glipa, X.; El Haddad, m.; Jones, D. J.; Roziere, J. *Solid State Ionics* **1997**, *97*, 323-331.
66. Agmon, N. *Chemical Physics Letters* **1995**, *244*, 456-462.
67. Qingfeng, L.; Hjuler, H. A. Bjerrum, N. J. *Journal of Applied Electrochemistry* **2001**, *31*, 773-779.
68. Aaron, D. S.; Liu, Q.; Tang, Z.; Grim, G. M.; Papandrew, A. B.; Turhan, A.; Zawodzinski, T. A.; Mench, M. M *Journal of Power Sources* **2012**, *206*, 450-453.

Chapter 7: Polybenzimidazole Membranes for Hydrogen and Sulfuric Acid Production in the Hybrid Sulfur Electrolyzer[5]

[5]Gulledge, A. L.; Garrick, T.; Weidner, J. W.; Benicewicz, B. C. *Journal of Power Sources* **2014**, In preparation.

7.1 Introduction:

Among the various electrochemical devices in which PBI has been utilized, one with great potential is the hybrid sulfur (HyS) electrolyzer. The HyS electrolyzer is capable of producing clean hydrogen on a large scale at efficiencies higher than those possible for water electrolysis.[1-10] The HyS electrolyzer relies on a two-step thermo-chemical process which involves the decomposition of H_2SO_4 to SO_2, O_2, and H_2O as well as an electrochemical oxidation of SO_2 in the presence of water to produce H_2SO_4 and H_2 illustrated in **Equation 7.1** and **Equation 7.2**. Since the sulfur compounds are internally recycled, the overall process is the decomposition of water into hydrogen and oxygen. The process is of interest because the high-temperature decomposition step could be coupled to next-generation nuclear power plants or high-temperature solar arrays.[11]

Eq 7.1: $SO_2 + 2H_2O \rightarrow H_2SO_4 + 2H^+ + 2e^-$

Eq 7.2: $2H^+ + 2e^- \rightarrow H_2$

Among the available materials utilized for the HyS device, Nafion has been utilized because the operating parameters are well-known.[12] One major drawback to the use of Nafion as a polymer electrolyte membrane (PEM) material for the HyS electrolyzer is that the conductivity of the material suffers greatly under low humidification conditions.[13,14] Production of concentrated H_2SO_4 at the anode dehydrates the PEM used in HyS electrolyzers, and significantly reduces the efficiency when Nafion is used.[12] This has led to the investigation of alternative materials that would be suited for operations in the HyS electrolyzer.

Polybenzimidazoles (PBIs) are a class of aromatic heterocyclic polymers with exceptional thermal and chemical stabilities.[15,16] Polybenzimidazole (PBI) membranes

have been shown to have exceptional performance in various electrochemical devices because of their high ionic conductivity when imbibed with various acid electrolytes.[17,18] PBI is a basic polymer (pka ~5.25)[19] and possesses both proton donor and acceptor sites. This property induces a specific interaction between the proton acceptor/donor sites and polar solvents, allowing direct acid incorporation into the polymer matrix. [20-22] To date, a large variety of PBI polymers have been synthesized and studied in the literature[23-45]; however, a sulfonated polybenzimidazole might be best suited for HyS electrolyzer applications. Sulfonated PBI (s-PBI) has been shown to be stable in a sulfuric acid environment[46,47], and could be incorporated in the HyS electrolyzer.

Herein, s-PBI PEM membranes doped with sulfuric acid were evaluated for the first time in the HyS electrolyzer at elevated temperatures. The prepared s-PBI membranes were characterized by molecular weight measurements, membrane composition, ionic conductivity, and mechanical properties. Performance evaluations were conducted under various conditions over temperatures ranging from 90˚C to 160˚C.

7.2: Polymerization of s-PBI

As illustrated in **Scheme 7.1**, this variant of PBI was synthesized with a pre-sulfonated monomer, mono-sodium 2-sulfoterephthalate. Using a pre-sulfonated monomer allows for controlled placement of and incorporation of the sulfonate group in every repeat unit of the polymer. Alternate sulfonation techniques, such as post polymerization sulfonation[48-50], or chemical grafting of functionalized motifs[51,52], often result in random placement of the sulfonate group in addition to non-uniform or uncontrolled sulfonation. Since proton conduction is proposed to occur by means of the Grotthuss-type (hopping) mechanism[53], it is surmised that uniform orientation of

sulfonate motifs along the polymer chain may facilitate the proton conduction of the material when doped with sulfuric acid. Ionic conductivities for s-PBI membranes imbibed in 30wt% sulfuric acid baths have been reported to be greater than 0.5S/cm at 100˚C.[22] For these reasons, s-PBI was chosen as a prime candidate to replace Nafion for use as a polymer electrolyte membrane in the HyS electrolyzer.

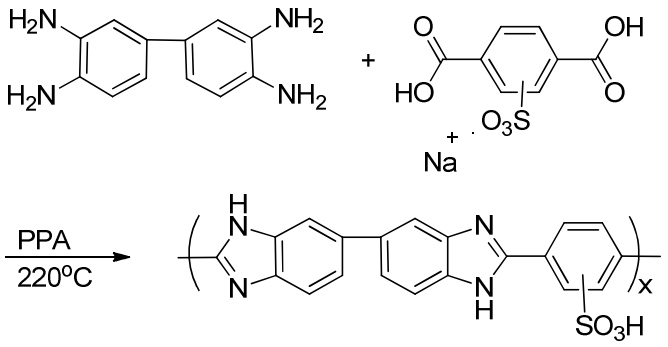

Scheme 7.1: Polymerization of s-PBI

7.3 Acid Exchange Process

The s-PBI utilized for the reported experimental evaluations was synthesized following a previously reported procedure.[22] The resulting polymer solution was cast as previously described resulting in a phosphoric acid doped membrane. To achieve the sulfuric acid doped analogue of the membrane, an acid exchange procedure was conducted. At this phase, prior to experimental evaluations of the material, removal of the phosphoric acid and subsequent sulfuric acid imbibing required verification. Acid exchange was confirmed via titration using the difference in pKa and equivalence points between sulfuric acid (-3, 1.92) and phosphoric acid (2.15, 7.20, 12.35) respectively. Moreover, titration across the full pH spectrum post acid exchange revealed only two equivalence points, verifying that only sulfuric acid remained in the membrane. Once the acid exchange was verified, subsequent evaluation of the material was conducted.

7.4 Ionic Conductivity

The anhydrous conductivity of s-PBI was measured as described in the experimental section of this thesis. The ionic conduction characteristics of the membrane were measured at temperatures from r.t. to 180˚C. **Figure 1.7** shows the ionic conductivity measured for s-PBI. The conductivity for the material exceeds 0.1 S/cm above 100˚C, but experiences a significant decline above 160˚C. This is indicative of the polymer softening (perhaps due to partial solubility) in sulfuric acid at high-temperature. Although the material softens above 160˚C , the membrane has a very desirable proton conductivity and is capable of operational temperatures well above that of Nafion.

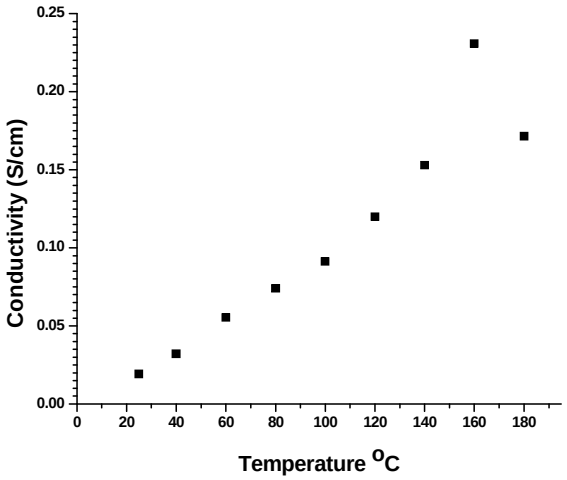

Figure 7.1: Anhydrous conductivity for s-PBI doped with sulfuric acid.

7.5 HyS Device Performance Evaluations

s-PBI membranes were evaluated in the HyS electrolyzer to determine the performance characteristics. Properties were measured over a range of temperatures at a constant flow rate of 30 sccm. Although PBI does not require water for proton

conduction,[54] water is a component of the thermo-chemical cycle in the HyS electrolyzer. Early attempts at supplying humidification at the cathode side of the cell to react at the anode side of the cell effectively washed out the acid electrolyte of the PBI membrane and resulted in poor performance. A new experimental setup was established in which the SO_2 stream was directly humidified prior to the anode feed of the cell. With this set-up, it was found that the humidifier temperature affected humidity levels of the SO_2 feed and subsequently affected the device performance. Evaluations were conducted over a range of current densities with a 30 sccm SO_2 flow rate with three humidifier temperatures; 90˚C, 95˚C and 98.5˚C, as shown in **Figure 7.2**, **Figure 7.3,** and **Figure 7.4**, respectively. The data in **Figure 7.2** shows similar performance for 90˚C and 95˚C and a significant drop in performance for 100˚C operation. This is likely due to the state flux of water as these temperatures are reached within the cell. At 100˚C, there is a competition between the boiling of water and the physical constraints of the system. Water is unstable in this system at this temperature and is likely responsible for the performance loss, as less liquid water would be available for the electrochemical reaction. **Figure 7.3** shows a similar trend, with lower performances due to the increased humidifier temperature. Increasing the humidifier temperature would send more water to the system, however, the temperature of the water sent would be closer to the boiling point of water, thus causing a faster conversion to the less reactive gas phase. **Figure 7.4** illustrates a similar trend at the highest humidifier temperature used, however, also indicates that above 110˚C some of the performance loss due to water is regained. This performance increase at elevated temperature is likely due to the increase in reaction kinetics of the electrochemical conversion. Despite the beneficial reaction kinetics of the system at temperatures above

110˚C, performance is still lower in comparison to the device performance at 90˚C with a humidifier temperature of 90˚C. The data from these performance studies suggests there may be a way to operate beneficially at elevated temperatures (>110˚C) while keeping the humidification temperature low enough as to not disrupt the system with excessive amounts of water boiling.

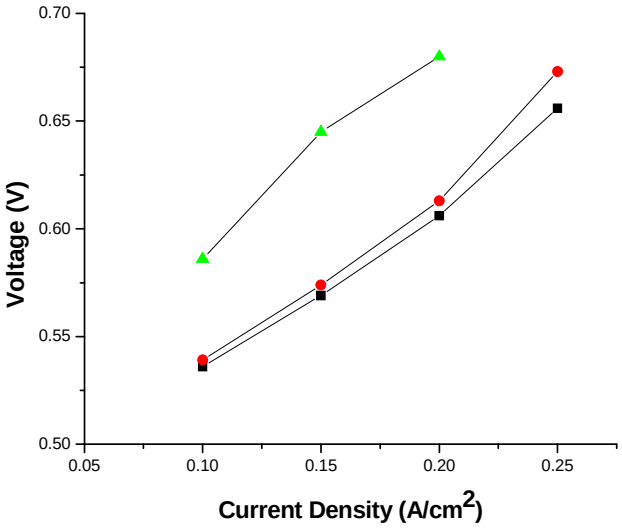

Figure 7.2: HyS device performance over a range of current densities with a humidifier temperature of 90˚C and a 30 sccm SO_2 flow rate. [Cell temperatures; squares: 90˚C, circles: 95˚C, triangles: 100˚C]

Another method of determining the performance efficiency of the HyS device is by the production of sulfuric acid at the anode exhaust. Samples were collected at various current densities and titrated against a standard to determine the concentration of the sulfuric acid produced. The molar concentration of sulfuric acid produced over a range of current densities with an SO_2 flow rate of 30 sccm with three humidifier temperatures; 90˚C, 95˚C and 98.5˚C, is shown in **Figure 7.5**, **Figure 7.6,** and **Figure 7.7** respectively. Looking at the H_2SO_4 concentration, these figures indicate similar trends as discussed for

Figures 7.2, 7.3, and 7.4. **Figure 7.7** does show unstable performance for the 120˚C operation with regards to sulfuric acid production. This is evidence of the system disruption caused by an imbalance of water available for the reaction and water escaping the system as a gas

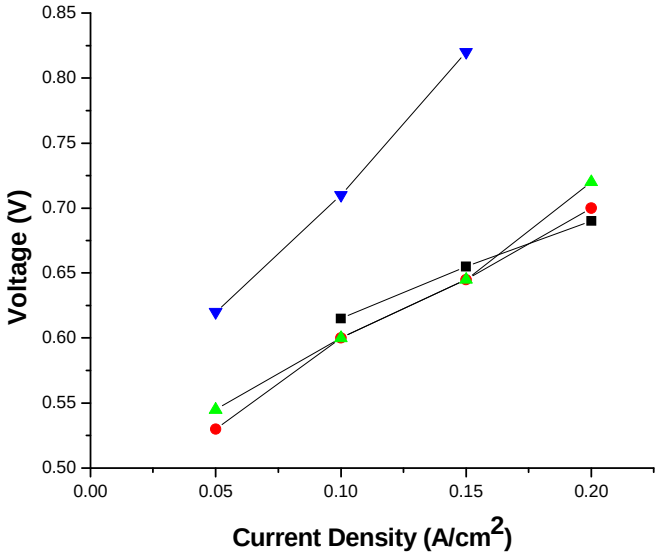

.

Figure 7.3: HyS device performance over a range of current densities with a humidifier temperature of 95˚C and a 30 sccm SO_2 flow rate. [Cell temperatures; squares: 90˚C, circles: 95˚C, triangles: 100˚C, inverted triangles: 105˚C]

Lifetime performance tests were also conducted on the HyS electrolyzer using sulfuric acid doped s-PBI. The device exhibited stable performance over the entire duration measured (approx 50hrs) as shown in **Figure 7.8**. Longer lifetime performance evaluations proved difficult as the experimental set up required constant supervision and monitoring. The lifetime evaluation did indicate that the device performance is stable over the duration measured, and would be suitable for HyS electrolyzer applications.

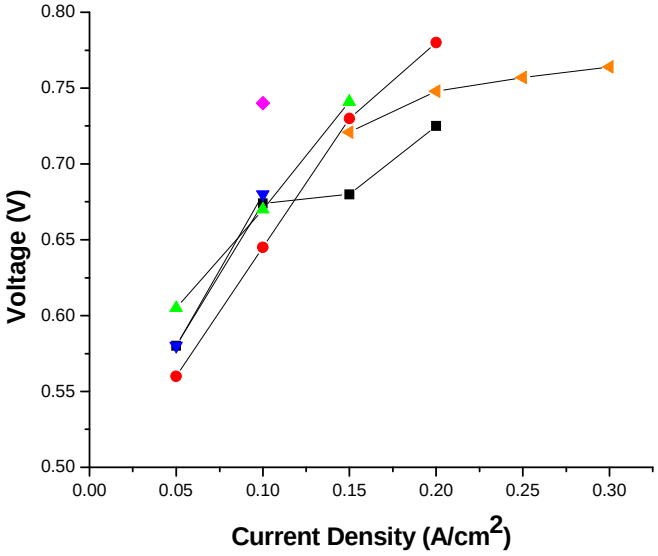

Figure 7.4: HyS device performance over a range of current densities with a humidifier temperature of 98.5˚C and a 30 sccm SO_2 flow rate. [Cell temperatures; squares: 90˚C, circles: 95˚C, triangles: 100˚C, inverted triangles: 105˚C, diamonds: 110˚C, left triangle: 120˚C]

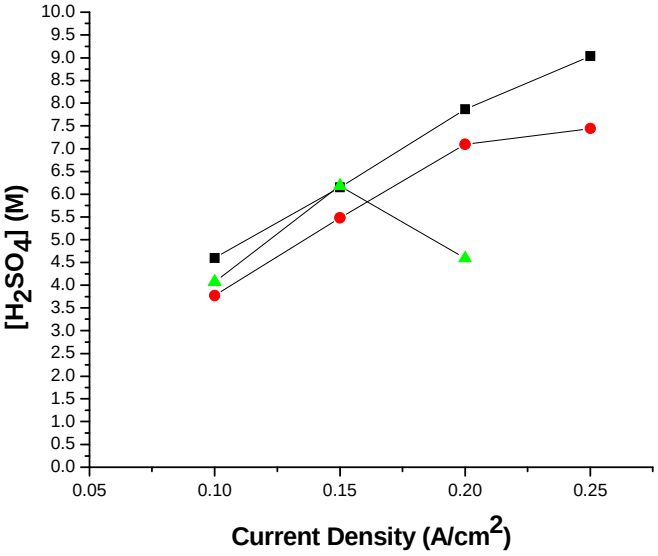

Figure 7.5: Sulfuric acid production over a range of current densities with a humidifier temperature of 90˚C and a 30 sccm SO_2 flow rate. [Cell temperatures; squares: 90˚C, circles: 95˚C, triangles: 100˚C]

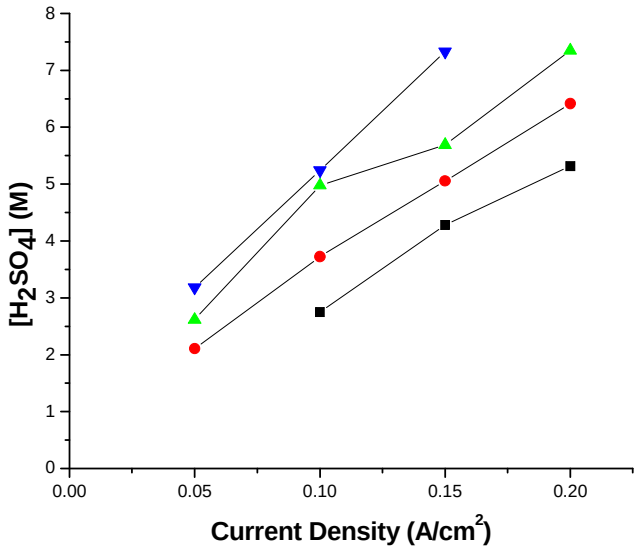

Figure 7.6: HyS device performance over a range of current densities with a humidifier temperature of 95˚C and a 30 sccm SO_2 flow rate. [Cell temperatures; squares: 90˚C, circles: 95˚C, triangles: 100˚C, inverted triangles: 105˚C]

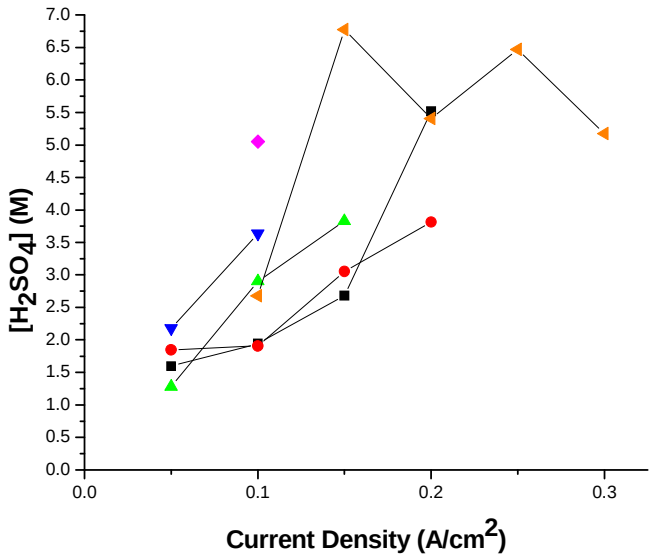

Figure 7.7: Sulfuric acid production over a range of current densities with a humidifier temperature of 98.5˚C and a 30 sccm SO_2 flow rate. [Cell temperatures; squares: 90˚C, circles: 95˚C, triangles: 100˚C, inverted triangles: 105˚C, diamonds: 110˚C, left triangle: 120˚C]

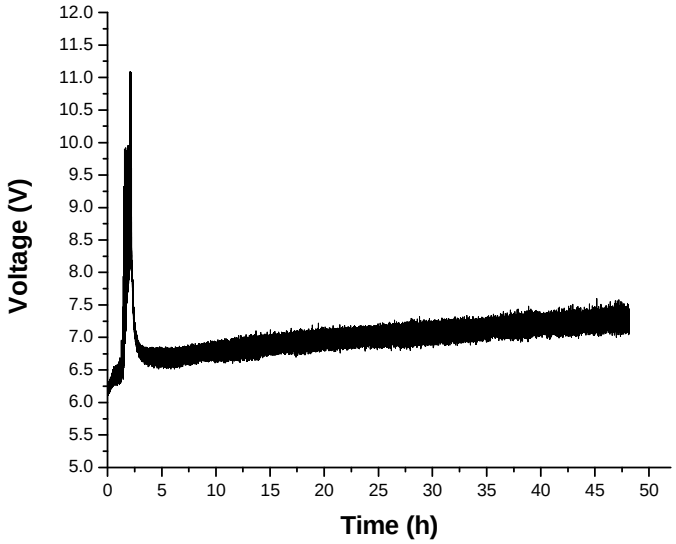

Figure 7.8: Lifetime evaluation of sulfuric acid doped s-PBI in the HyS electrolyzer with an SO_2 flow rate of 30 sccm at 130˚C cell temperature, 0.2 A/cm2 current density, and 90˚C humidifier temperature.

7.6 Conclusions

s-PBI was prepared via the PPA process and directly hydrolyzed to produce polymer electrolyte membranes doped with phosphoric acid. The membranes were then subjected to an acid exchange removal process and subsequently imbibed with sulfuric acid. Anhydrous proton conductivity measurements of the sulfuric acid doped s-PBI membranes revealed desirable conductivities (>2.0S/cm) at elevated temperatures. Conductivity measurements also indicated that the membrane was not stable at temperatures above 160˚C, and this was attributed to the softening or solubility of the s-PBI membrane in sulfuric acid.

Analysis of the HyS performance plots indicates that the device performance was optimal around 90˚C, and that once temperatures above 120˚C were reached, the device performance became unstable. Operation of the HyS electrolyzer with sulfuric acid doped s-PBI is a significant step towards the development of HyS systems capable of high-temperature operation. Since this was the first attempt at high temperature operation, it is surmised that stable performances could be obtained at higher temperatures once the experimental conditions concerning humidification of the SO_2 reactant feed are thoroughly evaluated. This work is the first application of PBI in a HyS electrolyzer. Additionally, this work is the first report of high temperature (>100˚C) device operation. This work has proven to be a significant mile-stone for the development and expansion of PBI PEM based electrochemical device applications.

7.7 References

1. Varkaraki, E.; Lymberopoulos, N. Zoulias, E. Guichardot, D.; Poli, G. *Int. J. Hydrogen Energy* **2007**, *32*, 1589-1596.
2. Shin, Y.; Park, W.; Chang, J.; Park, J. *Int. J. Hydrogen Energy* **2007**, *32*, 1486-1491.
3. Herring, J. S.; O'Brien, J. E.; Stoots, C. M.; Hawkes, G. L.; Hartvigsen, J. J.; Shahnam, M. *Int. J. Hydrogen Energy* **2007**, *32*, 440-450.
4. Hauch, A.; Jensen, S. H.; Ramousse, S.; Mogensen, M. *J. Electrochem. Soc.* **2006**, *153*, A1741-A1747.
5. Lu, P. W.; Garcia, E. R.; Ammon, R. L. *J. Appl. Electrochem.* **1981**, *11*, 347-355.
6. Lu, P. W.; Ammon, R. L. *J. Electrochem. Soc.* **1980**, *127*, 2610-2616.
7. Sivasubramanian, P.; Ramasamy, R. P.; Freire, F. J.; Holland, C. E.; Wiedner, J. W. Int. J. Hydrogen Energy 2007, 32, 463-468.
8. Gorensek, M. B.; Summers, W. A. *Int. J. Hydrogen Energy* **2009**, *34*, 4097-4114.
9. Jomard, F.; Feraud, j. P.; Caire, J. P. *Int. J. Hydrogen Energy* **2008**, *33*, 1142-1152.
10. Staser, J.; Ramaswamy, R. P.; Sivasubramanian, P.; Weidner, J. W. *Electrochemical and Solid-State Letters* **2007**, *10*, E17-E19.
11. Department of Energy (DOE) *Energy Information Administration, Hydrogen Use, Petroleum Consumption and Carbon Dioxide Emissions,* Washington, DC **2008**.
12. Staser, J. A.; Gorensek, M. B.; Weidner, J. W. *J. Electrochem. Soc.* **2010**, *157*, B952-B958.
13. Anantaraman, A. V.; Gardner, C. L. *J. Electroanal. Chem.* **1996**, *414*, 115-120.

14. Cappadonia, M.; Wilhelm Erning, J.; Saberi Niaki, S. M.; Stimming, U. *Solid State Ionics* **1995**, *77*, 65-69.
15. Yu, S.; Xiao, L.; Benicewicz, B.C. *Fuel Cells* **2008**, *No. 3-4*, 165-174.
16. Shogbon, C.; Brousseau, J.; Zhang, H.; Benicewicz, B.C.; Akpalu, Y. *Macromolecules* **2006**, *39*, 9409-9418.
17. Quan, G.; Benicewicz, B. C. *Journal of Polymer Science Part A: Polymer Chemistry* **2009**, *47*, 4064-4073.
18. Perry, K.; Eisman, G.; Benicewicz, B. *Journal of Power Sources* **2008**, *117*, 478-484.
19. Sannigrahi, A.; Ghosh, S.; Maity, S.; Jana, T. *Polymer* **2010**, *51*, 5929-5941.
20. Kojima, T.; *Journal of Polymer Science: Polymer Physics Ed.* **1980**, *18*, 1685-1695.
21. Sannigrahi, A.; Arunbabu, D.; Sankar, R. M.; Jana, T. *Macromolecules* **2007**, *40*, 2844-2851.
22. Mader, J. A.; Benicewicz, B. C. *Macromolecules* **2010**, *43*, 6706-6715.
23. Mader, J.; Xiao, L.; Schmidt, T. J.; Benicewicz, B. C.; *Adv. Polym. Sci.* **2008**, *216*, 63-124.
24. Li, Q.; Jensena, J.O.; Savinell, R.F.; Bjerrum, N.J. Prog. *Polym. Sci.* **2009**, *34*, 449-477.
25. Seel, D.C.; Benicewicz, B.C.; Xiao, L.; Schmidt, T.J. *Handbook of Fuel Cells* **2009**, *5*, 300-312.
26. Wainright, J. S.; Wang, J. T.; Savinell, R. F.; Litt, M.; Moaddel, H.; Rogers, C. *Proceedings of the Electrochemical Society* **1994**, *94*, 255-64.
27. Gilham J. K.; *Science* **1963**, *139*, 494-495
28. Strauss, E. L. *Polymer Eng. Sci.* **1966**, *6*, 24-29.
29. Weng, D.; Wainright, J. S.; Landau, U.; Savinell, R. F. *Proceedings of the Electrochemical Society* **1995**, *95-23*, 214-225.
30. Hill, J. R. *Adhesives Age* **1966**, *9*, 32-36.
31. Delman, A. D.; Kovacs, h. N.; Simms, B. B. *Journal of Polymer Science, Part A-1: Polymer Chemistry* **1968**, *6*, 2117-2126.
32. Wang, J. T.; Savinell, R. F.; Wainright, J.; Litt, M.; Yu, H. *Electrochim. Acta* **1996**, *41*, 193-197.
33. Wang, J. T.; Wainright, J. S.; Savinell, R. F.; Litt, M. *J. Appl. Electrochem.* **1996**, *26*, 751-756.
34. Szita, J.; Marvel, Carl S. *Journal of Applied Polymer Science* **1970**, *14*, 2019-2024.
35. Korshak, V. V.; Teplyakov, m. M.; Fedorova, R. D. *Journal of Polymer Science, Part A-1: Polymer Chemistry* **1971**, *9*, 1027-1043.
36. Bingham, M. A.; Hill, B. J. *Journal of Thermal Analysis* **1975**, *7*, 347-358.
37. Wang, J. T.; Wasmus, S.; Savinell, R. F. *J. Electrochem. Soc.* **1996**, *143*, 1233-1239.
38. Hilado, C. J.; LaBossiere, L. A.; Leon, H. A.; Kourtides, D. A.; Parker, j. A.; Hsu, M. S. *Journal of Combustion Toxicology* **1976**, *3*, 211-236.
39. Kovar, R. F.; Arnold, F. E. *Journal of Polymer Science, Polymer Chemistry Edition* **1976**, *14*, 2807-2817.

40. Chatfield, D. A.; Einhorn, I. N. *Journal of Polymer Science, Polymer Chemistry Edition* **1981**, *19*, 601-618.
41. Weng, D.; Wainright, J. S.; Landau, U.; Savinell, R. F. *J. Electrochem. Soc.* **1996**, *143*, 1260-1263.
42. Xing, B.; Savadogo, O. *J. New Mater. Electrochem. Syst.* **1999**, *2*, 95-101.
43. Savadogo, O.; Xing, B. *J. New Mater. Electrochem. Syst.* **2000**, *3*, 343-347.
44. Li, Q. F.; Niels, j. B. *Dianchi* **2002**, *32*, 174-177.
45. Asensio, J. A.; Borros, S.; Gomez-Romero, P. *Electrochem. Commun.* **2003**, *5*, 967-972.
    Coffin, D. R.; Serad, G. A.; Hicks, H. L.; Montgomery, R. T. *Textile Research Journal* **1982**, *52*, 466-472.
46. Mader J.; Benicewicz B. *Fuel Cells No. 2* **2011**, *11*, 212-221.
47. Jayakumar, J; Gulledge, A.; Staser, J.; Kim, C.; Benicewicz, B.; Weidner, J. *ECS Electrochem. Lett.* **2012**, *1*, F44-F48.
48. Ariza, M. J.; Jones, D. J.; Roziere, J. *Desalination* **2002**, *147*, 183-189.
49. Staiti, P.; Lufrano, F.; Arico, A. S.; Passalacqua, E.; Antonucci, V. *Journal of Membrane Science* **2001**, *188*, 71-78.
50. Asensio, J. A.; Borros, S.; Gomez-Romero, P. *Electrochim. Acta* **2004**, *49*, 4461-4466.
51. Bai, J. M.; Honma, i.; Murata, m.; Yamamoto, T.; Rikukawa, m.; Ogata, N. *Solid State Ionics* **2002**, *147*, 189-194.
52. Glipa, X.; El Haddad, m.; Jones, D. J.; Roziere, J. *Solid State Ionics* **1997**, *97*, 323-331.
53. Agmon, N. *Chemical Physics Letters* **1995**, *244*, 456-462.
54. Wainright, J. S.; Wang, J. T. Weng, D.; Savinell, R. F.; Litt, M. *J. Electrochem. Soc.* **1995**, *142*, L121-L123.

Chapter 8: Solution Polymerization of Polybenzimidazole[6]

[6] Gulledge, A. L.; Hoffman, J.; Steckle, W.; Benicewicz, B. *Journal of Polymer Science, Part A: Polymer Chemistry* **2014**, In preparation.

8.1 Introduction

Polybenzimidazoles (PBIs) are a class of aromatic heterocyclic polymers with exceptional thermal and chemical stabilities.[1,2] PBIs can be formed through a polycondensation of a diacid and tetra amine, as shown in **Scheme 8.1**. As with any polycondensation polymerization, and, as defined by the Carother's equation[3], an exact stoichiometric ratio is needed for the synthesis of high molecular weight polymer. Typical synthesis of bisbenzimidazoles involves a reaction between *o*-phenylenediamines with a diacid or diamide in HCl or polyphosphoric acid (PPA).[4] Synthesis of 2-substituted benzimidazoles from the reaction of *o*-phenylendiamine with an imidate are also well known.[5] Synthetic knowledge of these procedures can easily be applied to polymeric systems when di-functional monomers are incorporated. Di-functional monomers with various R groups and can be used to produce a variety of polybenzimidazole derivatives (**Scheme 8.1)**.

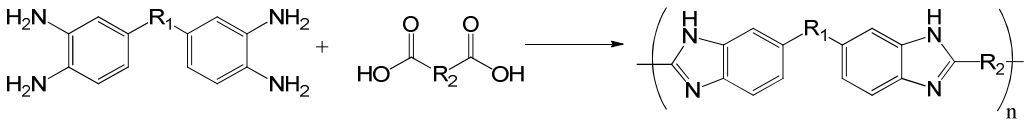

Scheme 8.1: Reaction of a tetra amine and a diacid to form a polybenzimidazole.

In 1959, the first aliphatic PBI was developed by Brinker and Robinson.[6] Shortly afterwards came the first development of an aromatic PBI by Marvel and Vogel in 1961.[7] In 1983, Celanese commercialized one type of polybenzimidazole (meta-PBI, poly(2,2'-m-phenylene-5,5'-bibenzimidazole), as shown in **Figure 8.1**. This commercialized polybenzimidazole was developed for use as fibers and textiles for thermal protective clothing and fire blocking applications.[8-11]

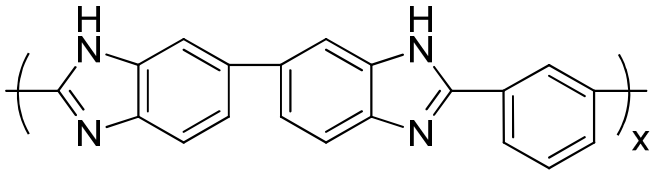

Figure 8.1: Poly(2,2'-m-phenylene-5,5'-bibenzimidazole)

Of all the derivatives of polybenzimidazoles, the aromatic PBIs have received the most attention due to their excellent thermal and chemical resistance properties[12-22]. Aromatic PBIs do not have a melting point due to their very high glass transition temperatures and exhibit very high decomposition temperatures. In addition to their high temperatures of decomposition (>500˚C), they are practically insoluble in most organic solvents.[23] Moreover, PBIs have shown outstanding stability when exposed to inorganic acids and bases when compared to other high performance fibers such as Nomex or Kevlar. [21,24]

Industrially, polybenzimidazole is polymerized by a two-stage melt/solid polymerization process. Di-phenyl isophthalate (DPIP) and 3,3',4,4'-tetraaminobiphenyl (TAB) are reacted in bulk to produce the meta-PBI product.[25] The condensate of this reaction (phenol) is however a gas and subsequent crushing of the resulting foam developed in the first stage is required. The second stage then involves reheating the mixture to synthesize high molecular weight polymer at temperatures upwards of 400˚C. The phenol gas by product of this reaction is hazardous and must be carefully collected and treated. The final product is a non-homogenous product that is separated based on particle size and molecular weight. Resulting powders from the bulk polymerization are then dissolved at high temperature and pressure in N,N-dimethylacetamide (DMAc) with LiCl. The polymer dope solution is then filtered and spun into fibers for commercial

application. These resulting fibers are then used as a raw material for thermally resistant fabrics and fire blocking applications.

In contrast to melt or bulk phase polymerization methods, a solution polymerization method for the synthesis of high molecular weight polybenzimidazole would be much more efficient and cost-effective when considering large-scale commercial production. Previous attempts at solution polymerizations of polybenzimidazoles have been unsuccessful in the development of commercially desirable high-molecular weight polymer. [26-29] Herein, a commercially viable solution polymerization for the synthesis of high molecular weight polybenzimidazoles in DMAc has been developed.

8.2 Reactivity Evaluations

To develop a viable method for the commercially favorable solution polymerization of high-molecular weight PBIs, a variety of monomer functionalities were investigated. DMAc was chosen as the solvent in which to develop the solution polymerization method because it is a commonly used industrial solvent and could be used directly for fiber spinning. To begin the monomer evaluations, chemical functionalities that are known to produce 2-phenylbenzimidazole were selected as shown in **Figure 8.2**. Mono-functional analogues were evaluated to allow for easier reaction kinetic studies and product evaluations.

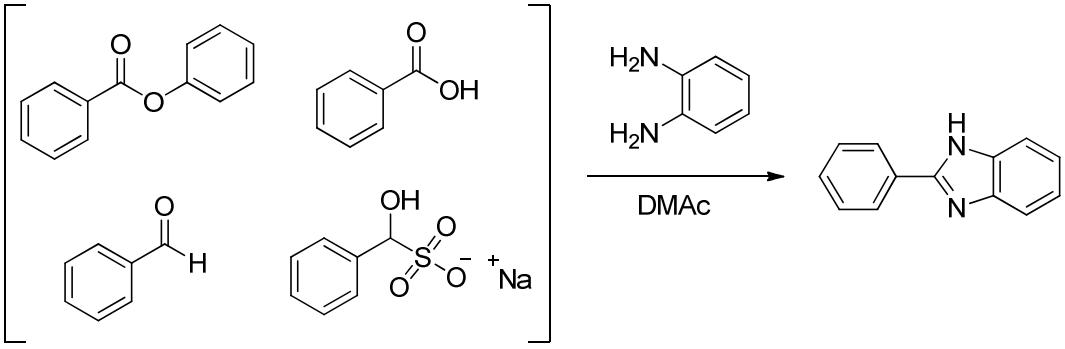

Figure 8.2: Chemical functionalities evaluated for the synthesis of 2-phenylbenzimidazole in dimethylacetamide (DMAc).

A series of reactions were conducted and monitored via GC/MS to evaluate the reaction efficiency and product formation in DMAc. Analysis of reaction kinetics on the mono-functional reactants in DMAc revealed only one successful chemical functionality in DMAc. The phenyl ester was found to be unreactive in DMAc at reflux, and only starting materials were recovered. The aldehyde functionality was found to be highly reactive and rapidly produced a product with a molecular weight of 284g/mol as shown in **Figure 8.3**. This was later determined to be the bis-imine (-CH=N-) product that corresponds to a 2:1 molar reaction between benzaldehyde and *o*-diaminobenzene. The carboxylic acid functionality was found to not form the desired product in high yield in DMAc as shown in **Figure 8.4**. The only chemical functionality found to be sufficiently reactive was the bisulfite adduct of benzaldehyde as shown in **Figure 8.5**. It is surmised that the bisulfite functionality maintains the high reactivity of the aldehyde and also incorporates steric hindrance which prevents reaction of a 2:1 ratio product. GC/MS analysis also indicated that this is a very fast, efficient reaction, free of unwanted by-products. Polymerization trials were conducted with the di-functional analogues at temperatures up to reflux in DMAc and similar results were obtained.

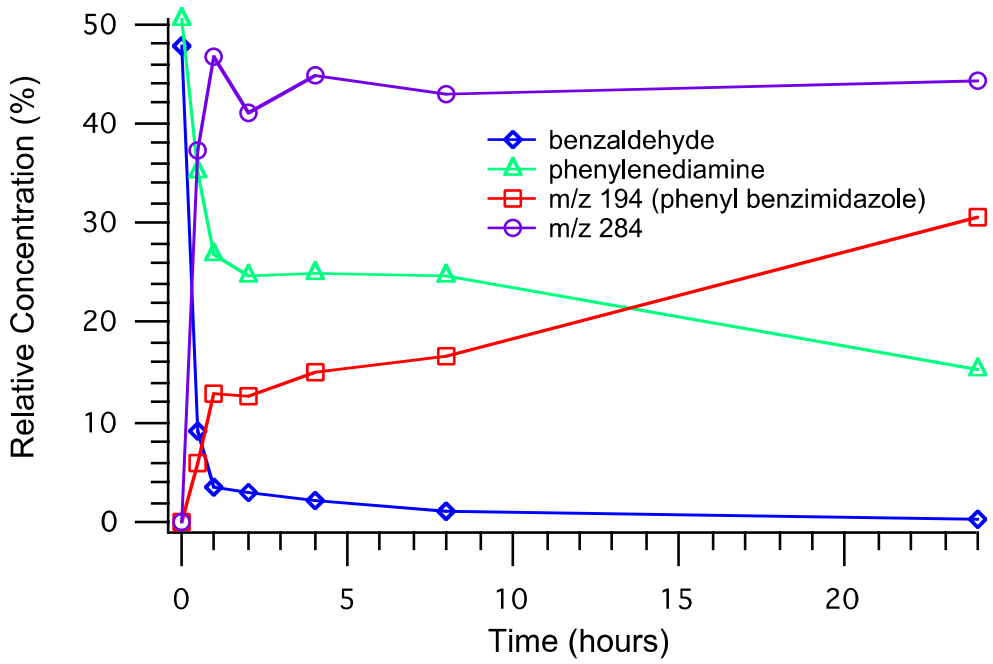

Figure 8.3: GC/MS reaction evaluation of benzaldehyde and diaminobenzene in DMAc at 100˚C.

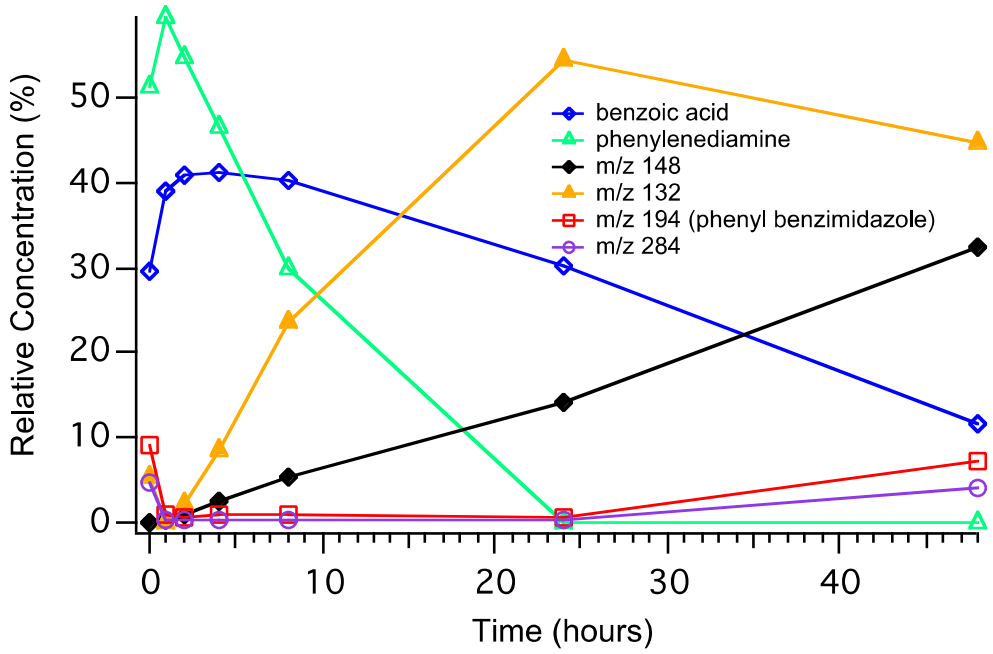

Figure 8.4: GC/MS reaction evaluation of benzoic acid and diaminobenzene in DMAc at 100˚C.

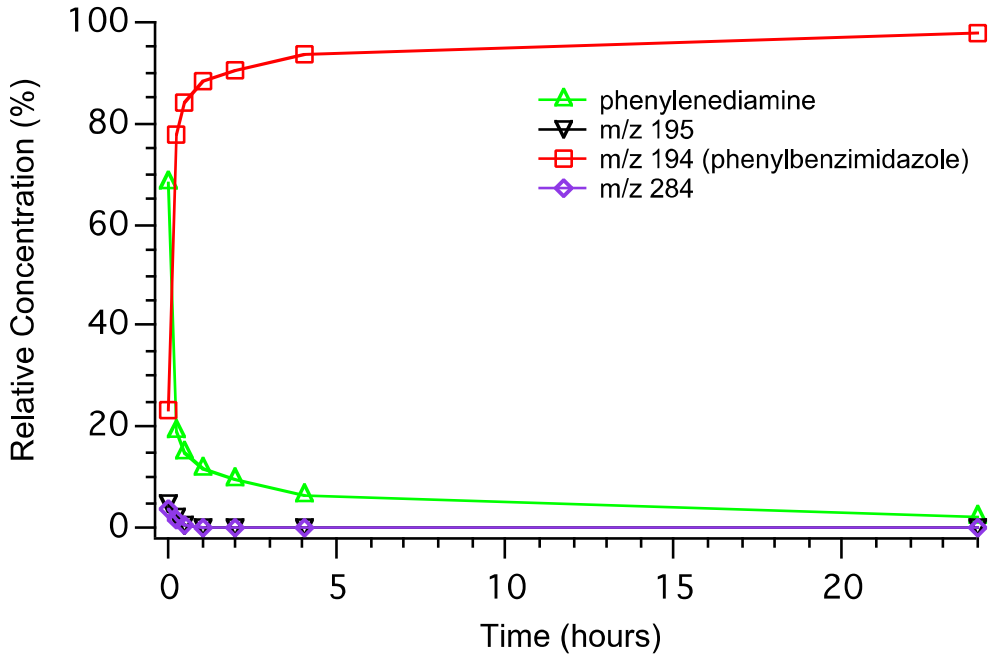

Figure 8.5: GC/MS analysis for reaction of benzaldehyde bisulfite adduct and *o*-diaminobenzene in DMAc at 100˚C.

8.3 Synthesis and Evaluation of Bisulfite Adduct

The bisulfite adduct was synthesized as shown in **Scheme 8.2**. The reaction of sodium bisulfite and isophthalaldehyde in a mixture of methanol and water produced a stable bisulfite adduct that was obtained as a white precipitated product. The reaction is mild and only requires ambient temperatures due to the high reactivity of the aldehyde functionality. The product from this reaction was obtained in high yield (>90%) and high purity (>98%), and was suitable for polymerization trials without further purification.

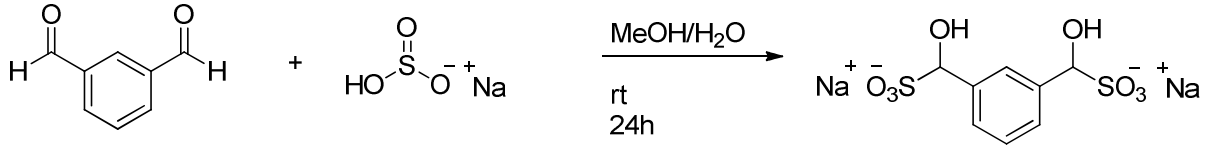

Scheme 8.2: Synthesis of isophthalaldehyde bisulfite adduct.

The bisulfite adduct product was analyzed via FT-IR and ^{1}H-NMR as shown in **Figure 8.6** and **Figure 8.7** respectively. The FT-IR comparison of isophthalaldehyde and the bisulfite adduct product confirmed the product formation as indicated by the disappearance of the carbonyl peak at ~1700cm^{-1}, and the appearance of two peaks at ~1175 and ~1000 cm^{-1} which correspond to the C-S stretching of the product. The ^{1}H-NMR comparison of isophthalaldehyde and the bisulfite adduct product also indicated successful synthesis of the desired product, as indicated from the disappearance of the aldehyde proton peak at ~10ppm and the appearance of peaks at ~5 and 6ppm which correspond to the alcoholic proton and aliphatic proton of the product, respectively. Further inspection of the product NMR reveals a very small amount (<1%) of the mono-substituted product, and some residual aldehyde (<2%). To compensate for the residual free aldehyde, a small amount (2 mol %) sodium bisulfite was added directly prior to polymerization to promote the conversion of the free aldehyde to the bisulfite adduct.

8.4 Solution Polymerization of Poly(2,2'-m-phenylene-5,5'-bibenzimidazole) (m-PBI)

Using the preformed isophthalaldehyde bisulfite adduct and commercially available 3,3',4,4'-tetraaminobiphenyl, poly(2,2'-m-phenylene-5,5'-bibenzimidazole) (m-PBI) was synthesized as shown in **Scheme 8.3**. Numerous reactions were conducted over a range of monomer concentrations to determine the optimal conditions for the synthesis of high-molecular weight polymer. Relative measures of molecular weight were conducted through inherent viscosity measurements in concentrated H_2SO_4 as PBI is insoluble in organic solvents commonly used for gel permeation chromatography. The inherent viscosities of the polymers synthesized at different monomer concentrations are

shown in **Figure 8.8** and plotted as a function of the final polymer solution concentration.

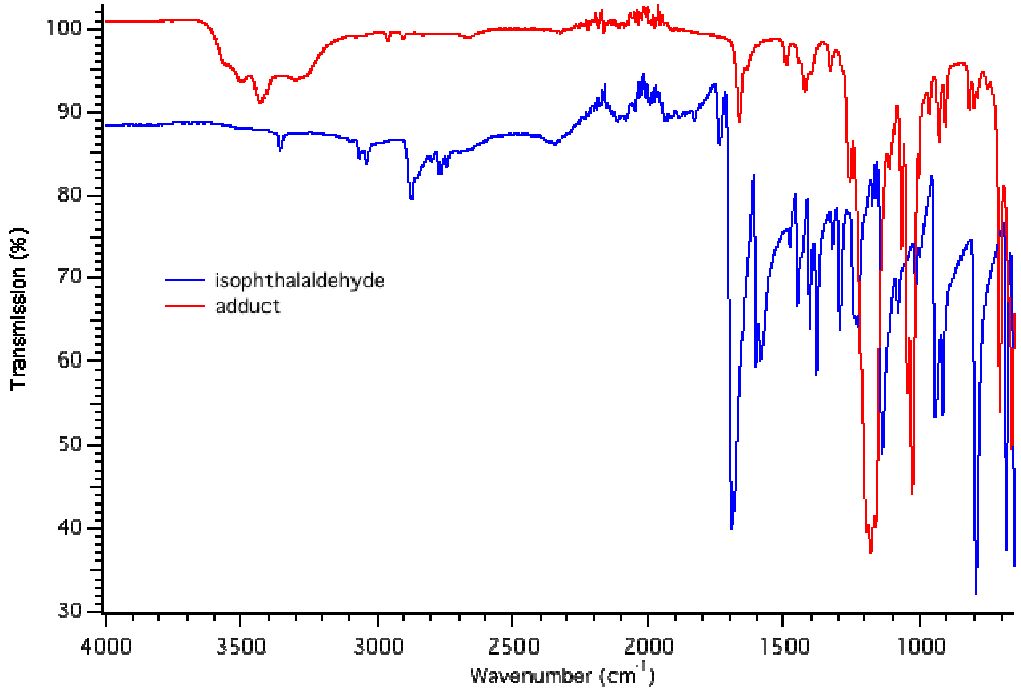

Figure 8.6: FT-IR spectral comparison of isophthaladehyde and the isophthalaldehyde bisulfite adduct.

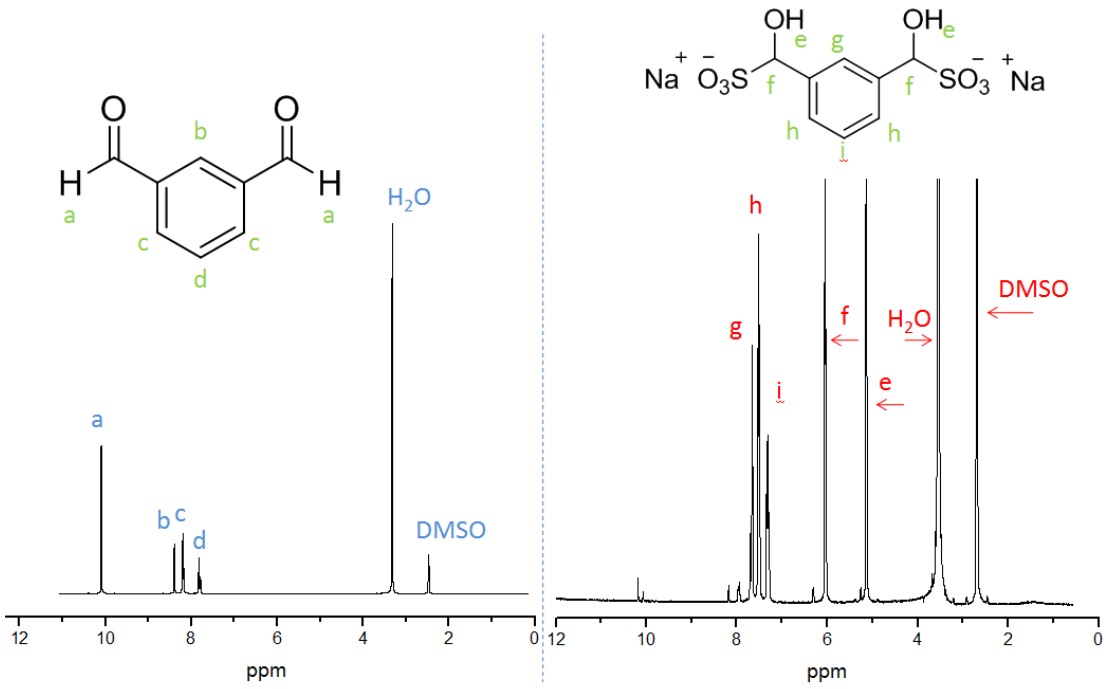

Figure 8.7: ^{1}H-NMR spectral comparison of isophthalaldehyde and the isophthalaldehyde bisulfite adduct.

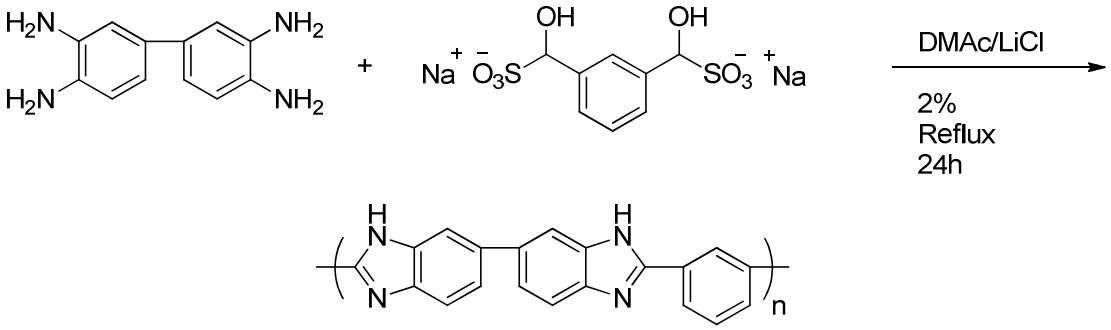

Scheme 8.3: Solution polymerization of poly(2,2'-m-phenylene-5,5'-bibenzimidazole) (m-PBI).

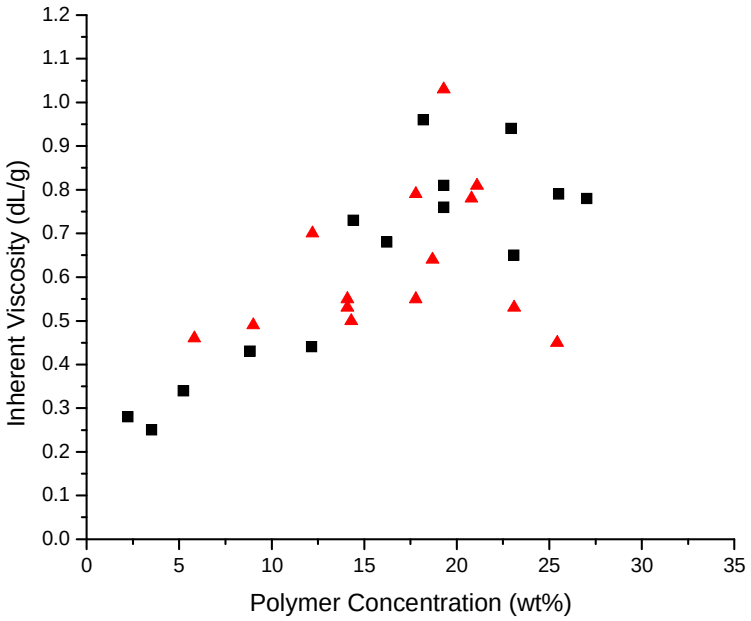

Figure 8.8: Polymer IV's for the polymerization of m-PBI in DMAc under reflux conditions. [Squares: No lithium chloride used, triangles: 2 wt% by solvent lithium chloride used]

Numerous polymerization trials were conducted with and without the use of LiCl as a solution stabilizer. Lithium chloride has been shown to increase the solubility of PBI in DMAc.[30] Evaluation of the polymerization of m-PBI in DMAc over a range of polymer concentrations revealed the optimal conditions to be at ~18% polymer by weight. The polymer product from these reactions was then compared to the commercially produced polymer via thermal gravimetric analysis (TGA), differential scanning calorimetry (DSC), FT-IR, and ^{1}H-NMR. TGA analysis is shown in **Figure 8.9**, and the polymer produced by the bisulfite route exhibited similar thermal stability to the commercially produced m-PBI (T_d ~600˚C). The differences in water loss were due to the different drying conditions of the starting powders.

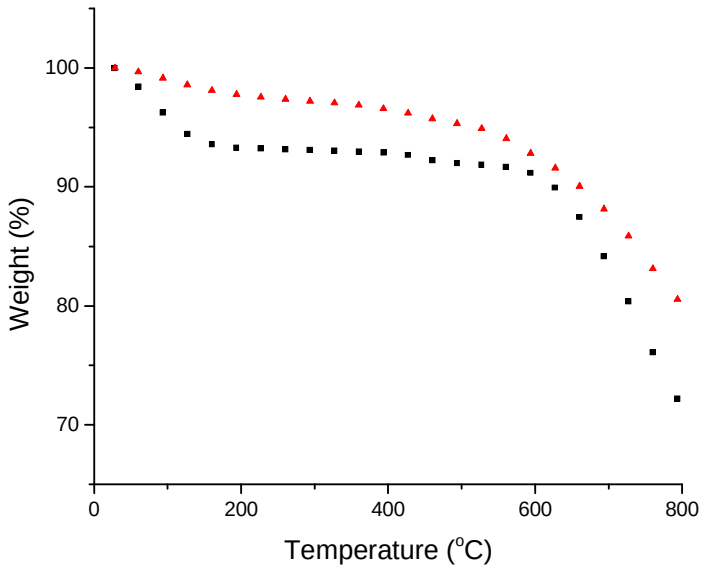

Figure 8.9: Thermal gravimetric analysis (TGA) of solution polymerization product and commercially produced m-PBI. [Triangles: solution polymerized m-PBI, squares: commercially produced m-PBI]

Differential scanning calorimetry (DSC) was conducted on the polymer product and the commercially produced m-PBI as shown in **Figure 8.10**. DSC indicated a glass transition (Tg) temperature of approximately 435˚C for both materials, as indicated by the baseline shift. The Tg of a polymer is affected by both the polymer structure and molecular weight. The Tg of a material becomes constant once a significant molecular weight is achieved, and therefore can be used as a supporting indication of the desired product.

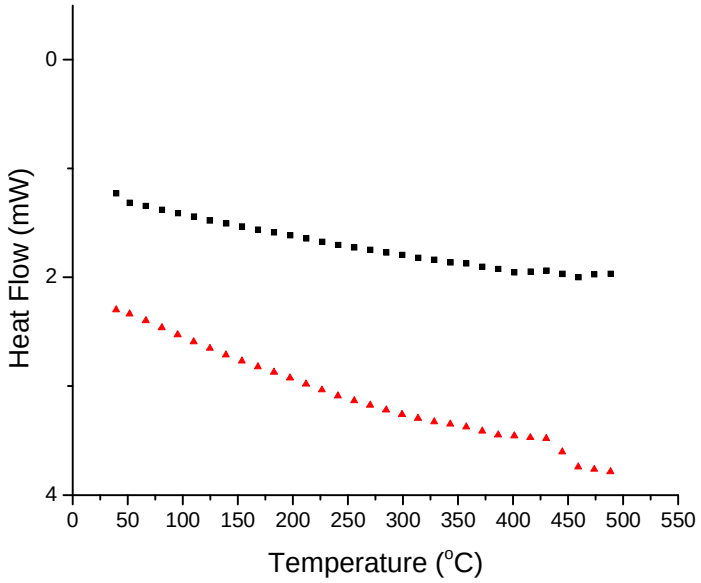

Figure 8.10: Differential scanning calorimetry of the solution polymerized m-PBI and commercially produced m-PBI. [Squares: solution polymerized m-PBI, triangles: commercially produced m-PBI]

^{1}H-NMR analysis of the solution polymerization product was conducted and compared to the reported ^{1}H-NMR of m-PBI as shown in **Figure 8.11**. The ^{1}H-NMR of the solution polymerized m-PBI directly corresponds to reported literature for the ^{1}H-

MNR of m-PBI[31], further confirming the successful polymerization and complete ring closure of the benzimidazole rings.

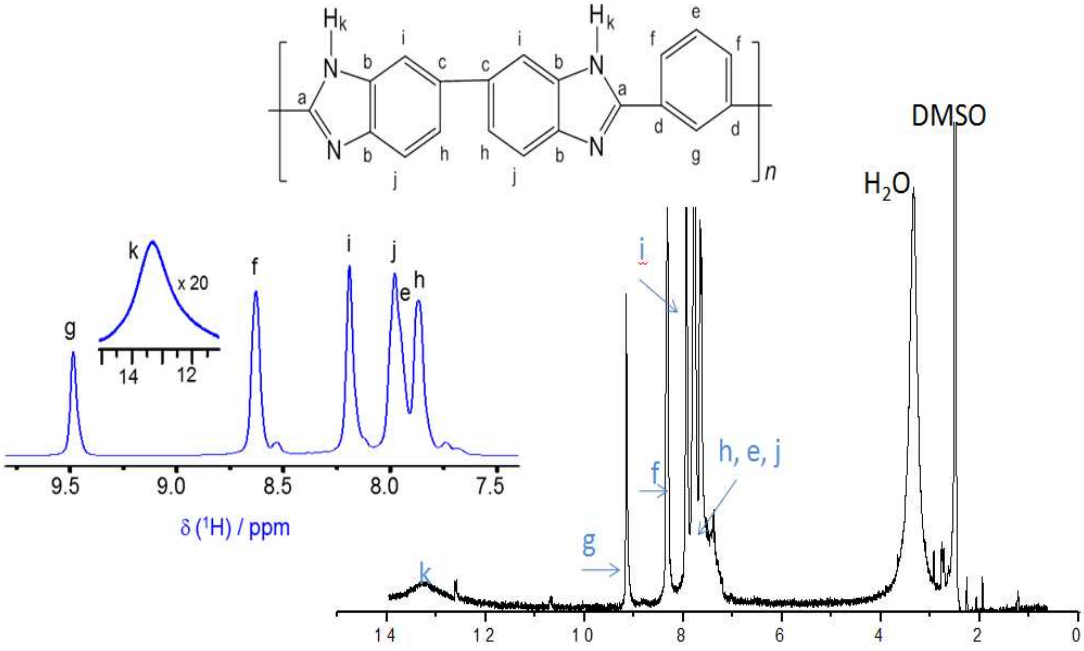

Figure 8.11: ^{1}H-NMR spectra for the solution polymerized m-PBI. Inset: reported ^{1}H-NMR for m-PBI.[31]

FT-IR analysis of the solution polymerized m-PBI was conducted and compared to the commercially produced m-PBI as shown in **Figure 8.12**. FT-IR spectra of several solution polymerization trials were compared to the commercially produced m-PBI and showed the same stretching frequencies and pattern distributions, indicating that m-PBI was successfully produced.

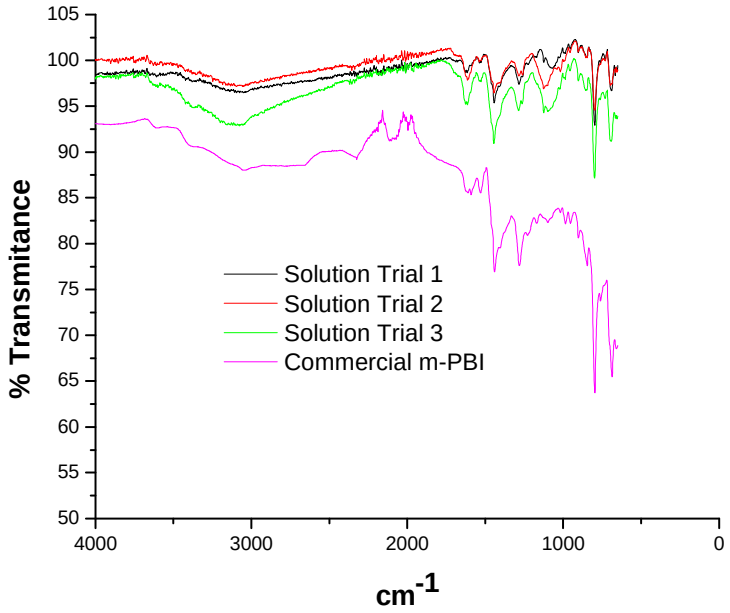

Figure 8.12: FT-IR spectral analysis for the solution polymerizations of m-PBI and commercially produced PBI.

8.5 Conclusions

In this work, the reactivity of several chemical functionalities were evaluated to determine an appropriate starting material for the solution polymerization of m-PBI in DMAc. Mono-functional analogues were reacted with *o*-diaminobenzene and the reactions were monitored via GC/MS. A bisulfite adduct of benzaldehyde was found to successfully produce the desired 2-phenylbenzimidazole in high-yield with fast conversion. Polymerization trials were also conducted with di-functional monomers, and similar results to the mono-functional analogues were obtained. A bisulfite adduct of isophthalaldehyde was synthesized and the product was confirmed via ^{1}H-NMR and FT-IR analyses. Numerous polymerization trials were conducted in which the isophthalaldehyde bisulfite adduct and commercially available 3,3',4,4'-tetraaminobiphenyl were reacted under reflux conditions in DMAc. Polymerization trials

were conducted with and without the use of LiCl as a solution stabilizer over a range of reaction concentrations. Optimal reaction conditions were determined to be at approx 18 wt % polymer concentration. Polymer product was analyzed via TGA, DSC, ^{1}H-NMR, and FT-IR and compared to commercially produced m-PBI. TGA, FT-IR and DSC showed identical characteristics to that of the commercially produced m-PBI. The ^{1}H-NMR spectrum was compared to the reported literature H^{1}-NMR spectrum of m-PBI and also confirmed the product formation.

Overall, a viable, commercially applicable, solution polymerization process for the synthesis of high-molecular weight PBI in DMAc was developed. This solution polymerization process has significant commercial and industrial applications to the large-scale production of m-PBI. In theory, this process could be applied to produce a variety of PBI derivatives.

8.6 References:

1. Yu, S.; Xiao, L.; Benicewicz, B.C. *Fuel Cells* **2008**, *No. 3-4*, 165-174.
2. Shogbon, C.; Brousseau, J.; Zhang, H.; Benicewicz, B.C.; Akpalu, Y. *Macromolecules* **2006**, *39*, 9409-9418.
3. Carothers, W. *Trans . Faraday Soc.* **1936**, *32*, 39-53.
4. Berrada, M.; Anbaoui, Z.; Lajrhed, N.; Berrada, M.; Knouzi, N.; Vaultier, M.; Sekiguchi, H.; Carriere, F. *Chem Mater* **1997**, *9*, 1989-1993.
5. Holan, G.; Samuel, E.L.; Ennis, B.C.; Hinde, R. W. *J. Chem Soc, C* **1967**, *1*, 20-25.
6. Brinker, K. C.; Cameron, D. D.; Robinson, I. M. *Linear Polybenzozazoles* 2904537, **1959**.
7. Vogel, H.; Marvel, C. S. *Journal of Polymer Science, Part A: Polymer Chemistry* **1961**, *34*, 511-539.
8. Powers, E. J.; Serad, G. A., *History and Development of Polybenzimidazoles*. **1986**, 355-73.
9. Chenevey, E. C.; Conciatori, A. B. *Polybenzimidazoles*. 65-517797 3433772, 19651230., **1969**.
10. Coffin, D. R.; Serad, G. A.; Hicks, H. L.; Montgomery, R. T. *Textile Research Journal* **1982**, *52*, 466-472.
11. Buckley, A.; Stuetz, D. E.; Serad, G. A. *Polybenzimidazoles*. **1987**, *11*, 572-601.
12. Gulledge, A. L.; Chen, X.; Benicewicz, B. C. J. Polym. Chem. 2014, 52, 619-628.

13. Perry, K. A.; More, K. L.; Payzant, A.; Meisner, R. A.; Supter, B. G.; Benicewicz, B. C. *J. Polym. Sci., Polym. Phys.* **2014**, *52*, 26-35.
14. Li, X.; Qian, G.; Chen, X.; Benicewicz, B. C. *Fuel Cells* **2013**, *5*, 832-842.
15. Li, X.; Chen, X.; Benicewicz, B. C. *J. Power Sources* **2013**, *243*, 796-804.
16. Jayakumar, J.; Gulledge, A. Staser, J. A.; Benicewicz, B. C.; Weidner, J. W. *ECS Electrochemistry Letters* **2012**, *1*, F44-F48.
17. Neutzler, J.; Qian, G.; Huang, K.; Benicewicz, B. C. *J. Power Sources* **2012**, *216*, 471-474.
18. Seel, D. C.; Benicewicz, B. C. *J. Membrane Sci.* **2012**, *405-406*, 57-67.
19. Gulledge, A. L.; Gu, B.; Benicewicz, B. C. *J. Polym. Sci. Part A: Polym. Chem.* **2012**, *50*, 306-313.
20. Mader, J.; Benicewicz, B. C. *Fuel Cells* **2011**, *11*, 212-221.
21. Molleo, M.; Schmidt, T. J.; Benicewicz, B. C. *Encyclopedia of Sustainability Science and Technology*, Ed. R. A. Meyers, Springer Science, **2013**, *Chapt. 13*, 391-431.
22. Yu, S.; Benicewicz, B. C. *Macromolecules* **2009**, *42*, 8640-8648.
23. Stuetz, D. E.; DiEdwardo, A. H.; Zitomer, F.; Barnes, B. P. *Journal of Polymer Science, Polymer Chemistry Edition* **1980**, *18*, 987-1009.
24. Chung, T. S. *Polybenzimidazoles*. Plastics Engineering (New York) **1997**, *41* (Handbook of thermoplastics), 701-731.
25. Chung, T. S. *Journal of Macromolecular Science, Reviews in Macromolecular Chemistry and Physics* **1997**, *C37*, 277-301.
26. Higgins, J.; Marvel, C. S. *Journal of Polymer Science, Part A-1: Polymer Chemistry* **1970**, *8*, 171-177.
27. Hedberg, F. L.; Marvel, C. S. *Journal of Polymer Science, Polymer Chemistry Edition* **1974**, *12*, 1823-1828.
28. Hedberg, F. L.; Marvel, C. S. *Nuova Chimica* **1974**, *50*, 51-54.
29. Neuse, E. W.; Loonat, Ms. S. *Macromolecules* **1983**, *16*, 128-136.
30. Hsiu-Li, L.; Chen, Y.; Li, C.; Cheng, C.; Yu, T. *Journal of Power Sources* **2008**, *181*, 228-236.
31. Conti, F.; Wilbold, S.; Mammi, S.; Korte, C.; Lehnert, W.; Stolten, D. *New J. Chem.* **2013**, *37*, 152-156.

Chapter 9: Summary, Conclusions, and Future Work

9.1 Summary & Conclusions

New sequence isomers of AB-PBI polymer and membranes were prepared using the PPA process and compared to reported literature on the known conventionally imbibed AB-PBI membranes. A new diacid monomer was synthesized from an imidate reaction with 3,4-diaminobenzoic acid. Polymerization of this diacid monomer with 3,3'-4,4'-tetraminobiphenyl yielded a new sequence isomer of AB-PBI, termed i-AB-PBI. Polymerization studies were conducted with the new diacid which showed an unusual dependence on monomer concentration, but revealed conditions where high I.V. polymers could be prepared. Membranes prepared from the PPA process exhibited higher levels of PA than typically reported for conventionally imbibed AB-PBI. The membrane mechanical property characterization and proton conductivity measurements indicated that the membranes formed from i-AB-PBI were suitable candidates for high temperature polymer membrane fuel cells.

The new sequence isomer, i-AB-PBI, was found to be less soluble in phosphoric acid and mechanically stable at elevated temperatures (120-180 ˚C) with high phosphoric acid doping levels (24-35 mol PA/mol polymer repeat unit). The changes in chain sequence incorporated into the new i-AB-PBI as compared to AB-PBI are believed to affect chain stiffness which may contribute to the observed decreased solubility and increased gel stability in phosphoric acid at high temperatures. AB-PBI membranes with

higher polymer content (~7-10.5 wt%) than those prepared from the traditional AB-PBI (~3 wt%) were obtained using the PPA process. The increased solids content of the i-AB-PBI films resulted in membranes that were more mechanically robust when compared to the in-house AB-PBI films prepared using the PPA process. Fuel cell performance evaluations were conducted using i-AB-PBI membranes and an output voltage of 0.65 V at 0.2 A/cm^2 for hydrogen/air at an operational temperature of 180 ˚C was observed.

A combination of monomer design and copolymerization techniques were used to prepare high molecular weight AB-type polybenzimidazoles comprised of a randomized benzimidazole sequence. Disrupted regularity of sequence in the polymer main chain was found to affect fundamental polymer properties, such as chain packing, solubility, glass transition (T_g) temperatures as well as membrane properties for high-temperature fuel cell application.

Phosphoric acid doped random co-polymer membranes of AB-PBI and *i*-AB-PBI were developed using the PPA process. The random AB-PBI polymers had inherent viscosities >2.0 dL/g, and formed mechanically robust films. Thermal evaluations of the randomized AB-PBI copolymers showed a slight decrease in thermal stability when compared to the ordered structures of AB-PBI and i-AB-PBI. Glass transition (T_g) values measured for the r-AB-PBI showed an unexpected depression when compared to theoretical values, and a maximum T_g depression of 140˚C was observed.

Randomized AB-PBI copolymers showed several differences across the compositional spectrum when compared to the AB-PBI and i-AB-PBI homopolymers, indicating primary chemistry and sequence affect properties of both the polymer and membranes derived thereof. A sequence dependence of solubility was observed as well as

trends regarding conductivity, PA retention, and fuel cell performance. Random AB-PBI copolymer membranes were evaluated for mechanical integrity, ionic conductivity and fuel cell performance. An output voltage ranging between 0.5 and 0.6 V at 0.2 A/cm^2 for hydrogen/air at an operational temperature of 180˚C was observed for several r-AB-PBI compositions, indicating these materials would be suitable candidates for high temperature fuel cell applications. When comparing films with similar PA doping and conductivity, an effect on fuel cell performance from sequence isomerism was observed. Thus it appears that both high PA loadings and a more ordered polymer structure contribute to high conductivities and membrane properties. This unique copolymer series provided an opportunity to evaluate fundamental properties of polybenzimidazole that would not be achievable in other copolymer systems. Because the copolymers evaluated consist of only repeating 2,5 benzimidazole units, without extraneous functionality or spacers, the fundamental properties of polybenzimidazole regarding sequence, orientation, and regularity could be investigated.

Random copolymer systems of AB-PBI and p-PBI termed AB/p-PBI and of i-AB-PBI and p-PBI termed i-AB/p-PBI were synthesized via the PPA process and evaluated for membrane composition, mechanical properties, ionic conductivities, and high-temperature fuel cell performances.

Compositional analysis of the AB/p-PBI copolymers showed similar membrane compositions in terms of phosphoric acid, water, and polymer content. Comparison of the random AB/p-PBI copolymers and the AB-PBI and p-PBI homopolymers indicated that the incorporation of a small amount of AB-PBI resulted in an increase in the acid retention of the membranes which remained relatively constant throughout the copolymer

compositional series. Compositional analysis of the i-AB/p-PBI copolymer system indicated the acid retention gradually increased as the composition was shifted from i-AB-PBI to p-PBI, however, was offset by the increase in polymer content of the final membrane, resulting in relatively consistent acid doping levels. These results were further supported when comparing the i-AB-PBI and p-PBI homopolymers.

Room-temperature mechanical evaluations were conducted for acid doped membranes for both copolymer systems. Evaluation of the ABp-PBI copolymer system indicated that mechanical properties were relatively constant as the copolymer composition varied. Changes that were observed in the mechanical properties were attributed to differences in inherent viscosity and acid loadings, and could not be credited to polymer compositional changes. However, evaluation of the i-AB/p-PBI copolymer system did indicate changes that were attributable to the polymer composition. The stress-at-break and elongation-at-break were found to decrease as randomization of the system increased. This is consistent with previous evaluations of randomization in ordered systems.[18] A decrease in Young's moduli of the i-AB/p-PBI copolymers was observed as the p-PBI content increased. This is attributed to the differences in bond angles of the para-phenyl moiety of p-PBI as compared to the benzimidazole structure of i-AB-PBI and the corresponding polymer repeat unit lengths which can affect inter-chain packing.

Ionic conductivity evaluations were conducted under anhydrous conditions over a range of temperatures for both random copolymer systems. For the AB/p-PBI random copolymers the ionic conductivity decreased as AB-PBI content increased. Since the AB/p-PBI copolymers evaluated had similar acid loadings, this effect was attributed to

the instability of AB-PBI gel membranes with high acid loadings at elevated temperatures. This effect is also evident by the rapid decreased ionic conductivity of the 90:10 (AB/p-PBI) copolymer, which showed a significant decrease in ionic conductivity with increasing temperature. AB-PBI homopolymers were unstable at elevated temperatures and ionic conductivity measurements could not be conducted. The i-AB/p-PBI copolymers exhibited an increased ionic conductivity with increasing p-PBI content. These effects were largely attributed to the acid-to-polymer ratio of the membranes evaluated. However, an effect of phenyl group incorporation on proton conduction cannot be ruled out.

Fuel cell performance evaluations were conducted on both the AB/p-PBI and i-AB/p-PBI copolymer systems. Studies of the AB/p-PBI copolymers indicated a correlation between fuel cell performance and the acid content in the membrane. Membranes with higher than 70% AB-PBI content were found to be unstable under the fuel cell operation conditions evaluated, indicative of the instability of PA-doped AB-PBI gel-membranes at elevated temperature. For the i-AB/p-PBI copolymers, fuel cell performance decreased as randomization of the system increased. Although the fuel cell performance decreased with randomization, all i-AB/p-PBI copolymers were found to have suitable high-temperature fuel cell performances. Lifetime evaluations were conducted for several i-AB/p-PBI compositions and all showed stable fuel cell performances for more than 1000 hours. These studies highlight an important design criterion for membrane gel stability. Copolymerization of PBI polymers that create highly randomized polymer sequences seem to disrupt chain packing in the highly swollen gel state. Thus, even when the phosphoric acid content in the membranes is retained, the gel

thermal stability is likely to decrease, thus rendering these membranes unsuitable for long-term stability at high temperatures.

s-PBI membranes were synthesized with uniformly placed sulfonate groups along the polymer backbone by utilizing a pre-sulfonated monomer. s-PBI membranes were prepared via the PPA process and subsequently imbibed with sulfuric acid. s-PBI membranes doped with sulfuric acid were selected for evaluations in a VRFB due to the exceptionally high conductivity and material stability in sulfuric acid. Mechanical analysis of the as-cast and sulfuric acid doped s-PBI membranes showed a significant increase in the Young's modulus of the material (295%) as compared to the phosphoric acid doped membranes. The increase in mechanical properties were attributed to membrane composition and thickness changes during the acid exchange process. Complete acid exchange was verified via titration analysis.

Performance evaluations were conducted on sulfuric acid doped s-PBI membranes in an operating single-cell VRFB. Polarization curves, OCV decay, and cycle testing were carried out. Exact replicate evaluations were performed on Nafion 117 and Nafion NR-211 for comparison. Obtained ASR data indicates a notably higher conductivity for s-PBI than Nafion in an operating VRFB. Differences in cell voltage at higher current densities were attributed to differences in membrane swelling. Swelling of the s-PBI membrane compressed the electrode, resulting in lower porosity and increased concentration polarization relative to Nafion-based materials.

Open circuit voltage decay studies indicate that the s-PBI membranes exhibited a slower rate of voltage decline and vanadium diffusion than that of Nafion NR-211. Cycle testing evaluations also indicated that s-PBI suppressed vanadium crossover much more

effectively than Nafion NR-211. Coulombic efficiency of s-PBI was measured to be nearly 100%, comparable with the much thicker Nafion 117 membrane. Discharge capacity evaluations show excellent discharge capacities for both Nafion NR-211 and s-PBI, allowing for a greater window of operation for VRFB systems. s-PBI also showed the least drastic normalized capacity fade, indicative of the vanadium crossover resistance of the material. Stable area specific resistances were observed for s-PBI, suggesting minimal performance degradation within the testing period. s-PBI was found to be an excellent material candidate as a high-performance membrane for VRFB systems. s-PBI appears to combine the superior coulombic efficiency of Nafion 117 with the high voltage efficiency of Nafion NR-211, resulting in the highest overall energy efficiency, with an average efficiency of 84% compared to 77% with Nafion 117 and 45% in Nafion NR-211.

s-PBI was utilized for the first time as a polymer electrolyte membrane in the hybrid sulfur electrolyzer (HyS). The HyS performance studies indicated that the optimal device performance was around 90˚C, and that temperatures above 120˚C caused the device performance to become unstable. Operation of the HyS electrolyzer with sulfuric acid doped s-PBI is a significant step towards the development of HyS systems capable of high-temperature operation. Since this was the first attempt at high temperature operation, it is surmised that stable elevated performances could be obtained at higher temperatures once the experimental conditions concerning humidification of the SO_2 reactant feed are thoroughly evaluated. This work was the first application of PBI in a HyS electrolyzer. Moreover, this work is the first report of high temperature (>100˚C) device operation. This work has proven to be a significant mile-stone for the development and expansion of PBI PEM based electrochemical device applications.

The reactivity of several chemical functionalities were evaluated to determine an appropriate motif for the solution polymerization of m-PBI in DMAc. Mono-functional analogues were reacted with *o*-diaminobenzene and the reactions were monitored via GC/MS. A bisulfite adduct of benzaldehyde was found to successfully produce the desired phenylbenzimidazole in high-yield with fast conversion. Polymerization trials were also conducted with di-functional monomers, and similar results to the mono-functional analogues were obtained. A bisulfite adduct of isophthalaldehyde was synthesized and the product was confirmed via ^{1}H-NMR and FT-IR analyses. Numerous polymerization trials were conducted in which the isophthalaldehyde bisulfite adduct and commercially available tetraaminobiphenyl were reacted under reflux conditions in DMAc. Polymerization trials were conducted with and without the use of LiCl as a solution stabilizer over a range of reaction concentrations. Optimal reaction conditions were determined to be at approx 18 wt % polymer concentration. Polymer product was analyzed via TGA, DSC, ^{1}H-NMR, and FT-IR and compared to commercially produced m-PBI. TGA, FT-IR and DSC studies showed identical characteristics to that of the commercially produced m-PBI. ^{1}H-NMR analysis compared to reported literature for the H^{1}-NMR spectrum of m-PBI also confirmed the product formation. A viable, commercially applicable, solution polymerization process for the synthesis of high-molecular weight PBI in DMAc was developed. This solution polymerization process has significant commercial and industrial applications to the large-scale production of m-PBI. In theory, this process could be applied to produce a variety of PBI derivatives.

Experimental development of new polybenzimidazole chemistry and evaluations of the structure-property relationships thereof have led to the developments of several

new types and classes of polybenzimidazole materials. Experimental electrochemical device applications were evaluated and expanded the applicability of these high-performance polymers as membrane materials. A newly developed solution polymerization for polybenzimidazoles has presented opportunities for highly-efficient, cost-effective, large-scale production of this widely studied polymer. Overall, the work presented in this thesis contributed to expanding the ever-growing knowledge of polybenzimidazole chemistry, and has expanded the electrochemical device applications of the material as well as development of a viable solution polymerization method for the large-scale production of polybenzimidazoles.

9.2 Future Work

Future work should consist of continuing to develop and explore structure-property relationships through the development of novel polybenzimidazole derivatives. Evaluations of AB-type copolymers with known PBI compositions could provide further insights into the material design and application. Experimental evaluations with new types of electrochemical energy conversion and energy storage devices should be conducted to fully understand the potential applications and performance capabilities of polybenzimidazole as a polymer electrolyte membrane material. Solution polymerization studies with other PBI derivatives using a bisulfite functionality should also be explored.

By applying the understanding developed from this research in terms of sequence regularity and stability, new systems can be developed in which performance properties are increased. The field of polymer electrolyte membrane (PEM) fuel cell technology is continuously expanding and provides a viable avenue for the development of environmentally friendly, stable, sustainable clean energy. As our population continues to

grow it's need for energy, fuel cells based on polymer science become an increasingly important field of study. Perhaps the combination of polybenzimidazole chemistry with other well suited systems such as PFSA membranes could produce the next generation of extremely high performance membranes. By imparting the known benefits and thermal stabilities of polybenzimidazoles with other well know chemistry, a polymer electrolyte membrane could be produced which does not fail. Many systems have been developed that have been shown to have stable performances over the entire duration of testing (thousands of hours). The understanding of these structure-property relationships could very well lead to the production of next-generation PEM fuel cell systems. This technology provides clean alternatives to fossil fuel based energy and other hazardous energy sources. Within the next 20 years, it is predicted that this technology will become common place, as our hydrogen economy continues to grow and develop.

Appendix A: Journal Authorizations

JOHN WILEY AND SONS LICENSE
TERMS AND CONDITIONS

Mar 05, 2014

This is a License Agreement between Alexander L Gulledge ("You") and John Wiley and Sons ("John Wiley and Sons") provided by Copyright Clearance Center ("CCC"). The license consists of your order details, the terms and conditions provided by John Wiley and Sons, and the payment terms and conditions.

All payments must be made in full to CCC. For payment instructions, please see information listed at the bottom of this form.

License Number	3342591051902
License date	Mar 05, 2014
Licensed content publisher	John Wiley and Sons
Licensed content publication	Journal of Polymer Science Part A: Polymer Chemistry
Licensed content title	Investigation of sequence isomer effects in AB-polybenzimidazole polymers
Licensed copyright line	Copyright © 2013 Wiley Periodicals, Inc.
Licensed content author	Alexander L. Gulledge,Xiaoming Chen,Brian C. Benicewicz
Licensed content date	Nov 30, 2013
Start page	619
End page	628
Type of use	Dissertation/Thesis
Requestor type	Author of this Wiley article
Format	Print and electronic
Portion	Full article
Will you be translating?	No
Title of your thesis / dissertation	ADVANCEMENTS IN THE DESIGN, SYNTHESIS AND APPLICATIONS OF POLYBENZIMIDAZOLES
Expected completion date	Mar 2014
Expected size (number of pages)	200
Total	0.00 USD
Terms and Conditions	

TERMS AND CONDITIONS

This copyrighted material is owned by or exclusively licensed to John Wiley & Sons, Inc. or one of its group companies (each a "Wiley Company") or a society for whom a Wiley Company has exclusive publishing rights in relation to a particular journal (collectively "WILEY"). By clicking "accept" in connection with completing this licensing transaction, you agree that the following terms and conditions apply to this transaction (along with the billing and payment terms and conditions established by the Copyright Clearance Center Inc., ("CCC's Billing and Payment terms and conditions"), at the time that you opened your RightsLink account (these are available at any time athttp://myaccount.copyright.com).

JOHN WILEY AND SONS LICENSE
TERMS AND CONDITIONS

Mar 05, 2014

This is a License Agreement between Alexander L Gulledge ("You") and John Wiley and Sons ("John Wiley and Sons") provided by Copyright Clearance Center ("CCC"). The license consists of your order details, the terms and conditions provided by John Wiley and Sons, and the payment terms and conditions.

All payments must be made in full to CCC. For payment instructions, please see information listed at the bottom of this form.

License Number	3342591382827
License date	Mar 05, 2014
Licensed content publisher	John Wiley and Sons
Licensed content publication	Journal of Polymer Science Part A: Polymer Chemistry
Licensed content title	A new sequence isomer of AB-polybenzimidazole for high-temperature PEM fuel cells
Licensed copyright line	Copyright © 2011 Wiley Periodicals, Inc.
Licensed content author	Alexander L. Gulledge,Bin Gu,Brian C. Benicewicz
Licensed content date	Oct 28, 2011
Start page	306
End page	313
Type of use	Dissertation/Thesis
Requestor type	Author of this Wiley article
Format	Print and electronic
Portion	Full article
Will you be translating?	No
Title of your thesis / dissertation	ADVANCEMENTS IN THE DESIGN, SYNTHESIS AND APPLICATIONS OF POLYBENZIMIDAZOLES
Expected completion date	Mar 2014
Expected size (number of pages)	200
Total	0.00 USD
Terms and Conditions	

TERMS AND CONDITIONS

This copyrighted material is owned by or exclusively licensed to John Wiley & Sons, Inc. or one of its group companies (each a "Wiley Company") or a society for whom a Wiley Company has exclusive publishing rights in relation to a particular journal (collectively "WILEY"). By clicking "accept" in connection with completing this licensing transaction, you agree that the following terms and conditions apply to this transaction (along with the billing and payment terms and conditions established by the Copyright Clearance Center Inc., ("CCC's Billing and Payment terms and conditions"), at the time that you opened your RightsLink account (these are available at any time athttp://myaccount.copyright.com).